Quaternary Science Reviews 241 (2020) 106390

Contents lists available at ScienceDirect

Quaternary Science Reviews

journal homepage: www.elsevier.com/locate/quascirev

Invited review

Segmentation and supercycles: A catalog of earthquake rupture patterns from the Sumatran Sunda Megathrust and other well-studied faults worldwide

Belle Philibosian [a, *], Aron J. Meltzner [b, c]

[a] U.S. Geological Survey Earthquake Science Center, P.O. Box 158, Moffett Field, CA, 94035, USA
[b] Earth Observatory of Singapore, Nanyang Technological University, 50 Nanyang Avenue, 639798, Singapore
[c] Asian School of the Environment, Nanyang Technological University, 50 Nanyang Avenue, 639798, Singapore

ARTICLE INFO

Article history:
Received 26 September 2019
Received in revised form
20 May 2020
Accepted 24 May 2020
Available online 8 July 2020

Keywords:
Holocene
Present
Earthquake science
Paleoseismology
Global
Historical records
Geomorphology
Sedimentology
Coral microatolls
Radiogenic isotopes

ABSTRACT

After more than 100 years of earthquake research, earthquake forecasting, which relies on knowledge of past fault rupture patterns, has become the foundation for societal defense against seismic natural disasters. A concept that has come into focus more recently is that rupture segmentation and cyclicity can be complex, and that a characteristic earthquake model is too simple to adequately describe much of fault behavior. Nevertheless, recognizable patterns in earthquake recurrence emerge from long, high resolution, spatially distributed chronologies. Researchers now seek to discover the maximum, minimum, and typical rupture areas; the distribution, variability, and spatial applicability of recurrence intervals; and patterns of earthquake clustering in space and time. The term "supercycle" has been used to describe repeating longer periods of elastic strain accumulation and release that involve multiple fault ruptures. However, this term has become very broadly applied, lumping together several distinct phenomena that likely have disparate underlying causes. We divide earthquake cycle behavior into four major classes that have different implications for seismic hazard and fault mechanics: 1) quasi-periodic similar ruptures, 2) clustered similar ruptures, 3) clustered complementary ruptures/rupture cascades, and 4) superimposed cycles. "Segmentation" is likewise an ambiguous term; we identify "master segments" and "asperities" as defined by barriers to fault rupture. These barriers may be persistent (rarely or never traversed), frequent (occasionally traversed), or ephemeral (changing location from cycle to cycle). We compile a catalog of the historical and paleoseismic evidence that currently exists for each of these types of behavior on major well-studied faults worldwide. Due to the unique level of paleoseismic and paleogeodetic detail provided by the coral microatoll technique, the Sumatran Sunda megathrust provides one of the most complete records over multiple earthquake rupture cycles. Long historical records of earthquakes along the South American and Japanese subduction zones are also vital contributors to our catalog, along with additional data compiled from subduction zones in Cascadia, Alaska, and Middle America, as well as the North Anatolian and Dead Sea strike-slip faults in the Middle East. We find that persistent and frequent barriers, rupture cascades, superimposed cycles, and quasi-periodic similar ruptures are common features of most major faults. Clustered similar ruptures do not appear to be common, but broad overlap zones between neighboring segments do occur. Barrier regions accommodate slip through reduced interseismic coupling, slow slip events, and/or smaller more localized ruptures, and are frequently associated with structural features such as subducting seafloor relief or fault trace discontinuities. This catalog of observations provides a basis for exploring and modeling root causes of rupture segmentation and cycle behavior. We expect that researchers will recognize similar behavior styles on other major faults around the world.

* Corresponding author.
E-mail addresses: bphilibosian@usgs.gov (B. Philibosian), meltzner@ntu.edu.sg (A.J. Meltzner).

https://doi.org/10.1016/j.quascirev.2020.106390

1. Introduction

1.1. A brief history of earthquake recurrence studies

Scientific study of earthquake recurrence dates back to the late 19th and early 20th centuries, when prescient hypotheses of fault scarp interpretation and elastic strain accumulation and release were developed by researchers such as Gilbert (1884) and Reid (1910). However, it was not until the theory of plate tectonics provided a cohesive scientific basis for the recurrence of earthquakes along major fault lines that attempts to anticipate earthquakes by examining patterns of past events began in earnest. "Seismic gaps," sections of un-ruptured fault between known recent ruptures, were identified as likely locations of future earthquakes on several plate boundary faults throughout the late 1960s and early 1970s, with some of these forecasts fulfilled shortly thereafter. Kelleher et al. (1973) summarized earlier efforts and produced the first comprehensive attempt at earthquake forecasting, integrating observations of seismic gaps around much of the Pacific Rim and introducing additional criteria involving the frequency and timing of previous historical events within the gap as well as consideration of the likely progression of cascading ruptures. This analysis was later expanded and updated by McCann et al. (1979), who incorporated the idea that some plate boundary regions might be persistently aseismic. Meanwhile, others pointed out that (then newly-determined) plate motion rates also provide slip budget constraints on earthquake recurrence intervals (Molnar, 1979; Rikitake, 1976), and that longer (though less precise) earthquake chronologies could be obtained from the geologic record (Allen, 1975; Clark et al., 1972; Plafker, 1969; Plafker and Rubin, 1978; Sieh, 1978; Sims, 1975; Wallace, 1970), both particularly useful where historical records are short. Plate motion or fault slip rates and paleoseismic data have been used to calculate individual average recurrence intervals (RIs) for each gap region in more recent forecasts (e.g., Nishenko, 1991).

Research has also been focused on explaining variability of rupture behavior in different settings. Kelleher and McCann (1976) were the first to suggest that average RIs and zones of aseismic slip on megathrust faults might be linked to subducting relief and properties of the subducting plate. The concept of a mechanical rupture barrier was first introduced by Das and Aki (1977) and connected to observed boundary zones between major earthquake ruptures by Aki (1979), who also noted that barriers could be related either to fault geometry or to heterogeneity in frictional properties. These inferences led to fault segmentation models blending rupture history and structural observations (e.g., Schwartz and Coppersmith, 1984). Rupture segmentation determines potential earthquake magnitude so it is highly desirable to identify barriers. However, this sometimes leads to unwarranted assumptions that ruptures will necessarily stop at structural discontinuities or that future ruptures will terminate in the same locations as past ruptures. For megathrust faults in particular, the realization that fault plane properties and the type of earthquakes they generate varies along dip introduced further complexity (Kanamori, 2014; Lay et al., 2012).

As the earthquake cycle conceptual framework developed, it was known that first-order models did not capture the full range of fault behavior, but once again oversimplification occasionally led to unfounded assumptions. Shimazaki and Nakata (1980) introduced the concepts of time- and slip-predictability, which relate stress on a fault to the timing or size of the next earthquake. These are useful models but are typically tested at only a single location, thus involving the potentially inaccurate assumption that all events affecting that location involve the same rupture area. RIs are most easily calculated either for a single paleoseismic site or for an entire region (based on historical accounts). While such RIs are useful for defining seismic hazard at a point or in a region, inaccuracies arise if a single-site or regional RI is improperly assumed to apply to an entire structurally-defined fault segment. In reality a single-site RI may reflect ruptures of various lengths and a regional RI likely includes non-overlapping ruptures on distinct sections of a fault, or perhaps even different faults. In a global analysis, Goes (1996) found significant irregularity in RI on many fault segments (particularly when smaller $M < 7.5$ subduction events were included) and hypothesized that this aperiodicity was due to stress interaction between neighboring fault segments. While some of the irregularity she observed can likely be attributed to conflation of non-similar events into single recurrence series, the facts remain that RIs are often best represented by ranges and that defining RIs for faults with variable rupture modes may not be straightforward. As an additional complication, Thatcher (1984) noted that real earthquake cycles could include inelastic deformation and aseismic slip, which must be accounted for when using plate motion budgets or time/slip predictable models to anticipate earthquakes.

Schwartz and Coppersmith (1984) noted that successive offsets on the Wasatch and San Andreas faults were similar and introduced the concept of a "characteristic earthquake": major faults or fault segments tend to produce earthquakes of a given size over the same rupture area. The characteristic earthquake model was originally intended to emphasize that earthquakes on individual faults did not follow the logarithmic Gutenberg-Richter magnitude distribution that is typically observed over large regions containing many faults. However, the degree of similarity implied by the term is not widely agreed upon, with some researchers requiring earthquakes to be virtually identical in order to qualify as "characteristic," and/or using a strictly segmented model with characteristic earthquakes on each segment as the default assumption for fault rupture behavior. Overly rigid implementation of this model is a factor behind skeptical evaluations of earthquake forecasts (Jackson and Kagan, 1993; Kagan and Jackson, 1991, 1995; Nishenko and Sykes, 1993). Based on the larger dataset that was available a decade later, Sieh (1996) proposed a more flexible "characteristic slip" model: the idea that individual asperities slip by a characteristic amount in each event, though they may rupture independently or in tandem with others creating a variety of rupture lengths. In this model, variable slip primarily occurs in transition zones between asperities. More recently, Zielke (2018) proposed that the observations are best reproduced by a recurrence model dominated by large, quasi-periodic similar ruptures but including a distribution of less regularly timed moderate earthquakes with variable rupture areas.

Thus, the relevant parameters for understanding both earthquake hazards and fault mechanics have evolved from their original simplistic forms, and knowledge of the variability of fault behavior has necessitated caution in making assumptions. Researchers now seek to discover the maximum, minimum, and typical rupture areas; the distribution, variability, and spatial applicability of RIs; and patterns of earthquake clustering in space and time. In this review, we compile rupture chronologies for major faults worldwide where data are sufficient to provide substantive constraints on rupture segmentation and recurrence patterns.

1.2. Data requirements for evaluating rupture segmentation and cyclicity

In order to assess earthquake cycle behavior and rupture segmentation along a given fault, the known earthquake chronology must be long enough to span several full system seismic cycles (in which the entire fault is re-ruptured), and must be established at many locations along the fault. Observing a wide variety of faults

for a short period (as can be done with modern instrumental techniques), while valuable, cannot substitute for observing the long-term behavior of a single fault over multiple rupture cycles. Very long earthquake chronologies that are limited to a single point along the fault (e.g., Clark et al., 2013; Klinger et al., 2015) are also less informative because the rupture extent of each event is not known. Further, the data must be temporally and spatially precise enough to delineate individual ruptures. Technically speaking, determinations of rupture extent based on correlating geologic observations from site to site are able to establish only the maximum rupture extent of an individual earthquake, with the caveat that any "single event" could in theory be composed of multiple non-overlapping smaller events within the time resolution of the geologic data. Occam's Razor is generally applied to interpret the smallest number of individual ruptures that are permitted by the data, but with the emerging knowledge (discussed more fully in section 3) that rupture cascades—temporally clustered series of earthquakes on neighboring fault sections—are common, this assumption may not be strongly justified. As the time resolution of an earthquake chronology becomes more precise, the likelihood increases that an apparent single event truly represents a single event, so high-resolution techniques are required (with historical records being ideal). Finally, for any detailed chronology, it is also important to evaluate the strength of the evidence of absence of earthquakes; i.e., how confidently the occurrence of earthquakes can be excluded during periods when there is no positive evidence for earthquakes. Geologic or historical records that are likely to have significant temporal gaps are far less valuable than continuous records.

Thus, favorable conditions for identifying rupture patterns include short rupture RIs and long, continuous, spatially distributed historical or high-resolution geologic records of earthquakes. Faults that contribute to our catalog are highlighted on the global map in Fig. 1, with RIs and quality of earthquake chronologies detailed in Table 1. Among the primary and secondary contributors, the South American and Japanese subduction zones stand on the strength of their long historical records while most others include a combination of historical and paleoseismic data. Minor contributors demonstrate notable patterns via a few recent ruptures and/or a more limited paleoseismic dataset. A comparison of site density and record length for prominent regional examples of three paleoseismic techniques is shown in Fig. 2.

Analysis of coral microatolls (Fig. 2A), a technique first applied to tectonic research by Taylor et al. (1987) and subsequently developed along the Sumatran Sunda Megathrust (e.g., Natawidjaja et al., 2004; Sieh et al., 1999, 2008; Zachariasen et al., 1999, 2000), is one of the only geologic methods with sufficient temporal precision to provide strong constraints on cyclicity and segmentation. The combination of precise uranium-thorium disequilibrium dating and annual band counting can produce absolute age uncertainties of a decade or less, with relative age uncertainties (time intervals between events recorded in a single continuous coral record) of less than a year. Furthermore, continuous growth of a coral not only records sudden, presumably coseismic vertical deformation events but also precludes the occurrence of coseismic deformation at all other times. However, it must be admitted that even the coral technique, though extremely precise by geologic standards, would likely conflate earthquakes on neighboring fault segments that occurred within a few years of each other. Thus, a rupture cascade within a short time interval (such as the 2004 Aceh–Andaman and 2005 Nias–Simeulue earthquakes on the Sunda Megathrust) might be interpreted as a single event, and those very closely spaced in time (such as the 8.4 and 7.9 Mentawai Sunda Megathrust earthquakes in 2007, which were separated by only 12 hours) almost certainly would be.

Of the other geologic techniques, turbidite paleoseismology (Fig. 2B) is one of the most promising for detailed earthquake recurrence studies. The connection between fault rupture and turbidite deposition, via seismic shaking and sediment transport along often complex flow paths, is less direct than for most other paleoseismic techniques. Nevertheless, because subaqueous sedimentation records are generally more complete, more continuous, and longer than those on land, turbidite paleoseismology is attractive for resolving details of fault rupture chronologies. While turbidite flows can be triggered by a variety of processes, it is argued (e.g., Goldfinger et al., 2012) that turbidite deposits resulting from large earthquakes may plausibly be identified based on their synchronicity and similar characteristics across widespread independent submarine deposition systems. Furthermore, turbidite records provide additional criteria to correlate individual earthquakes between sites, which may help to overcome the inherent limitations of correlation based on radiometric ages. In addition to radiocarbon age constraints, Goldfinger et al. (2012, 2013b; 2017) based their well-known correlations of Cascadia turbidites on turbidite count confluence tests (which rely on understanding the details of the offshore flow paths) and on matching the patterns of laminae within individual turbidite deposits. These techniques, if accurate, have the potential to distinguish between neighboring events in rupture cascades even if they occurred only a few days apart, whereas radiocarbon techniques alone could not. However, there is significant debate about the accuracy of both techniques, as well as other aspects of the Goldfinger et al. analysis (e.g., Atwater and Griggs, 2012; Atwater et al., 2014), and it is difficult to rigorously evaluate turbidite paleoseismology in Cascadia because there is no independent high-temporal-precision earthquake chronology to compare.

It would be ideal to apply the turbidite technique to a subduction zone with a record of historical earthquakes, in order to evaluate the correlation between turbidites and earthquake ruptures and to determine whether it is typically easy to distinguish neighboring ruptures within a cascade via turbidite event signatures, or whether they might be misinterpreted as a single event. So far, the only case where known neighboring ruptures have been examined in the turbidite record is for the 2004 and 2005 Sunda Megathrust earthquakes. Patton et al. (2015) found it easy to distinguish between turbidite deposits from the 2004 and 2005 events because those from 2005 were much thinner and different in character. However, in comparison to the 2004 turbidites, the 2005 turbidites were also much more intermittently distributed, perhaps due to the lack of shallow slip in 2005 (Goldfinger et al., 2014; Patton et al., 2015; Sumner et al., 2013, 2014). Therefore, events like the 2005 rupture could easily be missed in prehistoric turbidite records, particularly if sampling sites are not selected specifically for maximum seismogenic turbidite preservation. Furthermore, it remains unclear whether turbidites from neighboring ruptures that are more similar in size and depth would be as easy to distinguish.

Japan and South America, with their long historical records of subduction earthquakes including many rupture cascades, would be better places to verify the accuracy and precision of marine turbidite paleoseismology. So far, most analyses in these areas have been limited to a small handful of core locations, and the sites have usually not been selected with this specific research goal in mind. Due to climate or depositional environment, many of the cores that have been studied contain very few turbidites for the last several thousand years (Bernhardt et al., 2015; Blumberg et al., 2008; Garrett et al., 2016; Völker et al., 2008). Nevertheless, a few successful (though geographically limited) studies in both Japan and South America suggest that broader application is likely possible

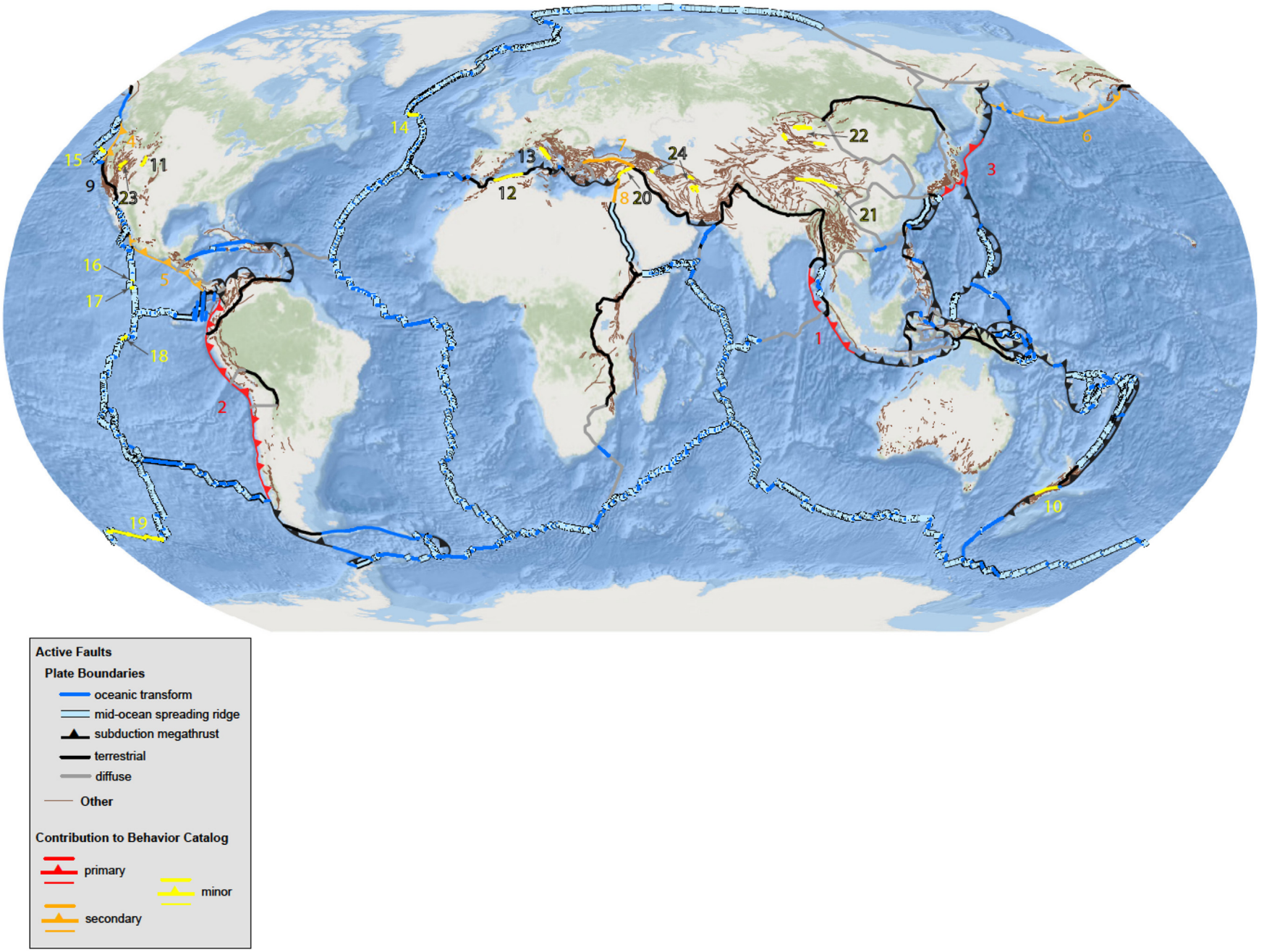

Fig. 1. Active faults of the world and their contributions to this study. Plate boundary faults are adapted from Bird (2003). Other faults are from the Global Earthquake Model Active Fault Database (Styron, 2019). Primary and secondary contributors to our catalog are faults with historical and/or high-temporal-resolution paleoseismic data covering multiple earthquake cycles (which are more likely to exist for faults with short rupture recurrence intervals). Minor contributors have particularly illustrative lower-resolution paleoseismic data and/or recent ruptures demonstrating notable patterns. Most other faults on this map have little or no paleoseismic data and/or at most one historical rupture along any given section. Numbers refer to Tables 1 and 2 which give specifics for each fault zone.

Table 1
Featured and other notable fault zones.

No.	Name	Rupture RI[a]	Historical Period	Paleoseismic Site Density	Paleoseismic Time Resolution[b]	Catalog Contribution
1	Sumatran Sunda Megathrust	200–500 yrs	~250 yrs	high	annual	primary
2	South American Megathrust	~100 yrs	~450 yrs	low	decades	primary
3	Japanese Megathrusts	100–500 yrs	400–1000 yrs	low	decades	primary
4	Cascadia Megathrust	200–500 yrs	200 yrs	high	decades + strat. corr.	secondary
5	Middle America Megathrust	50–100+ (?)	~200 yrs	low	decades	secondary
6	Alaska-Aleutian Megathrust	~500 yrs	150 yrs	low	decades	secondary
7	North Anatolian Fault	~300 yrs	~1000 yrs	moderate	decades	secondary
8	Dead Sea Fault	~500 yrs	~2000 yrs	moderate	decades	secondary
9	San Andreas Fault	~200 yrs	200 yrs	moderate	decades	none
10	Alpine Fault	~300 yrs	200 yrs	moderate	decades	minor
11	Wasatch Fault	>1000 yrs	150 yrs	moderate	centuries	minor
12	El Asnam Fault	~700 yrs	300 yrs	low	decades + strat. corr.	minor
13	Central Italian normal faults	>1000 yrs	700–2000 yrs	low	centuries	minor
14	Charlie-Gibbs Transform	~30 yrs	100 yrs	none		minor
15	Blanco Transform	~14 yrs	50 yrs	none		minor
16	Clipperton Transform	~20 yrs	100 yrs	none		minor
17	Siqueiros Transform	~2 yrs	30 yrs	none		minor
18	Gofar-Discovery Transform	~5 yrs	30 yrs	none		minor
19	Eltanin Transform	4–10 yrs	40 yrs	none		minor
20	East Anatolian Fault	centuries	~500 yrs	very low	centuries	minor
21	Kunlun Fault	centuries	~300 yrs	low	centuries	minor
22	Mongolian strike-slip faults	millennia	~300 yrs	very low	millennia	minor
23	Nevada Basin & Range normal faults	millennia	150 yrs	low	centuries	minor
24	Iranian strike-slip and thrust faults	100s–1000s yrs	~1000 yrs	very low	centuries	minor

[a] Ranges indicate variability between asperities rather than for a single asperity.
[b] strat. corr. abbreviates stratigraphic correlation.

Table 2
Observation of fault behavior types[a].

No.	Name	Persistent/Frequent Barriers	Quasi-Periodic Recurrence	Rupture Cascades	Super-imposed Cycles	Clustered Similar Ruptures
1	Sumatran Sunda Megathrust	yes	yes	yes	yes	no
2	South American Megathrust	yes	yes	yes	yes	no
3	Japanese Megathrusts	yes	yes	yes	yes	no
4	Cascadia Megathrust	yes	yes	no	yes	weak
5	Middle America Megathrust	likely	likely	yes	likely	
6	Alaska-Aleutian Megathrust	possible	likely	yes	likely	
7	North Anatolian Fault	yes	yes	yes	yes	no
8	Dead Sea Fault	likely	weak	yes		possible
9	San Andreas Fault					
10	Alpine Fault		yes			no
11	Wasatch Fault	likely	yes	possible	possible	no
12	El Asnam Fault					possible
13	Central Italian normal faults			yes		likely
14	Charlie-Gibbs Transform	likely	yes			no
15	Blanco Transform	yes	yes	yes		no
16	Clipperton Transform[b]	N/A	yes	N/A	N/A	no
17	Siqueiros Transform	possible	possible			no
18	Gofar-Discovery Transform	yes	yes	yes	possible	no
19	Eltanin Transform	likely	yes	yes		no
20	East Anatolian Fault			yes		
21	Kunlun Fault			yes		
22	Mongolian strike-slip faults			yes		
23	Nevada Basin & Range normal faults			yes		
24	Iranian strike-slip and thrust faults	possible	possible	yes		

[a] Blank entries indicate lack of necessary data.
[b] Segmentation and related cycle types not applicable to single asperities such as the Clipperton case.

(Bernhardt et al., 2015; Ikehara et al., 2016; Noda et al., 2008). To better constrain the capabilities of the technique, we recommend that the marine paleoseismology community prioritize a broad study of seismically generated turbidites in an area with well-constrained neighboring historical ruptures.

To mention a final important paleoseismic tool, lacustrine turbidites (particularly those in small lakes) have many of the same benefits as marine turbidites (non-erosive environment, long periods of continuous deposition, high temporal resolution of deposition including potentially annual varves) with several additional advantages: simpler radiocarbon analyses without the need for a marine reservoir correction, fewer potential non-seismic triggers due to less wave action and lack of large river influx, and less complex sediment flow paths. The method does have a few comparative disadvantages in a subduction environment, such as the relatively sparse distribution of lakes and a greater variety of proximal earthquake sources. Nevertheless, where comparisons have been made, earthquake chronologies based on lacustrine

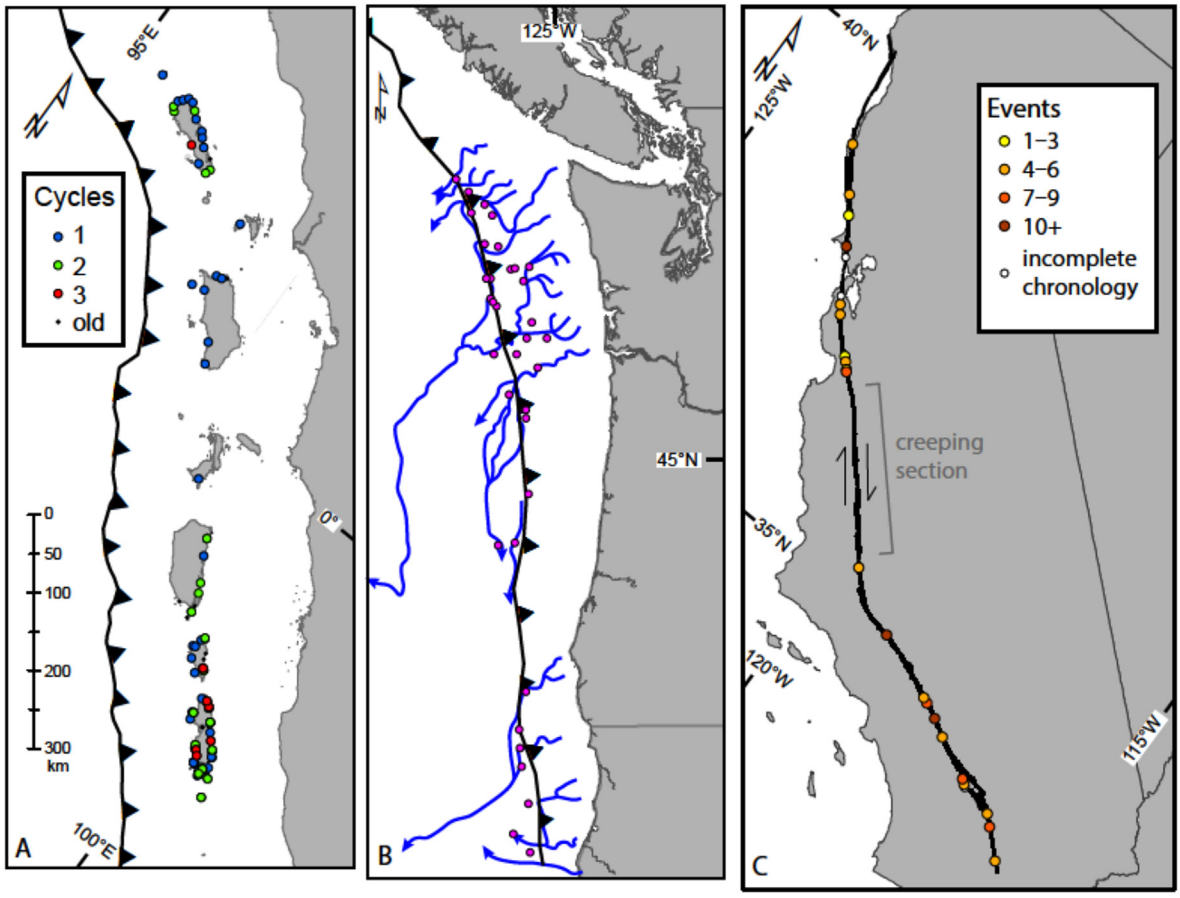

Fig. 2. Site density and earthquake chronology length comparison for (A) coral microatolls in Sumatra, (B) marine turbidites in Cascadia, and (C) trench studies on the San Andreas fault in California, each the best-developed example of the respective geologic technique. All maps are shown at the same spatial scale. Each "cycle" along the Sumatran margin includes multiple individual earthquakes that dominantly rupture different sections of the fault. Data at "old" Sumatra sites are limited to times prior to the most recent three cycles. Cascadia turbidite sites shown in (B) are those used by Goldfinger et al. (2017) to delineate the limits of past megathrust ruptures; most span much of the Holocene and range from ~20 events at the northern end to ~40 events at the southern end according to their interpretation, which could be considered ~20 full cycles of the system. Turbidite flow paths from Goldfinger et al. (2012, 2017, blue lines) illustrate the less direct link between fault rupture and marine core observations. San Andreas event tallies (compiled by Scharer and Streig, 2018) at some sites may overestimate the number of full system cycles if tail ends of neighboring ruptures overlap.

turbidites agree well with historical records of subduction events (e.g., Moernaut et al., 2014) and various data from this promising technique contribute to paleoseismic catalogs for many of the faults discussed in this review.

While the techniques discussed above provide a great deal of valuable information, it is important to reiterate that even the most precise geologic techniques currently available could potentially lead to conflation of neighboring ruptures within a cascade. While the broader-scale rupture RI would still be accurate in the case of such a misinterpretation, there is potential for segment boundaries to be missed and the length of individual ruptures to be overestimated. This should not deter researchers from utilizing geologic techniques, but it is a limitation that should be kept in mind. Fortunately, from an earthquake hazards perspective, this limitation cannot lead to an underestimation of maximum earthquake magnitude. However, conversely, care should be taken not to overemphasize the worst-case scenarios that result from considering the longest possible rupture, as doing so may lead to paralysis in disaster mitigation efforts.

In terms of historical records, as noted above the Japanese and South American subduction zones have the best overall documentation of earthquakes. The only two terrestrial plate boundary faults with records covering a comparable number of seismic cycles, the North Anatolian Fault and Dead Sea Fault in the Middle East, lie in more sparsely populated areas. To evaluate rupture patterns on these faults, historical records must be combined with paleoseismic data. Historical data alone are inadequate, because ancient reports of seismic shaking and other effects are typically too geographically limited or imprecise to determine exactly which part of a fault ruptured. However, the radiocarbon-based ages of terrestrial paleoseismic events are also inadequate on their own, as they are typically too imprecise to positively correlate events between geographically separated sites. Only if the two data sets are combined and paleoseismic data are used to tie historical reports to specific fault segments, can long, precise earthquake chronologies be developed for terrestrial faults. The San Andreas Fault, arguably the best-studied in terms of trenching paleoseismology (Fig. 2C), cannot contribute much to the discussion as its historical records extend only ~200 years into the past, and one section has not had even one historical rupture. Events recorded at an individual paleoseismic site can be correlated with others only by means of absolute age, and these ages typically have uncertainties of decades or more. Therefore, there are typically many different rupture scenarios that can fit all the paleoseismic data, with various degrees of cycle regularity and segmentation persistence (Biasi and Weldon, 2009).

Our catalog includes faults drawn from most tectonic environments, though the sampling is highly non-uniform (Fig. 1).

Unsurprisingly, there is little contribution from oceanic transforms or mid-ocean spreading ridges, as the former are dominantly aseismic and the latter nearly completely so (e.g., Bird et al., 2002). Furthermore, the long distance from land essentially eliminates the possibility of paleoseismic or historical records, and even the instrumental records are limited in precision for these remote areas. Nevertheless, a few oceanic transforms with very short RIs exhibit notable behavior patterns during the instrumental period and are discussed in later sections.

For both historical and geological techniques, subduction zones have a number of advantages over terrestrial faults as case studies. Historical earthquakes can often be confidently attributed to the megathrust based on very broad affected areas and tsunami reports, whereas the causative fault for non-subduction earthquakes is more frequently ambiguous. Two geologic techniques with potential for high temporal resolution, based on coral microatolls and marine turbidites, are both more easily applicable in offshore subduction environments. The availability of these techniques confers an additional advantage in that it is relatively logistically simple to establish chronologies at many locations along a fault: the Sumatra and Cascadia margin studies shown in Fig. 2 were each done by a single research group (each with about five people dominantly or wholly dedicated to the project) while numerous groups have worked along the San Andreas fault with each site requiring at least one graduate thesis or equivalent analysis effort. While Cascadia researchers have examined hundreds of marine cores collected over past decades as they developed the turbidite paleoseismology method, the subset of cores that ultimately proved useful could have been collected in one or two field campaigns targeted for that purpose (as has been done for more recent work along the Sunda Megathrust; Patton et al. (2015)). Given these various advantages, it is no surprise that the bulk of our behavior catalog is drawn from subduction environments. We must therefore be somewhat cautious in applying our findings to fault zones more generally, as certain aspects of subduction megathrusts do not apply to most terrestrial faults (such as the much larger width and depth of the seismogenic zone). Nevertheless, we have enough data from multiple types of terrestrial faults (and a few oceanic transforms) to argue that many of the behaviors we observe are universal.

As high-temporal-precision records such as those discussed above are required to build an accurate model of rupture recurrence, we include fault zones in our catalog based on the availability of such data. However, for each fault zone in our compilation we also incorporate any available less precise geologic data (such as paleotsunami deposits) that significantly extend the length of the record. While these extended records may not be complete or temporally precise, they still provide valuable insight into the persistence of fault behavior over longer time periods.

2. Along-strike rupture segmentation

We begin this section with a practical view of how along-strike segmentation has traditionally been assessed for faults and ruptures. Unfortunately, the terminology surrounding fault and rupture segmentation has become somewhat muddled. Fault "segments" have been delineated based both on structural discontinuities or changes in fault orientation (dominantly on terrestrial faults) and on limits of past ruptures (dominantly on megathrust faults, where structural discontinuities are often less obvious). It has generally been assumed that structural segmentation has some effect on rupture segmentation, but as is discussed in section 2.7 below, there is not always a clear correspondence. Additionally, segments defined based on past rupture patterns are highly dependent on the specifics of known recent ruptures. If known ruptures were relatively short at the time of definition, longer ruptures which occur or are discovered later are then referred to as "multi-segment" ruptures. However, if only long ruptures were known at the time of definition and shorter ruptures subsequently occur or are discovered, researchers must break up originally defined segments or refer to parts of segments. None of this terminology is particularly appropriate for discussing the maximum size of events that may occur on a fault zone.

In the context of assessing patterns of rupture behavior, we find it useful to approach segmentation via the concepts of rupture barriers and asperities, adapted and modified from Lay and Kanamori (1981). We define three types of barriers: persistent, frequent, and ephemeral. There is likely a continuum between persistent barriers, which are very rarely or never traversed by fault ruptures, and frequent barriers, which often stop ruptures but are occasionally traversed. We call barriers "persistent" only if there is no known past rupture traversal, because one of our aims is to determine the limits on the largest ruptures that can occur. Additionally, if even one traversal has occurred during the typically relatively short period of observation, it is probably not an extremely rare event. Ephemeral barriers are qualitatively different from persistent/frequent barriers, in that the boundaries between fault ruptures shift locations from cycle to cycle. A persistent or frequent barrier implies a structural or rheological control on rupture extent, whereas ephemeral barriers indicate that rupture extent is dependent on the distribution of stress on the fault, and the hazard at a given time will depend on the specifics of past fault ruptures. Any rupture terminations that do not correspond to persistent or frequent barriers can be assumed to be ephemeral barriers.

Between two persistent barriers, we define "master segments" which represent, to the best of our ability to determine, the maximum-length rupture that can plausibly occur on that section of the fault. A master segment is composed of one or more "asperities" which can rupture individually. (While the term "asperity" has various connotations in different contexts, making it less than ideal, we use it to mean a fault patch that slips primarily during large earthquakes, without any specific implications about fault plane geometry or radiated energy produced.) After defining this segmentation based on past rupture patterns alone, we then compare the distribution of identified barriers to structural features that may be related.

2.1. Sunda Megathrust

The reliably complete historical record of $M > 7.5$ earthquakes along the Sumatra–Andaman portion of the Sunda Megathrust, from 8°S to 15°N, extends about 250 years, beginning at the time of consistent record-keeping at a network of coastal European outposts in the mid-1700s (Bilham et al., 2005; Newcomb and McCann, 1987). Intermittent colonial records and more distant Indian records extend back into the 1600s and arguably preclude the occurrence of giant earthquakes and tsunamis similar to the 2004 event, but are not necessarily complete for $M < 8.5$ ruptures (Rajendran et al., 2007; Reid, 2016). Prior to that time there are few if any historical earthquake records, as many indigenous groups did not keep written records and local Malay and Indonesian records rarely mentioned earthquakes, likely because their wooden construction was not significantly damaged by seismic shaking and there were few coastal settlements to be affected by tsunamis (Reid, 2015). Along the outer arc islands of Sumatra, the rupture chronology (Fig. 3) has been extended hundreds of years via extensive study of coral microatoll records (Meltzner et al., 2010, 2012; 2015; Philibosian et al., 2012, 2014; 2017), though there remain spatio-temporal data gaps where no microatolls covering a given time

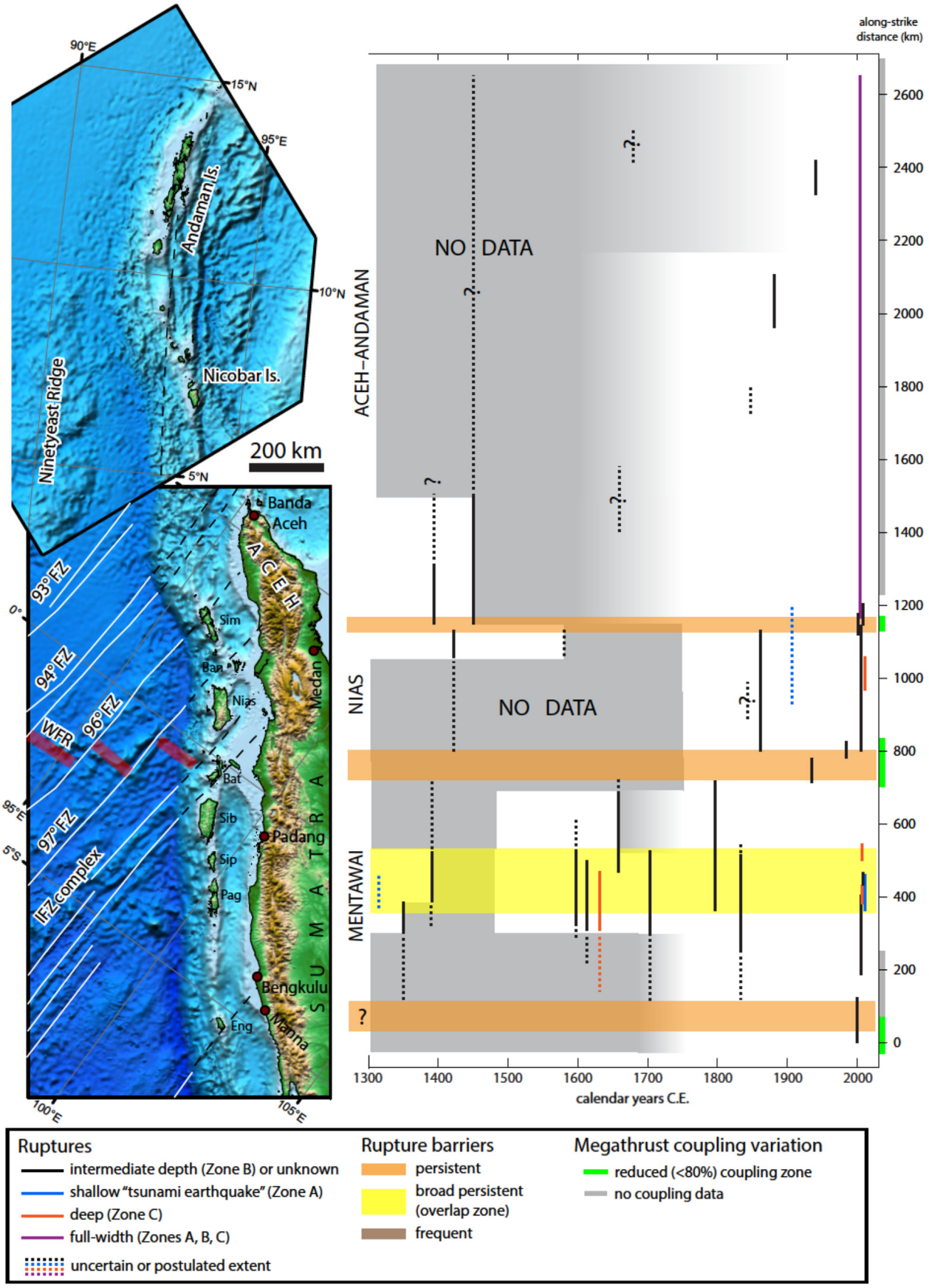

Fig. 3. Rupture history of the Sumatra–Andaman Sunda Megathrust in space and time, from historical and geologic records (sources in supplementary Table S1). A version of this figure with year labels for each earthquake rupture is given in Figure S1. On the map, fracture zones (white lines, dashed black post-subduction) and fossil spreading ridge segments (red bars) on the subducting plate are from Jacob et al. (2014). WFR: Wharton Fossil Ridge, IFZ: Investigator Fracture Zone, Sim: Simeulue, Ban: Banyak Islands, Bat: Batu Islands, Sib: Siberut, Sip: Sipora, Pag: Pagai Islands, Eng: Enggano. Siberut, Sipora, and the Pagai Islands are collectively known as the Mentawai Islands. This figure (as well as Figs. 4–6) uses the NOAA ETOPO1 global relief dataset (Amante and Eakins, 2009) as a basemap. Time-space regions labeled "no data" do have some coverage from distant paleotsunami records, but it is difficult to tie such records to precise source areas. Sections with reduced interseismic coupling (according to Chlieh et al., 2008; Tsang et al., 2015a) are indicated by green bars along right plot axis. Gray bars indicate unconstrained interseismic coupling.

period have yet been found. While coral microatolls are also present in the Andaman and probably Nicobar islands, these have unfortunately not yet been studied in detail (Som et al., 2009). Rupture lines are dotted in Fig. 3 when the extent is inferred but not precisely constrained by the data.

2.1.1. Observations along the Sunda Megathrust

Two likely persistent barriers, beneath Simeulue and the Batu Islands, can be readily identified in the rupture history of the Sumatran Sunda Megathrust (Meltzner et al., 2012; Philibosian et al., 2014), separating the Aceh–Andaman, Nias, and Mentawai master segments. Over the past 700–1100 years, both barriers have served as the endpoints of numerous ruptures and no M > 8 rupture is known to have traversed either one (though due to data gaps, the possibility cannot be entirely excluded). Based on the southern termination of the 2007 Mentawai rupture and the beginning of transition toward the Java section of the megathrust, a third barrier may lie beneath Enggano Island, but this is not well constrained by the data (Fig. 3). All three of these locations have hosted more moderate M 7–8 megathrust ruptures: Simeulue in 2002 and 2008 (Morgan et al., 2017), the Batu Islands in 1935 and 1984 (Natawidjaja et al., 2004; Rivera et al., 2002), and Enggano in 2000 (Abercrombie et al., 2003). (Note, while the 2000 Enggano event had by far the highest magnitude at 7.9, it was a complex earthquake with likely less than half the total moment released on the megathrust interface.)

Both the Aceh–Andaman and Nias segments have had end-to-end ruptures, confirming their status as single master segments. Several M_w 7.5–8 historical earthquakes have also occurred within the 2004 rupture zone (Bilham et al., 2005; Malik et al., 2011; Rajendran et al., 2007), indicating that the Aceh–Andaman segment is made up of multiple distinct asperities. The Mentawai behavior is different, with no known single segment-spanning rupture. Instead, events are typically centered in the northwest or southeast but overlap significantly in the middle, beneath Sipora and the Pagai Islands (Philibosian et al., 2014, 2017). This 150-km-long overlap zone could be considered an extremely broad persistent barrier. However, it is likely more accurately described as a patchwork of small asperities that can participate in larger ruptures extending northward or southward, but nevertheless inhibit the continuation of rupture through this zone. This interpretation is supported by the "patchy" quality of the 2007 M_w 7.9 rupture, which involved two spatially separated asperities (Konca et al., 2008), by the later individual rupture of another asperity in 2008 (Salman et al., 2017), and by the general variability of past ruptures in this region (Philibosian et al., 2017).

2.1.2. Segmentation mechanisms along the Sunda Megathrust

Rupture segmentation along the Sumatran Sunda Megathrust is argued by many researchers to link to features on the subducting plate, which include numerous fracture zones offsetting segments of the Wharton Fossil Ridge (WFR) inactive spreading center (Jacob et al., 2014, Fig. 3). One such fracture zone subducts beneath Simeulue Island, forming a morphological high along the plate interface that is interpreted to act as the rupture barrier and to structurally control small asperities responsible for more moderate earthquakes (Morgan et al., 2017 and references therein). Both the WFR and the multi-stranded Investigator Fracture Zone (IFZ) subduct beneath the Batu Islands. Based on gravity and seismic reflection data, the subducted WFR continues as a morphological ridge along the plate interface and coincides with the southern edge of the 2005 rupture (Henstock et al., 2016). The subducted IFZ has a weaker geophysical signature that is discontinuous along its strike (Henstock et al., 2016), but is associated with a well-defined streak of seismicity (Lange et al., 2010). Kopp et al. (2008) noted that subduction of the IFZ substantially disrupts the deformation front of the accretionary wedge (though they erroneously stated that the point of subduction migrates northward along the trench; it actually migrates southward). The northern termination of the 1797 northwestern Mentawai rupture is only loosely constrained (Philibosian et al., 2014), and the IFZ is a wide feature, but it is certainly plausible that the two were related.

Yet another fracture zone (FZ) subducts beneath Enggano Island, though no authors have specifically proposed a connection with rupture termination. There are several other fracture zones which are not associated with rupture terminations. Three subduct north of Simeulue and were traversed by the 2004 rupture, though that is perhaps unsurprising since they have been covered by the thick sediment of the Nicobar Fan and are not associated with seafloor relief at the trench (Gulick et al., 2011). Another subducts beneath the Banyak Islands and is less thickly buried in sediment, yet was traversed by the 2005 rupture. The latter FZ may have some effect, as the 2005 rupture was divided into two main asperities north and south of the Banyak Islands (Briggs et al., 2006). However, it clearly does not form a persistent barrier, as it was also traversed in 1861 (Meltzner et al., 2015). Therefore, the FZ beneath Enggano is by no means guaranteed to produce rupture segmentation. Singh et al. (2011) suggest that rupture termination near Enggano is instead related to a subducted seamount, though the feature they detect via seismic reflection is quite deep on the plate interface, largely past the seismic zone. In that case it would have to be the zone of disruption left behind by the subduction of the seamount, not the seamount itself, that inhibits rupture propagation.

Concentrations of permanent uplift on the overriding plate, which are thought to be related to rupture segmentation along some other subduction zones (see section 2.2.2), have not been found along the Sumatran Sunda Megathrust. None of the islands west of Sumatra bears flights of marine terraces, and analyses of corals with ages throughout the Holocene on Nias and the Mentawai Islands limit permanent uplift rates in most areas to a few tenths of a millimeter per year (Briggs et al., 2008; Philibosian et al., 2012). Variations in rate appear related to the trends of fold axes in the accretionary prism. The Andaman and Nicobar Islands do have more significant long-term uplift, with variations along strike (Rajendran et al., 2008), but these cannot be related to persistent barriers as they are all within the 2004 rupture area. Analysis of satellite imagery (such as is available on Google Earth) reveals uplifted terraces along the coast of mainland Sumatra, from about Manna (4.5°S, 102.9°E) southeastward. However, no formal analysis of these terraces has yet been published, and the uplift does not appear to be concentrated in narrow zone, so it is unclear whether this may relate to a rupture barrier. Regardless, these terraces lie largely outside the limits of the section of the Sunda Megathrust we analyze in this paper.

Although the fault slip budget in barrier regions could be balanced in a number of ways (e.g. overlapping "tails" of large ruptures, slow slip events, or more frequent moderate earthquakes), a likely scenario is that persistent barriers have reduced long-term interseismic coupling in comparison to asperities. Interseismic coupling on the Aceh-Andaman segment is essentially unconstrained before the 2004 rupture (Paul and Rajendran, 2015) and since then has been dominated by postseismic signals (Paul et al., 2012), so we cannot assess the potential connection with rupture segmentation in that area. Farther south, models based on a combination of interseismic GPS and 20th-century coral data suggest that plate interface coupling is indeed reduced beneath Simeulue, the Batu Islands, and Enggano (Chlieh et al., 2008; Tsang et al., 2015a), consistent with the interpretation that these regions of the megathrust accommodate plate motion largely through continuous creep and relatively moderate "large" (M_w < 8)

earthquake ruptures, rather than "great" to "giant" ($M_w \geq 8$) earthquake ruptures. However, comparison of GPS deformation rates in the 1990s to those in the 2000s suggests that the Batu and Enggano regions were more highly coupled in the earlier period (Prawirodirdjo et al., 2010). This and other evidence that interseismic deformation rates (and, thus, the underlying fault slip deficit rates) can fluctuate on decadal time scales (Meltzner et al., 2015; Tsang et al., 2015a) indicate that short-term observations of interseismic deformation (e.g. limited to the GPS era) are not necessarily representative of long-term averages and should not be the only method used to identify asperities and barriers.

2.2. South America

With a continuous historical record in most areas since the late 1500s and typical RIs of ~100 years, the South American subduction zone is one of the better areas to evaluate segmentation (and recurrence) behavior. We have compiled the approximate rupture lengths of all historical megathrust earthquakes with estimated magnitudes >7.5 (Fig. 4). This record should be complete for the entire South American margin except for four regions: the Atacama Desert region of northernmost Chile, which had little European settlement (and thus written record) until the 1830s (Comte and Pardo, 1991), north-central Chile where records are sparse until the latest 1700s (Beck et al., 1998), southern Chile where records are sparse until the early 1800s (Kelleher, 1972), and remote southernmost Chile which had no significant settlement until the mid-1800s (Barrientos, 2007). It should be noted that in general, endpoints for progressively earlier ruptures are progressively less precisely known, but this variable uncertainty is typically not well quantified in the literature. We use dotted lines on Fig. 4 only in places where there is notable debate about rupture extent or where evidence is considered particularly weak. We include only those earthquakes which the evidence strongly suggests occurred on the megathrust; note that this criterion excludes some of the deadliest earthquakes in South American history, such as the 1939 Chillán earthquake (inland from Concepción in Chile) and the 1970 Ancash earthquake (inland from Chimbote in Peru), both of which according to most analyses occurred within the subducting slab. While our catalog is dominantly derived from historical records, a growing body of paleoseismic work has revealed additional details about some events and hints about longer-term behavior in some areas.

2.2.1. Observations in South America

Based on the patterns of past ruptures, we can divide the megathrust into 10 master segments, which we refer to by the names typically given to them in the literature (left axis of Fig. 4). These segments range between 300 and 1000 km long and all but two have had at least one end-to-end rupture in a single earthquake during historical times (and one of those two is likely freely slipping). The boundaries between these segments appear to be persistent barriers to rupture, in that a rupture of one segment has never extended far into a neighboring segment. Although endpoints for earlier historical ruptures are generally less precisely known, based on the available information it appears that some of the boundaries are quite sharp (e.g. Arica), whereas others are more diffuse with a potentially significant zone of overlap between neighboring ruptures (e.g. Arauco). Like the segment boundaries identified along the Sunda Megathrust, some of the South American boundary zones host M 7–7.5 events, suggesting relatively small asperities surrounded by areas of otherwise low coupling. Within these master segments, regions where many (but not all) ruptures terminate are identified as frequent barriers.

The area where the Carnegie Ridge subducts beneath Ecuador is the northernmost segment boundary. It produced several M ~7 events in 1896, 1956, and 1998 but served as an end point for the larger 1906, 1942, and 2016 ruptures to the north (Nocquet et al., 2016; Yepes et al., 2016). As discussed in more detail later, there were no historical subduction earthquakes before 1896 in Ecuador and very few at all in northern Peru, so the number of events with which to assess barrier persistence is small in comparison to most of the other segment boundaries, but what evidence exists does suggest a persistent barrier. At the southern end of the potentially creeping Chiclayo segment, another boundary exists between the quiescent zone and numerous historical ruptures that have occurred southeast of Chimbote (Dorbath et al., 1990). Within the Lima segment (which has not ruptured end-to-end historically), there are two potential frequent barriers where numerous ruptures have terminated, but both have likely been traversed by at least one historical rupture.

Farther south, another apparently persistent segment boundary is associated with the subduction of the Nazca Ridge. No M8+ rupture has been centered in this area and numerous ruptures on both the north and south sides terminated in that vicinity (Dorbath et al., 1990; Okal et al., 2006). Based on tsunami modeling, Okal et al. (2006) argued that the giant 1868 Arica rupture traversed the 175-km-wide Nazca Ridge, yet it clearly did not extend north of the ridge zone. At least one M ~7.5 earthquake, in 1996, was centered on the ridge, and an earlier event in 1942 ruptured much of that same area but also extended southeastward (Bilek, 2010). Saillard et al. (2017) indicate that a 1687 rupture may have traversed the Nazca Ridge, but Dorbath et al. (1990) concluded that there were actually two events, with the southern one occurring one day later and geographically separated from the northern event (thus likely indicating a rupture cascade).

Continuing southward, Arica, Mejillones, Taltal, and Tongoy have served as fairly sharp endpoints for numerous historical ruptures while no historical M8+ rupture has traversed any of these boundaries (Beck et al., 1998; Bilek, 2010; Comte and Pardo, 1991). The historical record is shorter for the region surrounding Mejillones and Taltal since the Atacama Desert was settled relatively late, so the evidence that they are persistent barriers is less strong than for most of the others we propose; however, Victor et al. (2011) argued that long-term deformation of the Mejillones Peninsula is consistent with a persistent barrier. M ~7.5 earthquakes centered on the Arica boundary occurred in 1681 and 1833 (Comte and Pardo, 1991). South of Tongoy, numerous ruptures (in 1822, 1873, 1880, 1906, 1943, 1971, and most recently the 2015 Illapel rupture) terminated near Valparaíso (Barnhart et al., 2016; Beck et al., 1998). We do not place a persistent boundary there because the earlier 1730 and possibly 1647 ruptures are thought to have traversed it (Beck et al., 1998; Carvajal et al., 2017a), making this area merely a frequent barrier.

Even farther south, two additional boundary zones can be identified in the vicinities of Constitución–Pichilemu and Arauco, separating the Concepción segment from the Valparaíso segment to the north and the Valdivia segment to the south. These boundaries may be less sharply defined than those farther north, in that while historical ruptures have never involved more than one of the three master segments (Beck et al., 1998; Melnick et al., 2009), there has likely been significant overlap between ruptures on neighboring segments, even those that are fairly closely spaced in time. Two notable examples are the estimated ~150 km of overlap in the Constitución–Pichilemu region between the 1730 Valparaíso and 1751 Concepción ruptures (Beck et al., 1998; Carvajal et al., 2017a; Melnick et al., 2009), and the more certain ~150 km of overlap in the Arauco region between the 1960 Valdivia and 2010 Maule

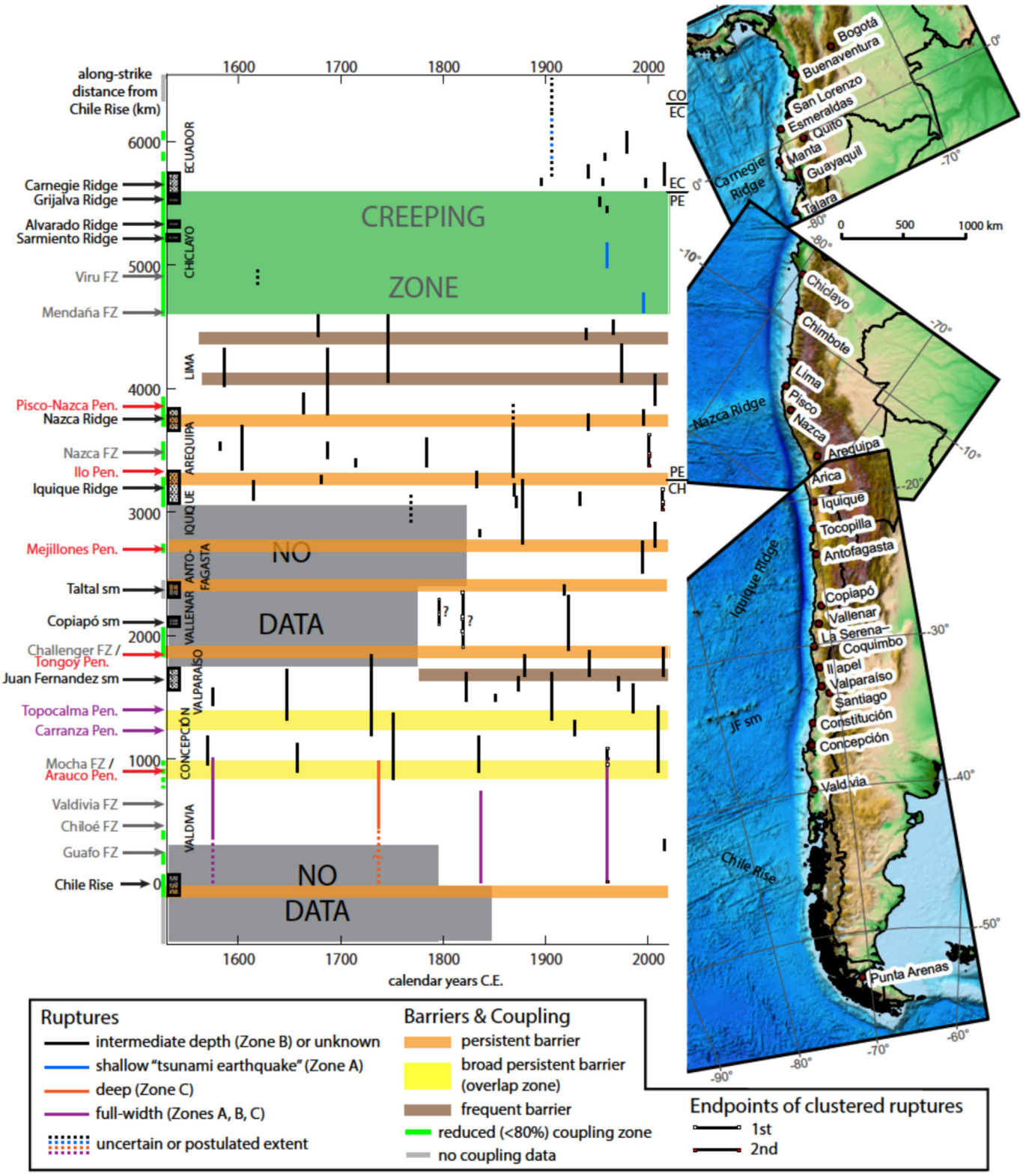

Fig. 4. Rupture history of the South American megathrust in space and time, from historical records (sources in supplementary Table S2). A version of this figure with year labels for each earthquake rupture is given in Figure S2. Gray areas had insufficient European settlement to have reliable historical records. Small squares at rupture endpoints differentiate multiple adjoining or overlapping ruptures that occurred within a few years. Queried rupture groups in the Vallenar segment were clusters of 2 and 3 earthquakes but the precise extent of each individual event is not known. Green band indicates the Chiclayo segment which has had no ruptures other than tsunami earthquakes for over 400 years and appears to be freely creeping. Along the y-axis, areas with subducting seafloor relief >1 km high (from Sparkes et al., 2010, with the addition of features off northern Peru and Ecuador), are indicated by black spotted bars and labeled in black (sm = seamounts). Subducting fracture zones (FZ) are labeled in gray. Uplifting peninsulas associated with low megathrust coupling (labeled in red) and normal to high megathrust coupling (labeled in purple) have been assessed for the Arequipa through Concepción segments only (Jara-Muñoz et al., 2015; Saillard et al., 2017). Green bars along the y-axis indicate areas of low interseismic coupling compiled from Chlieh et al. (2014), Villegas-Lanza et al. (2016), Saillard et al. (2017), and Moreno et al. (2011); gray bars indicate lack of data to constrain coupling. Locations of international borders are indicated along the right edge of the plot (CO: Colombia, EC: Ecuador, PE: Peru, CH: Chile).

(Concepción segment) ruptures (Moreno et al., 2011). Historical records are not sufficiently precise to determine definitively whether most earlier ruptures on these three segments overlapped or not (Kelleher, 1972). One possibility is that the Constitución–Pichilemu and Arauco boundary zones consist of individual asperities that may be involved in ruptures of either of the two neighboring master segments, yet are sufficiently inhibitory to rupture to prevent continuation from one master segment to the other. Another possibility is that successive earthquakes within these "overlap zones" may not actually rupture the same asperities, if there is segmentation along dip: in fact, Carvajal et al. (2017a) argue based on historical observations that within the overlap zone, the 1730 rupture was dominantly deep and the 1751 rupture was dominantly shallow. The 1906 and 2010 ruptures that later overlapped in this same region may have had a similar relationship (Carvajal et al., 2017b). Geologic evidence supports the persistent nature of the Arauco boundary and suggests that previous ruptures from north or south overlapped along strike but involved different asperities along dip (Dura et al., 2017). These Chilean overlap zones are similar in absolute size to the central Mentawai overlap zone, though ~150 km represents a much smaller percentage of the total rupture length of the Chilean earthquakes than the Mentawai earthquakes.

South of the subduction of the Chile Rise, the plate convergence rate is much slower and the seismicity rate of small to moderate earthquakes is also much lower than in the rest of Chile (Barrientos, 2007). It would be premature to assume that this segment never produces great earthquakes, but there have been no M > 7.5 subduction earthquakes since reliable historical records began in this remote and sparsely populated region, c. 1870. The termination of the 1960 earthquake rupture, the ridge subduction, and the significant change in plate boundary kinematics all suggest that the Chile Rise is likely a persistent barrier to rupture, but this cannot be assessed critically based on the available data.

It should be noted that rupture terminations that do not correspond to one of the barriers described above may indicate the presence of additional frequent barriers (e.g., within the Arequipa and Iquique segments). With shorter historical records or imprecisely known rupture endpoints, it can be difficult to distinguish whether a barrier is frequent or ephemeral. However, we can be confident that we have identified every potential persistent barrier.

2.2.2. Segmentation mechanisms in South America

Numerous studies have searched for patterns linking South American megathrust segmentation to structural features and interseismic coupling. Sparkes et al. (2010) assessed the correlation between M > 8 earthquake rupture terminations and subducting topography along the Peru–Chile subduction zone. Of the 14 such earthquakes that had sufficiently precisely determined rupture endpoints (those that occurred between 1868 and 2010), all but one had exactly one endpoint within 40 km of subducting relief >1 km high. The only exception is the 1939 Chillán earthquake which may actually have been an intraplate event, and if not must have occurred very deep on the plate interface (Beck et al., 1998). Therefore, it is perhaps not surprising that the latter event behaved differently (we do not include it on our space-time diagram). Of the six subducting seafloor features with >1 km relief, only the narrowest member (a sparse seamount chain that enters the trench near Copiapó, Chile) was traversed by a megathrust rupture in the Sparkes et al. (2010) study, and this feature is also the only one of the six that did not serve as a rupture endpoint during 1868–2010. According to their statistical analysis, it is highly unlikely (~1.5% chance) that the observed correlation between rupture endpoints and relief is merely a coincidence. However, they note that subducting relief cannot be the only factor to influence rupture limits, as each of the 13 studied ruptures had one end that was not associated with subducting relief.

Four of the six subducting relief features identified by Sparkes et al. (2010) correspond well to the persistent barriers we identify: the Nazca Ridge, Iquique Ridge (Arica), Taltal seamount chain, and Chile Rise. The fifth, the Juan Fernandez seamount chain, corresponds to the frequent barrier near Valparaíso. The sixth feature, the Copiapó seamount chain, lies in the middle of the Vallenar segment and was (as mentioned above) certainly traversed by the 1922 Vallenar rupture. It may also have been traversed by earlier ruptures in 1819 and 1796, although the precise extent of these earlier ruptures is less well known. Sparkes et al. (2010) speculate that the wide spacing between Copiapó seamounts reduces their effectiveness as a barrier. Nevertheless, seismograph analysis of the 1922 event suggests it involved three separate asperities, while the 1819 rupture involved three separate events over the course of a week and the 1796 rupture involved two events several months apart (Beck et al., 1998). This past rupture complexity suggests the possibility that there is megathrust heterogeneity associated with the Copiapó seamounts that contributed to the multi-asperity nature of the 1922 rupture and may even have divided the 1819 and/or 1796 ruptures.

In summary, the conclusion made by Sparkes et al. (2010) that subducting relief is a factor (but perhaps not the only factor) influencing persistent segmentation remains robust when the full historical record is examined. In addition, applying the criterion of subducting relief >1 km to the northern extension of the subduction zone (outside the region analyzed by Sparkes et al.), the Carnegie Ridge would also be correctly identified as a likely persistent barrier. The Grijalva, Alvarado, and Sarmiento ridges also have relief greater than the 1 km threshold (Lonsdale, 2005), but as they subduct within the historically aseismic Chiclayo segment, their effect on megathrust ruptures is unknown. Yepes et al. (2016) suggest that the Grijalva Ridge (which is a rifted margin) separates a more-coupled section from a less-coupled section of the megathrust at the northern end of the Chiclayo segment, but without historical large earthquakes on either section this is difficult to test.

Subducting features with lesser relief may also inhibit rupture, though perhaps less reliably. Carena (2011) argued that subducting oceanic fracture zones (FZs) would behave as lateral ramps and noted that several FZs are associated with rupture terminations along the South American megathrust. Indeed, there are three FZs potentially associated with persistent segment boundaries we identify: the Challenger FZ (Tongoy), the Mocha FZ (Arauco), and the Mendaña FZ (Chimbote). The Viru FZ subducts within the historically aseismic Chiclayo segment so its effects are unknown. Three FZs within the Valdivia segment were entirely traversed by the 1960 rupture and likely by earlier ones, perhaps because they are mantled in sediment (Carena, 2011), and the Nazca FZ subducts within the Arequipa segment (traversed in 2001 and 1868, and likely by earlier ruptures). However, these FZs still had some effect: areas of high slip in the 1960 rupture appear bounded by FZs (Barrientos and Ward, 1990), indicating that the FZs may divide the segment into several distinct asperities and may have served as endpoints for past events. Also, Robinson et al. (2006) suggest that the Nazca FZ did inhibit rupture propagation in 2001, though this barrier was ultimately overcome.

In addition to the influence of features on the subducting plate, the relationship between upper plate features and rupture segmentation has also been explored in this region. Saillard et al. (2017) investigated segmentation along the Peru–Chile section of the megathrust by correlating geodetically-derived recent

megathrust coupling with rapid long-term coastal uplift and the locations of prominent peninsulas along the coast. They propose that the formation and uplift of these peninsulas is related to inelastic deformation in the upper plate that occurs above low-coupling regions on the megathrust during the interseismic period. They found the strongest correlations between these factors at the Pisco-Nazca, Ilo, Mejillones, Tongoy, and Arauco peninsulas, all of which except Ilo coincide with persistent barriers we identify. In our earlier discussion of rupture endpoints in Section 2.2.1, with regard to the Ilo peninsula, we placed the nearest barrier at Arica, 140 km to the south. Saillard et al. argue that the Ilo peninsula has served as an endpoint for numerous ruptures on the Arequipa segment that did not extend as far south as Arica, but due to the assumed greater uncertainty of endpoints it is difficult for us to confidently determine whether older historical ruptures ended at Ilo or Arica. The two most recent events in this region were the 2001 Arequipa earthquake doublet, where rupture did indeed stop at the Ilo peninsula, and the 1868 Arica earthquake for which, as the name suggests, most researchers are confident rupture extended to Arica. It may be that Ilo, like the Juan Fernandez seamounts, frequently (but not always) behaves as a rupture barrier. It is also worth noting that the reduced coupling zone identified by Saillard et al. seems more closely associated with the Nazca FZ than with the Ilo peninsula, which are at the same latitude but separated by ~150 km along strike (see Fig. 4). In addition, Saillard et al. do find low coupling in the Arica region, though there is no associated uplifting peninsula there. Although Saillard et al. infer that the areas of low coupling are most likely related to patches of rate-strengthening friction, they do not propose a structural or rheological reason for these apparent heterogeneities. The Pisco-Nazca and Ilo regions are associated with subducting relief >1 km identified by Sparkes et al. (2010) and the Tongoy and Arauco regions with fracture zones, but the Mejillones peninsula is not associated with any subducting plate feature.

It should be noted that not all uplifting peninsular regions are clearly associated with reduced coupling, but even those that are not may be related to segmentation. Saillard et al. compile data from an earlier study by Jara-Muñoz et al. (2015) indicating rapid uplift on the Carranza and Topocalma peninsulas, but do not find significantly reduced coupling in those areas. However, as Jara-Muñoz et al. point out, these two uplifting peninsulas are located at either end of the Constitución–Pichilemu boundary zone discussed above, which can apparently rupture along with either the Valparaíso or Concepción segments. Jara-Muñoz et al. propose that upper-plate structures are causing the uplift and presumably acting as rupture barriers, though again the precise mechanisms are uncertain.

In summary, upper and/or lower plate structures can be identified that correspond to all of the persistent barriers and at least one frequent barrier that we delineate. Conversely and equally important, every subducting feature with >1 km relief and every peninsula associated with either rapid uplift or low coupling corresponds to a barrier (although some of these are occasionally overcome by very large ruptures). Subducting fracture zones have less consistent effects, as some correspond to persistent or frequent barriers and others apparently do not, although some could correspond to unidentified frequent barriers. Some of the upper plate peninsulas correspond to subducting features that could be the underlying cause of both the rupture barrier and the upper plate deformation, but other peninsulas appear unrelated to the subducting plate and might indicate influence of upper plate structures alone.

A more complex model of the relationship between subducting topography and rupture segmentation along the Peru-Chile megathrust proposed by Contreras-Reyes and Carrizo (2011) offers a potential explanation for the observed divergent effects of similar features. They argue that the subduction of high oceanic features (which increases normal stress) can produce either barriers or asperities depending on the smoothness of the megathrust interface. According to their hypothesis, the fracture zones in southern Chile correlate to areas of high slip in the 1960 earthquake due to their increased normal stress, but did not disrupt rupture propagation because they are mantled in sediment. Other similarly-sized features in sediment-poor sections of the margin (such as the Mocha FZ and Juan Fernandez ridge) act as barriers due to the interface heterogeneity. Also, the top of the broad, obliquely-subducting Iquique ridge may act as a strongly-coupled asperity along most of the Iquique segment despite its lack of sediment cover, simply because it is large enough to form a homogenous surface with high normal stress. The persistent barrier at Arica would then be controlled by transitions in stress and geometry along the northern edge of the Iquique ridge.

Considered separately from upper plate deformation, there is reasonably good correspondence between zones of reduced interseismic coupling (green bars on distance axis of Fig. 4) and barrier regions, though the caveat remains that the effects of great earthquakes within the last few decades may pollute interseismic coupling models. Megathrust coupling is as yet poorly constrained in northern Colombia (Mora-Páez et al., 2019), but interface coupling is strong in southern Colombia and northern Ecuador and becomes patchy and ultimately very low at the Carnegie Ridge segment boundary (Chlieh et al., 2014). Coupling is persistently low throughout the Chiclayo segment, transitioning at the Mendaña FZ to high throughout the Lima segment (Villegas-Lanza et al., 2016). As previously discussed, Saillard et al. (2017) used a GPS dataset covering the Arequipa through Concepción segments with time periods chosen to exclude 21st-century great earthquakes, finding reduced coupling zones coinciding with the Nazca Ridge, Arica, Mejillones, Tongoy, and Arauco barriers, with an additional low coupling zone associated with the Nazca FZ within the Arequipa segment. Moreno et al. (2011) modeled interseismic coupling on the Valdivia segment including a viscoelastic relaxation correction for the 1960 earthquake, finding a low-coupling patch shifted southward from the Arauco peninsula (in contrast to Saillard et al.), low coupling in the vicinity of the Chile Rise barrier, and two smaller patches of low coupling within the segment. The small decoupled patches roughly coincide with lower slip areas in 1960, but do not seem to align well with subducting fracture zones.

2.3. Japan

Japan's >1300-year written history of subduction earthquakes and significant paleoseismic data provides another excellent region in which to assess cyclicity and segmentation. We review the earthquake history of the three subduction zones, the Japan-Kurile Trench, Nankai Trough, and Sagami Trough (Fig. 5). As in South America, though specifics of earlier ruptures are generally less precisely known, we use dotted lines only where there is notable debate about rupture extent or where constraints are considered particularly weak. Dashed lines are used in a few cases when evidence is dominantly based on paleoseismic data. While the Nankai and Sagami Troughs both involve subduction of the Philippine Sea Plate beneath Japan, the sharp 90° change in orientation of the plate boundary, collision of the Izu-Bonin volcanic arc with the Japan block, and associated potential transition between the overriding Amur and Okhotsk Plates (e.g., Bird, 2003) suggest that a contiguous megathrust rupture across the Izu Peninsula is extraordinarily unlikely. The hypothesis of a persistent barrier to

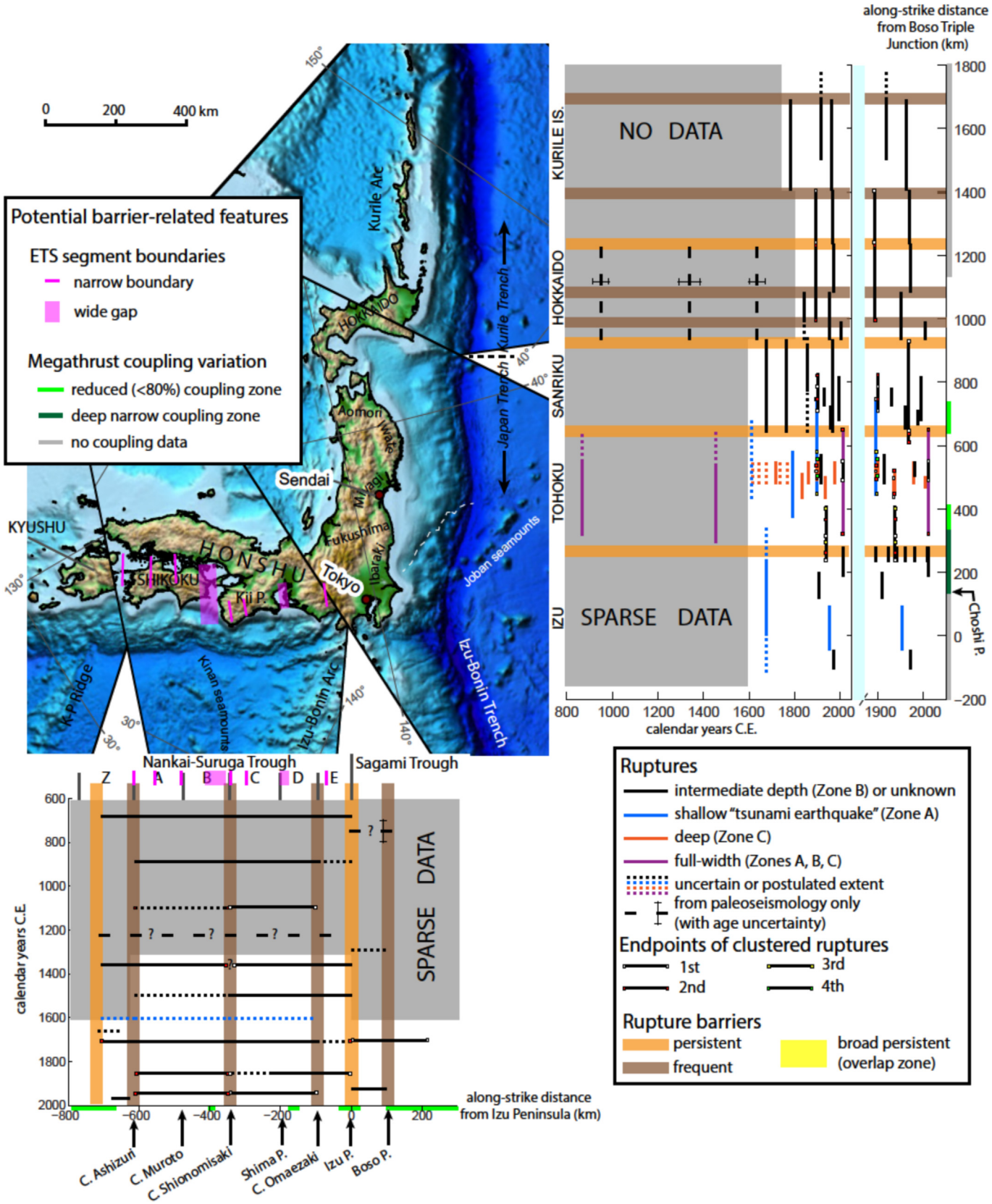

Fig. 5. Rupture history of the Japanese megathrust faults in space and time, from historical and geological records (sources in supplementary Tables S3–S4). A version of this figure with year labels for each earthquake rupture is given in Figure S3. Gray areas had intermittent to absent historical record keeping; dashed rupture lines are based on geologic data alone during periods with few historical documents. Question mark in the middle of the 1361 Nankai rupture indicates debate as to whether it was a single event or separate A-B and C-D ruptures a few days apart. Along the Nankai-Suruga Trough, the commonly defined segments are shown with capital letters; these are also sometimes named Hyuga-nada (Z), Nankai (A–B), Tonankai (C–D), and Tokai (E). Nankai Trough ETS segment boundaries (magenta marks) are from Obara (2010). Locations of capes and peninsulas potentially associated with segmentation are indicated with black arrows. Coupling model (green bars along distance axes) from Loveless and Meade (2016) did not extend south of the Choshi Peninsula or north of Hokkaido (gray bars indicate lack of data). For the Japan-Kurile trench, an expanded view of the last century (including M 7–7.5 events) is shown at right. Dashed white line on map shows potential offshore extension of Median Tectonic Line from Bassett et al. (2016). K-P abbreviates Kyushu-Palau.

rupture below the Izu Peninsula is further supported by the historical earthquake record, during which both the northernmost (Tokai) portion of the Nankai megathrust and the western (Kanto) portion of the Sagami megathrust have ruptured numerous times, but never simultaneously.

2.3.1. Nankai-Sagami Trough observations

The Nankai Trough is one of the first places where rupture segmentation and variable rupture modes became apparent, beginning with a now-classic paper by Ando (1975). He originally divided the megathrust into four segments (A, B, C, D) based on characteristics of historical earthquakes, though the division between A and B was based on a modeled transition in earthquake source parameters—there is actually no evidence that segments A or B have ever ruptured individually. Numerous researchers have since refined the Nankai Trough rupture history through historical and paleoseismic studies. In a recent review, Garrett et al. (2016) compiled (from both English and Japanese language literature) all the historical and paleoseismic evidence for past Nankai Trough earthquakes, updating the analysis by adding a segment Z to the southwest and dividing the original segment D into smaller D and E components. Based on their compilation, it is likely that in addition to the Izu Peninsula, another persistent barrier exists offshore Kyushu in their segment Z. Between Kyushu and the Izu Peninsula, the entire Nankai Trough can be considered a master segment and is known to have ruptured from end to end in 1707 as well as in earlier historical events (Fig. 5). Within this segment there are three frequent barriers, located at the Z/A, B/C, and D/E boundaries. Subsequent studies (Fujiwara et al., 2020; Garrett et al., 2018; Kitamura et al., 2018) have largely supported the chronology of Garrett et al. (2016); the primary difference is that some researchers espouse an interpretation that the 1854 Tokai rupture did not extend west to the C asperity (Seno, 2012). For the purposes of earthquake cycle studies, it may not be meaningful to define either of the segment pairs A-B or C-D as two separate asperities, since other than the alternate interpretation of 1854 there are no historical examples of rupture limits on the A/B or C/D boundaries. All 14 historical earthquakes are consistent with various combinations of four asperities: Z (Hyuga-nada), A-B (Nankai, not to be confused with the entire Nankai Trough), C-D (Tonankai), and E (Tokai).

Historical records for the Sagami Trough region are less extensive than for Nankai, with reliable reports remaining sparse until Edo (ancestral Tokyo) became a Shogunate capital in 1603 (Shimazaki et al., 2011). Megathrust earthquake RIs are also apparently longer than along the Nankai Trough, which further reduces the number of well-known events (Fig. 5). Only two historical megathrust events are well-documented: the 1923 Taisho-era Kanto-region earthquake that devastated Tokyo and its port of Yokohama, and the 1703 Genroku-era earthquake that is thought to have ruptured essentially the entire Sagami Trough (making it a single master segment). There is a general consensus that a historical earthquake in 1293 was probably also a Taisho-type event, but other correlations between earthquake reports and paleoseismic data are uncertain (Satake, 2015; Shimazaki et al., 2011; Shishikura, 2014). Analysis of marine terraces and paleotsunami deposits suggest that there is probably a frequent barrier in the vicinity of the Boso Peninsula, defining the east boundary of the asperity that ruptured individually in 1923, and that Taisho-type events are significantly more frequent than Genroku-type events (Shishikura, 2014). However, there is some debate about the precise relationship between megathrust rupture, long-term uplift, and terrace formation in this area (e.g., Sato et al., 2016), and it is therefore difficult to deduce exact rupture extent and timing from terrace extent. Also, higher-resolution topographic data have revealed additional, less-studied intermediate terraces (Komori et al., 2017; Shishikura, 2014) that might be linked to ruptures of other types (i.e. not matching Taisho- or Genroku-type). Therefore, there may be additional frequent barriers and/or ephemeral barriers along the Sagami Trough, but the geologic record of past ruptures is too imprecise to illuminate them clearly.

2.3.2. Japan-Kurile Trench observations

Along the east-facing coast of Honshu, likely complete historical records of subduction earthquakes extend about 400 years into the past, with more sporadic accounts for the preceding millennium (e.g., Satake, 2015). However, most historical Japan Trench subduction earthquakes prior to 1896 (and several since) have had little treatment outside Japanese-language publications, presenting a challenge for the authors of this review. It is clear from the 20th-century record that the Japan Trench has numerous small asperities that can rupture individually in relatively moderate (M_w 7–7.5) earthquakes (Yamanaka and Kikuchi, 2004). Prior to the giant 2011 Tohoku earthquake, several asperities with repeating historical ruptures had been identified: a pair off the Sanriku coast (Iwate and Aomori prefectures) which can rupture either together or separately, with M ~8 two-asperity ruptures occurring about every 100 years (most recently in 1968); a smaller asperity off Miyagi with M ~7.5 ruptures every ~40 years, and a very small asperity off Ibaraki that has produced M ~7 earthquakes every ~20 years during the 20th century (Earthquake Research Committee, 2011; Mochizuki et al., 2008; Satake, 2015). (Note: while the 1968 event is commonly known as a "Tokachi-oki" earthquake, the rupture area was actually not adjacent to the Tokachi region but located off the Sanriku coast.) Other regions of the megathrust were considered less predictable, such as the area off Fukushima which had a cluster of ruptures in 1938 but no other known major ruptures, and another small asperity between the Miyagi-oki asperity and the trench which ruptured in 1915, 1981, and 2011 (Abe, 1977; Earthquake Research Committee, 2011; Hatori, 1976; Kubota et al., 2017; Satake, 2015). Historical tsunami earthquakes had also occurred along most of the shallow subduction interface of the Japan Trench (Earthquake Research Committee, 2011; Hatori, 1975a, b, 1987; Yanagisawa et al., 2016).

Based on the historical record alone each of these megathrust regions would have been considered separate master segments, but geological observations of vast tsunami deposits hinted that larger events linking several of these asperities had occurred in the more distant past (Minoura et al., 2001; Sawai et al., 2007, 2008a; b). These suspicions were confirmed with the occurrence of the 2011 event, tragically before the new geologic knowledge had been incorporated into tsunami hazard education and planning. One might still consider there to be a potential persistent barrier separating the Sanriku asperities (roughly the 1968 rupture area) from the Tohoku asperities (roughly the 2011 rupture area) and perhaps another at the south end of the 2011 rupture (the frequent M ~7 Ibaraki-oki earthquakes might be associated with this latter barrier). Additionally, no known ruptures have traversed the "corner" that separates the Japan Trench from the Kurile Trench off Hokkaido. These potential barriers outline the Tohoku(-oki) and Sanriku(-oki) master segments (Fig. 5). However, this segmentation may not extend to the shallow domain of the megathrust; an 1896 tsunami earthquake (Tanioka and Satake, 1996) appears to have traversed the Tohoku/Sanriku barrier. Regardless, within these segments, it is perhaps more meaningful to define and discuss "frequent asperities" as has been done in the past rather than frequent barriers, especially given that there are clearly separations between asperities along dip as well as along strike. South of the Tohoku segment, the Izu section of the subduction zone seems to have less frequent earthquakes in general, with no two rupture areas alike during the last 400 years (Fig. 5). Thus, it is difficult to

identify any rupture patterns there.

Along the Kurile Trench, the historical period is significantly shorter, with no written records from the Hokkaido coast before the year 1800 (e.g., Satake, 2015). There is an extensive record of 19th- and 20th-century earthquakes, including several large to great intraslab events (Earthquake Research Committee, 2004; Satake, 2015; Takahashi and Hirata, 2003) which we do not include in this analysis. The entire Kurile–Hokkaido margin ruptured in a ~20-year cascade of M_w 8+ earthquakes during the mid-20th century, with a previous more temporally distributed series having occurred in the 19th century (Fig. 5). Ruptures had similar (though perhaps not identical) extents in both historical cascades, leading to division of segments and alphabetical labeling similar to the Nankai Trough (Fukao and Furumoto, 1979). However, as was later discovered for the Japan Trench, extensive tsunami deposits along the Hokkaido coast indicate that much larger events, most likely joining several asperities along strike, occurred in prehistoric times (Hirata et al., 2009; Nanayama et al., 2003, 2007; Satake et al., 2008; Sawai et al., 2009). As these events are known only from geologic data, the exact rupture extent is uncertain, but the master segment likely extends at least along the full length of Hokkaido. Within this segment, it appears there are at least three along-strike asperities (named southwest to northeast Tokachi-oki, Akkeshi-oki, and Nemuro-oki by Hirata et al., 2009), which ruptured either individually or in pairs during each of the historical events. The divisions between these asperities can be considered frequent barriers. Common boundaries of historical ruptures off the Kurile Islands to the northeast are likewise at least frequent barriers, but it is uncertain whether longer ruptures can occur there as well. We label this the "Kurile Islands" segment but it may be composed of more than one master segment.

As a whole, in comparison to the Nankai Trough, the Japan-Kurile Trench has a less extensive historical earthquake record, more heterogeneous distribution of asperities (along both strike and dip), and longer RIs between large multi-asperity ruptures, all of which make its behavior more difficult to characterize. Therefore, while we propose a master segment and asperity structure which is consistent with the available data, we are necessarily less confident in this interpretation than for our assessment of the Nankai Trough.

2.3.3. Segmentation mechanisms in Japan

In comparison to South America, there is a relative dearth of subducting plate features in Japan that could be associated with barriers (Fig. 5), though some connections between the two may still be inferred. The most prominent subducting feature on the Philippine Sea plate is the Izu-Bonin volcanic arc, the crest of which is clearly associated with the Izu Peninsula persistent barrier. The arc is such a broad bathymetric feature that its edges could additionally be associated with the D/E frequent barrier on the southwest and the Boso Peninsula frequent barrier on the northeast. Farther southwest, the Kyushu-Palau Ridge subducts in the vicinity of the potential persistent barrier within segment Z, and a causative relationship was suggested by Yamamoto et al. (2013). As is the case for several other persistent barriers we have identified, M_w ~7 earthquakes are common in the vicinity of the subducting ridge, with seven having occurred since 1899 (Nakata et al., 2012; Yamashita et al., 2012).

Along the Nankai Trough between the Kyushu-Palau ridge and the Izu-Bonin volcanic arc, the subducting plate is relatively smooth except for the Kinan seamount chain. However, the latter does not line up with any of the persistent or frequent barriers: the most recently subducted seamount is located below the B segment and is arguably forming an asperity rather than a barrier (Cummins et al., 2002). While the Z/A and B/C frequent barriers do not seem to be associated with subducting relief, they could still be related to discontinuities in the Philippine Sea Plate that form during subduction: in fact, a likely tear in the subducting slab lies beneath the B/C barrier (Cummins et al., 2002). Kodaira et al. (2006) further suggest that a plutonic body intruded into the upper plate and accretionary wedge may contribute to the B/C barrier by increasing normal stress, inhibiting rupture propagation. Both upper and lower plate heterogeneities are also associated with the Z/A boundary: there is a marked transition in slab curvature, as well as a low velocity zone in the upper plate, potentially indicating different rheology or fluid content (Yamamoto et al., 2014). However, the B/C boundary area is associated with a high velocity zone, illustrating that the relationship between seismic velocity structure and rupture barriers is not simple (Yamamoto et al., 2017). Numerous modeling studies have attempted to reproduce the Z/A and B/C frequent barriers and the ensuing rupture patterns (e.g., Hok et al., 2011; Hori, 2006; Hyodo et al., 2016; Nakata et al., 2012).

The Joban seamount chain is the only notable bathymetric feature that subducts along the Japan Trench. It is indeed associated with a likely persistent barrier off Ibaraki, where it has been posited that seamount subduction inhibits megathrust rupture. The source area of the frequent M ~7 earthquakes appears to be confined by the incoming flank of a subducting seamount and by the disruption in the accretionary prism left by previously subducted seamounts (Mochizuki et al., 2008). The M_w7.9 aftershock that occurred half an hour after the giant Tohoku earthquake also seems to have been bounded by the seamount in this area (Kubo et al., 2013). Another feature potentially related to this segment boundary is a transition in bathymetry and gravity data interpreted as an offshore continuation of the Median Tectonic Line (Bassett et al., 2016). This feature cuts diagonally northeast across the forearc from the Ibaraki region to the trench (Fig. 5), with most of the known historical earthquake rupture areas limited to the northwest side of the line.

Regarding upper plate features, along the Nankai Trough, uplifting peninsulas (Fujiwara et al., 2010; Matsu'ura, 2015; Okuno et al., 2014; Ota and Omura, 1991) coincide with each of the divisions between lettered asperities (Fig. 5), though only a subset of these have historically acted as rupture barriers. The most pronounced uplift is on Cape Muroto (Matsu'ura, 2015), aligned with the A/B boundary which does not seem to be a barrier. Along the Sagami Trough, the proposed frequent barrier beneath the Boso Peninsula is indeed associated with upper plate deformation, as evidenced by the aforementioned flights of terraces that are assumed to be coseismically generated (Shishikura, 2014). Along the Japan-Kurile trench, the coastline is generally too far from the trench to expect much barrier-related uplift there. The Choshi Peninsula is the only exception, and it does not obviously correlate with a barrier. All things considered, the relationship between uplifting peninsulas and rupture barriers is not as clear-cut in Japan as it appears to be along the South American margin.

The distribution of interseismic coupling on the Japanese subduction interfaces has fluctuated significantly during the instrumental era due to the numerous subduction earthquakes that have occurred (most recently summarized by Loveless and Meade, 2016). Nevertheless, there is some correlation between persistent barriers we identify and zones with consistently low to moderate coupling identified by Loveless and Meade (2016; green bars in Fig. 5). Correlations between coupling variations and frequent barriers are generally less apparent, except along the Sagami Trough: the western (Kanto) asperity has been more strongly and consistently coupled than the (unnamed) asperity east of the Boso Peninsula, with the eastern asperity producing significant slow-slip events (Loveless and Meade, 2016; Ozawa et al., 2007). This lower rate of strain accumulation along the eastern Sagami Trough may underlie the very long RI for full-Sagami (Genroku-type) ruptures (see

section 3.3.1).

Along the Nankai Trough, an intriguing comparison can be made between segmentation in seismic rupture and in the episodic tremor and slip (ETS) that have been well documented by GPS and seismic networks in the recent instrumental period (Obara, 2010). Akin to the more widely known ETS in Cascadia (discussed in section 2.4), these Nankai ETS events occur over days to weeks along the transition zone between the coupled and freely slipping depths of the megathrust interface. As with seismic ruptures, along-strike boundaries and gaps (indicated by magenta lines and bars on Fig. 5) can be identified between different "families" of ETS events. A large gap and shift in ETS position corresponds to the potential slab tear linked to the B/C frequent barrier. Many of the other boundaries between ETS families also appear to align with lettered asperity boundaries, including the A/B and C/D boundaries (which have not historically served as rupture endpoints). Some additional ETS boundaries lie within lettered asperities, so while there is evidence that rupture and ETS segmentation may be linked, not all of the boundaries that exist in the transition zone necessarily extend into the seismogenic zone.

2.4. Cascadia

Although the Cascadia megathrust lacks a local historical record, there is excellent geological and remote historical evidence that the most recent rupture (in 1700) stretched the full length of the margin from Cape Mendocino in California to northern Vancouver island (Atwater et al., 2005; Goldfinger et al., 2012, 2017; Hutchinson and Clague, 2017). Therefore, the entire Cascadia megathrust can be considered a single master segment. To go further, interpretations must necessarily be primarily based on the offshore turbidite record—evaluation of potential frequent barriers within the master segment cannot be done based on terrestrial data alone, because the temporal and spatial resolution of those data are too low. As previously noted in section 1.2, there is significant debate regarding the accuracy of the interpretation of the turbidite record, and it is beyond the scope of this review to examine the intricacies of Cascadia turbidites. However, it is a worthwhile exercise to evaluate the implications of the turbidite-based paleoseismic record, making the assumption that it is accurate.

Based on the Holocene-spanning history of turbidite deposition along the Cascadia margin, Goldfinger et al. (2012, 2017) have identified "families" of ruptures that suggest at least four frequent barriers within the master segment, dividing the margin into five asperities (Fig. 6, left). In this case, dotted lines represent ruptures inferred to extend into regions where data are more limited or where conflicts have arisen between interpretations of offshore and coastal data. Goldfinger et al. (2013b, 2017) also note a few very spatially limited mud turbidites within the southernmost asperity that could suggest a further subdivision. However, thinner, less spatially extensive turbidites potentially have non-seismic origins and even if seismic are likely $M < 7.5$ events that are less confidently attributed to the megathrust: in that southernmost part of Cascadia, $M > 7$ strike-slip earthquakes within the deforming Gorda block are a frequent occurrence (e.g., Rollins and Stein, 2010). Terrestrial paleoseismic records along the coast of Cascadia, which extend up to 6500 years, are at least roughly consistent with the turbidite-based history (e.g., Leonard et al., 2010), though some conflicts have arisen (e.g., Atwater and Griggs, 2012; Hutchinson and Clague, 2017). Along-strike variations in coastal subsidence during the 1700 event are consistent with slip divided into four asperities, roughly coincident with those defined based on turbidite extent (Kemp et al., 2018; Wang et al., 2013). Subsidence distributions during past ruptures are generally too poorly constrained to determine whether this asperity pattern has persisted over many earthquake cycles, but the available data suggest that past distributions have not been wildly different (Milker et al., 2016). However, it should be noted that coseismic subsidence measurements in Cascadia have large uncertainties so they generally do not provide strong constraints on asperity distribution.

As with the Nankai case, in Cascadia it is interesting to compare segmentation in seismic rupture and in ETS. Brudzinski and Allen (2007) first noted that ETS RIs were divided into three broad groups roughly corresponding to different terranes in the overriding North American Plate, and further proposed additional segment boundaries between recurring families of events. These segment boundaries were later refined based on more recent, more precise data, for a total of eight ETS "asperities" (Boyarko et al., 2015), and the observed patterns continue to persist for successive ETS events (Fig. 6, right). When slow slip propagates into barrier regions, tremor generation and slip speed may be reduced (Wech and Bartlow, 2014). Three of the four frequent rupture barriers (Cape Blanco, Yaquina Bay, and Astoria) potentially align with ETS barriers, but there is a significant offset between the Quillayute rupture barrier and the Johns River ETS barrier. The southernmost ETS barrier does align with the additional rupture barrier at the California/Oregon border suggested by Goldfinger et al. (2017), and the detailed rupture history along Vancouver Island is not sufficiently well constrained to assess whether the two northernmost ETS barriers might also correspond with seismic rupture barriers. Boyarko et al. (2015) note that there appears to be some correspondence between ETS/rupture segmentation and sedimentary basins/gravity anomalies in the forearc identified by Wells et al. (2003) (hypothesized to correspond to megathrust asperities). Li and Liu (2017) reproduced similar ETS behavior in a model system, finding that segmentation is dominantly controlled by variation in ETS zone width along strike and that RI is strongly influenced by spatially varying effective normal stress.

There is essentially no large-scale subducting seafloor relief that might be producing rupture or ETS barriers in Cascadia. While the Juan de Fuca plate and slab has numerous northeast-trending age discontinuities produced by propagating transform faults throughout the complex spreading history of the Juan de Fuca Ridge (Wilson, 2002), relief associated with these structures has been completely drowned by the vast amount of sediment shedding off the coastline. It is nevertheless possible that these buried structures contribute to rupture/ETS segmentation, but co-location with barriers is difficult to evaluate because these plate discontinuities are so oblique to the strike of the subduction zone. The active plate discontinuities, i.e., the Blanco fracture zone and Nootka fault that separate the main Juan de Fuca plate from the remnant Gorda and Explorer deforming zones, are perhaps the most likely to induce rupture segmentation. Indeed, the Blanco fracture zone subducts in the vicinity of the Cape Blanco ETS/rupture barrier, and the Nootka fault potentially corresponds to the northernmost ETS barrier. In addition to linear discontinuities, individual subducted seamounts that appear to affect the upper plate have also been identified based on geophysical surveys (Tréhu et al., 2012). Some of these seamounts may correspond to barrier zones, but the strength of the correlation cannot be evaluated without a more comprehensive search for subducted seamounts.

Overall the rupture segmentation in Cascadia seems more likely driven by variations in the overriding plate (e.g., the terrane boundaries) than in the subducting plate. Wells et al. (2017) noted that zones of low tremor density (which are the barriers) are associated with upper plate faults and hypothesized that fluid escape along these faults reduces stress on the megathrust interface. They also proposed that upper plate faults (some of which

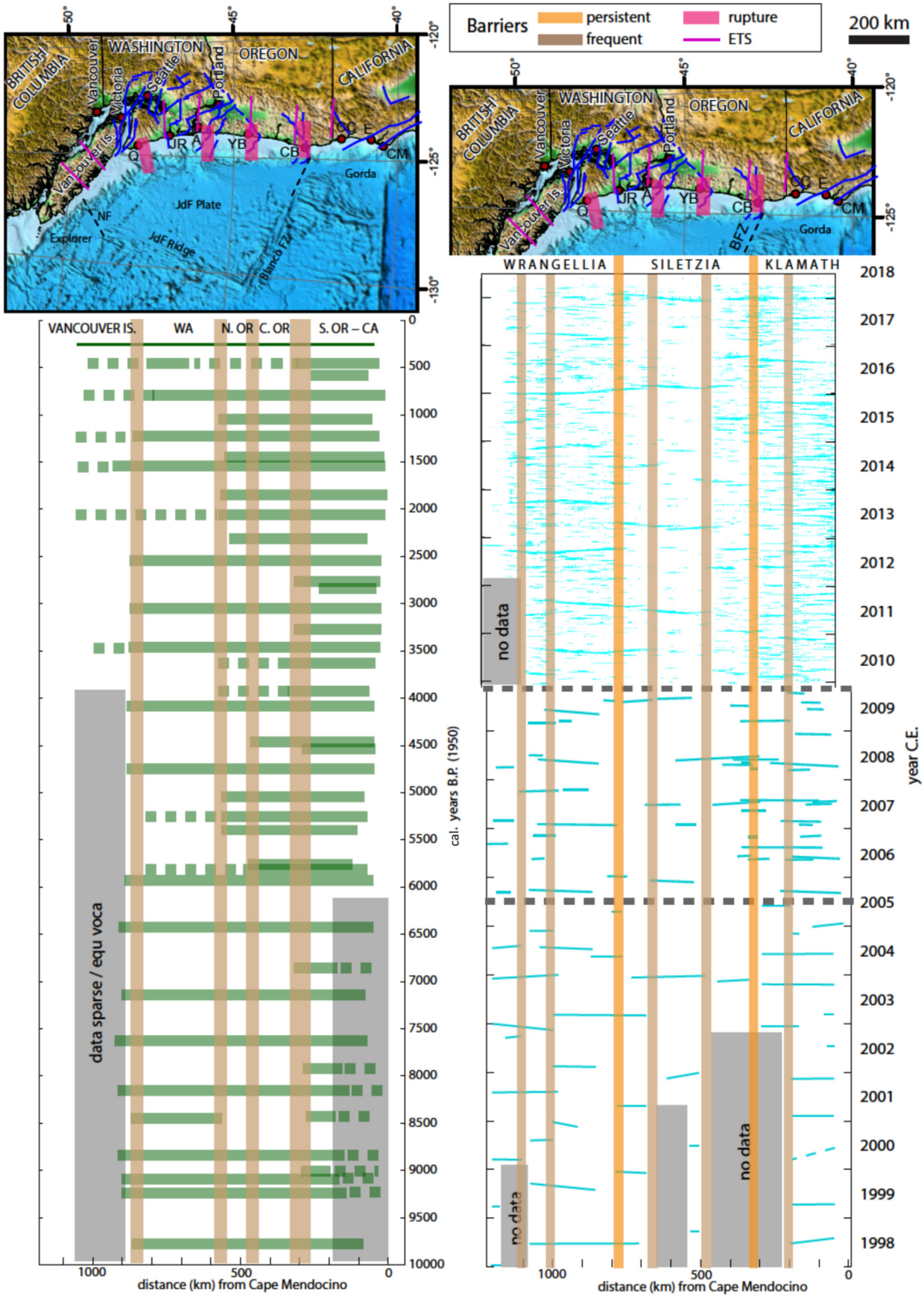

Fig. 6. Holocene rupture history interpreted from turbidite records (left, compiled from Goldfinger et al., 2012, 2017) and recent ETS history (right) of the Cascadia Megathrust. Except for the most recent (1700) event, line thickness illustrates the typical ~100-year age uncertainty for seismic ruptures; dotted lines indicate where ruptures are inferred to extend into regions where data are more limited or where conflicts have arisen between interpretations of offshore and coastal data. Heavy gray dashed lines on the right-hand plot indicate transitions between progressively more precise and complete data sources: 1998–2005 (Brudzinski and Allen, 2007); 2005–2009 (Boyarko et al., 2015); 2010–2018 (https://pnsn.org/tremor, Wech, 2010). Barriers are shown by vertical brown and orange lines in the rupture history plots and by pink lines on the maps, broad for rupture barriers and thin for ETS barriers. (Both types are shown on both maps for comparison.) Frequent rupture barriers divide the single master segment into five asperities which we name for the adjacent onshore regions, while the ETS events can be broken into three zones based on recurrence interval that correspond to major terranes in the overriding plate. Barriers potentially correspond to upper plate faults (blue lines, from Wells et al., 2017). Q: Quillayute, JR: Johns River, A: Astoria, YB: Yaquina Bay, CB: Cape Blanco, CC: Crescent City, E: Eureka, CM: Cape Mendocino, WA: Washington, N./C./S. OR: Northern/Central/Southern Oregon, CA: California, NF: Nootka fault, JdF: Juan de Fuca, BFZ: Blanco Fracture Zone.

extend offshore above the seismogenic zone) might similarly produce barriers to seismic rupture propagation. Zones of rapid long-term coastal uplift associated with these faults (Kelsey and Bockheim, 1994; Kelsey et al., 1996) coincide with frequent barriers at Yaquina Bay, Cape Blanco, and potentially the CA/OR border. The distribution of interseismic coupling is very poorly constrained in Cascadia since the assumed seismogenic zone lies almost entirely offshore, and there have been few seafloor geodesy measurements (Wang and Tréhu, 2016). Therefore, it is not possible to evaluate a correlation between along-strike coupling variations and proposed barrier locations.

2.5. Other subduction zones

While their established rupture chronologies are too short to serve as primary examples, some relevant observations have been made along the Middle America and Alaska-Aleutian subduction zones.

2.5.1. Middle America

While the historical record in Central America began at roughly the same time as in South America, the record of subduction earthquakes is not as complete, for several reasons. Kelleher et al. (1973) found that they could not assemble pre-1900 earthquake chronologies for the Middle American megathrust with the same confidence as they had for South America because settlement along the Pacific coast of Central America was persistently sparse, and remains so to this day. Even recent concerted efforts to expand the earthquake history based on local historical documents have failed to locate many records prior to 1800 (Castillo-Aja and Ramírez-Herrera, 2016). Additionally, the tendency of the Middle American megathrust to rupture in relatively moderate M_w ~7.5 events, with only a few exceeding M_w 8, means that megathrust ruptures were generally less likely to be remarked upon in historical records. Finally, based on historical records alone, it is more difficult to confidently assign a M_w ~7.5 event to the subduction interface, as opposed to intraslab or crustal faults in the overriding plate. In fact, the 2017 Chiapas earthquake, at M_w 8.2, was the largest ever instrumentally recorded in Mexico and generated a significant tsunami, yet was an intraslab event (Okuwaki and Yagi, 2017; Ramírez-Herrera et al., 2018). Based on historical records alone, it would be nearly impossible to determine whether such an earthquake occurred along the subduction interface or within the slab.

For these reasons, we do not attempt to compile an accurate long-term rupture chronology for the Middle American megathrust. Nevertheless, we can note some relevant features. It is clear that there are numerous barriers to rupture along the plate interface, dividing it into 20 or more distinct asperities with variable RIs (Astiz and Kanamori, 1984). It is less clear which of these barriers should be classified as persistent, as the 200-year historical record is likely not long enough to encompass potential rare multi-asperity ruptures. Indeed, the largest known historical event, which occurred offshore Oaxaca in 1787, likely encompassed several asperities that later ruptured individually during the 20th century (Suárez and Albini, 2009). The distribution of relief on the subducting plate is typical and does not seem especially rough, so there is no reason to expect the Middle American megathrust to be more segmented than others. The two most prominent subducting features, the Tehuantepec Ridge/Fracture Zone and the Cocos Ridge, are associated with zones of little or no $M > 7$ seismicity throughout recorded history, leading to the suggestion that these are persistent aseismic zones or barriers (Astiz and Kanamori, 1984).

2.5.2. Alaska-Aleutians

The Alaska-Aleutian subduction zone is an excellent example of the way recently observed ruptures are often initially assumed to indicate persistent segmentation. Nearly the entire margin ruptured in a series of great to giant earthquakes during the 20th century, and the boundaries between these events have been used to define segments (Nishenko and Jacob, 1990; Wesson et al., 2007). Based on the 20th-century record alone, six of these could be master segments. However, the historical record is only ~100 years long over most of the margin, which is much too short to evaluate the true persistence of the proposed segment boundaries, as most areas have had only one rupture during this period. Even some of the 20th-century rupture areas are uncertain, such as for the enigmatic 1946 tsunami earthquake (López and Okal, 2006). In the one region where historical records extend over 200 years (Kodiak Island), they describe a prior rupture (in 1788) that was clearly different in extent from those that occurred in the 20th century. In combination with geologic data, these records indicate the presence of additional frequent barriers and suggest that some of the barriers between 20th-century events may not be persistent (Briggs et al., 2014; Shennan et al., 2014). Geologic data also suggest that the 1964 M_w 9.2 earthquake may not be the largest possible event, due to the impermanence of another 20th-century barrier (Shennan et al., 2009).

Most analyses do support the persistence of one barrier, the Shumagin Gap, which like a number of other megathrust rupture barrier regions has hosted several M_w 7–7.5 earthquakes and is currently not accumulating much interseismic strain (Witter et al., 2014), but everything to the east could potentially be a single master segment composed of at least five individual asperities (Shennan et al., 2016). To the west of the Shumagin area, the Aleutian Islands portion of the megathrust is made up of no more than three master segments, delineated by extremely long $M_w > 8.5$ ruptures in 1957 and 1965 and a third un-ruptured section in the far west. However, since then, three smaller (M_w 7.5–8) earthquakes have occurred within the 1957 and 1965 rupture areas (Wesson et al., 2007), indicating that there are several individual asperities within the master segments that sometimes rupture independently.

Mueller et al. (2015) recently suggested updating the seismic hazard map for Alaska to reflect the more variable megathrust segmentation that these and other studies have revealed. Porto and Fitzenz (2016) offer an alternative segmentation model based on detecting along-strike changes in $M > 4$ earthquake activity rates, but there is no particular reason to expect the latter to be indicative of large earthquake boundary zones. Through future geologic studies and analysis of historical records, understanding of Alaska-Aleutian segmentation will continue to improve.

2.6. Non-subduction examples

Terrestrial faults are commonly structurally segmented, and it has generally been assumed that step-overs and major bends that divide segments inhibit through-going ruptures (e.g. Segall and Pollard, 1980). However, most of these segment boundaries are not persistent barriers to rupture, as many well-documented historical and recent fault ruptures have clearly involved multiple structurally defined segments. Analysis of well-documented historical ruptures suggests that larger step-overs are more likely to arrest rupture propagation, and beyond a certain gap width (perhaps 3–4 km for strike-slip faults and 7 km for normal faults) through-going rupture may become impossible (Wesnousky, 2006, 2008). Higher-angle bends are also more likely to arrest rupture (Biasi and Wesnousky, 2017). These analyses are consistent with

the hypothesis of a continuum of barrier persistence, in which moderate discontinuities would function as frequent barriers and large discontinuities as persistent barriers. However, since in general no more than one well-mapped rupture exists for any given section of fault, it is possible that many of the smaller step-overs that did arrest rupture do function as persistent barriers on those particular faults. Among the endpoints of well-mapped terrestrial fault ruptures, the only example that can be demonstrably excluded as a persistent barrier is the southern endpoint of the 1979 Imperial Fault rupture in southern California, as that segment boundary was previously traversed by the earlier 1940 rupture which involved the entire Imperial Fault (King and Thatcher, 1998).

Furthermore, about a third of the strike-slip rupture endpoints were not associated with any identifiable structural complexity (Wesnousky, 2006, 2008). It is unclear whether these endpoints are associated with less visibly obvious structural barriers (in which case they could be persistent or frequent barriers to rupture) or whether they have to do with stress state on the fault (in which case they would be ephemeral). The latter is probably more likely, but the fact remains that it is impossible to judge without observing repeat rupture of the same fault segment. Although repeat ruptures have been identified from historical and paleoseismic data, the endpoints are typically not sufficiently well constrained to judge whether any barriers are persistent. For example, the San Gorgonio Pass "structural knot" on the San Andreas Fault has been suggested as a possible persistent barrier (Yule, 2009 and references therein). However, with terrestrial paleoseismic data alone, it is very difficult to distinguish between a single through-going rupture that traverses the barrier and a pair of events that rupture on either side of the barrier within a short period. Conversely, while several regions of the world have historical records spanning a few thousand years (typically long enough to encompass multiple seismic cycles on primary faults of the region), these regions have historically been more sparsely populated than the Japanese and South American coasts, such that historical reports alone are often insufficient to precisely delineate rupture extent and thus test rupture barrier persistence.

The Dead Sea Fault (DSF) and the North Anatolian Fault (NAF) are approaching the point when there will be enough paleoseismic data (in conjunction with the historical data) to test barrier persistence, but as of yet there is too much uncertainty. Two recent companion reviews of the chronology of DSF ruptures, both combining paleoseismic/archaeological and historical data, produced space-time distributions that were similar overall but differed in terms of precise rupture extent (Agnon, 2014; Marco and Klinger, 2014). This is not surprising since most historical DSF events have so far been identified at only one paleoseismic site (at most), and assumptions are generally made based on subjective historical macroseismic reports. Nonetheless, where paleoseismic data do exist, familiar features can be identified, such as likely frequent barriers at minor fault discontinuities within the Wadi Araba between Aqaba and the Dead Sea (Klinger et al., 2015; Lefevre et al., 2018), and potential persistent barriers associated with major discontinuities: the large stepover bounding the Dead Sea (e.g., Lefevre et al., 2018) and the transition in the Jordan Gorge from a single fault strand to multiple splays to the north in Lebanon (Wechsler et al., 2018). In the latter case, the authors describe the 20-km-long Jordan Gorge section of the DSF as a "weak segment" which has ruptured along with neighboring segments to the north or south, as well as producing its own more moderate events. This behavior bears a striking similarity to that of barrier zones on megathrust faults, detailed above.

On the North Anatolian Fault, authors of a recent review (Fraser et al., 2010) acknowledge that even historical records in that region are often insufficiently temporally precise to assess segmentation of past ruptures: reports of destruction of multiple villages by different earthquakes might be lumped into a single historical earthquake if they occurred in the same year. In the case of a rupture cascade, to which the NAF is prone, day-level or even hour-level precision is sometimes required to distinguish individual earthquakes. Nevertheless, a combination of historical and paleoseismic data allows many events to be identified at multiple sites, enabling a more rigorous review. The compilation by Fraser et al. (2010), which extends thousands of years, suggests likely persistent barriers associated with the two largest fault step-overs near Bolu and Niksar, dividing the fault into western, central, and eastern segments. The persistence of other barriers is less certain. During the 20th-century cascade (which has reasonably well documented ruptures), though rupture on parallel fault segments did overlap when projected across strike, there was at most a few km of re-rupture of any part of the fault (Barka, 1996; Hartleb et al., 2002). An upcoming reanalysis of paleoseismic and historical earthquake dates raises the possibility that some or all of the ~10 asperities defined by various 20th-century ruptures may be persistent features (Rockwell and Biasi, 2017), separated by frequent or even persistent barriers. However, paleoseismic records do suggest an additional frequent barrier within the 1939 eastern segment rupture (Fraser et al., 2012).

Evidence of persistent rupture segmentation also exists for certain oceanic transform faults. Due to the hot, thin crust in the vicinity of spreading ridges, the seismogenic zones of oceanic transform faults are generally narrow and the interfaces are often poorly coupled (e.g., Bird et al., 2002), limiting most earthquakes below magnitude 7. However, the earthquakes' relatively small size results in shorter RIs, particularly on transforms with very fast slip rates. Given the remote location of oceanic transforms from both human and instrumental observers, location and analysis of earthquakes is generally only possible for magnitudes above ~5.5 and only since they have been observable by global seismometer networks (roughly the last 50–100 years, depending on magnitude). Despite these limitations, multiple seismic cycles have been observed on several oceanic transforms during this brief instrumental period, and these cycles often exhibit rupture segmentation. The neighboring Gofar and Discovery transforms on the East Pacific Rise are perhaps the most spectacular example, with at least 10 separate asperities identifiable by their distinct series of repeating ruptures (Froment et al., 2014; McGuire, 2008; Wolfson-Schwehr et al., 2014). These asperities are separated by barrier regions comparable in size to the repeating rupture regions, in which slip is accommodated through smaller earthquakes and likely aseismic creep. A few of these barriers correspond to visible geometric discontinuities, but others do not, leading to the hypothesis that this spatially variable slip behavior is dominantly linked to geology-driven variation in frictional properties (e.g., Froment et al., 2014; Wolfson-Schwehr et al., 2014). Though location precision varies and is generally poor for older events, similar persistent rupture segmentation is suggested by sequences of repeating earthquakes on the Blanco, Siqueiros, Eltanin, and Charlie-Gibbs transforms (Aderhold and Abercrombie, 2016; Boettcher and McGuire, 2009; Kuna et al., 2019; McGuire, 2008; Sykes and Ekström, 2012).

2.7. Summary of mechanisms, models, and observational proxies of rupture segmentation

As noted by Aki (1979), persistent and frequent rupture barriers must ultimately be related to geometric discontinuities or heterogeneity in fault frictional properties. Identifying these features or their proxies is critical both for understanding fault mechanics and

for earthquake hazard analysis (particularly in areas without a long earthquake chronology). Frictional properties connected to rupture segmentation generally cannot be directly observed. They can sometimes be inferred from fault rock rheology, temperature, and hydration conditions (e.g., Moore and Rymer, 2007). Holtkamp and Brudzinski (2014) identified an apparent correlation between earthquake swarms and rupture termination in subduction earthquakes and argued that swarms indicate frictional heterogeneity. On terrestrial faults, large discontinuities in the surface trace are readily observed and provide a first-order proxy for likely geometric barriers at depth in the seismogenic zone (Biasi and Wesnousky, 2017; Wesnousky, 2006, 2008), though how and why these discontinuities arise is usually unclear. In subduction environments, there are typically fewer obvious discontinuities in the surface trace. Observable surface features on the upper and lower plates may be causally linked to rupture barriers, though interpretations are less straightforward since the exact mechanism (friction or geometry) that halts rupture propagation is subject to debate, and upper plate features may be either the result or the cause of fault rupture behavior.

Kelleher and McCann (1976) first proposed (based on the distribution of historical earthquakes alone) that subducting bathymetric highs inhibited great megathrust earthquakes. Although many of the specifics of their hypothesis were contradicted by later ruptures, there is abundant evidence (detailed throughout section 2 above, and noted locally and globally by numerous authors) that features in the subducting plate influence rupture segmentation, particularly when they are associated with significant seafloor relief. As is the case for terrestrial faults, larger features are more likely to be associated with barriers and large-feature barriers are more likely to be persistent rather than merely frequent. Ridges, seamounts, and fracture zones all have the potential to act as barriers when they are subducted, although it is clear from our worldwide analysis that the relationship is not strictly one-to-one. Some examples of these features do not act as barriers and some barriers are not obviously associated with such structures; thus, it is important to avoid confirmation bias when proposing segmentation mechanisms. Statistical analyses do indicate that significant earthquakes (dominantly $M > 5$) are more likely to initiate near subducting features (Landgrebe and Müller, 2015). These observations are consistent with the idea that fault interface heterogeneity creates a patchwork of small asperities which generate frequent earthquakes, but inhibit the propagation of larger ruptures. As suggested by Bassett and Watts (2015a), broader subducting features such as aseismic ridges may form individual asperities large enough to produce M ~7 earthquakes, consistent with common observations of more moderate-magnitude events within barrier zones. Analogous large barrier zones may similarly produce more moderate earthquakes on terrestrial faults.

It should be noted that while subducting features (especially those associated with significant relief) would clearly introduce geometric discontinuity to the fault interface, it has also been suggested that they would halt rupture through the mechanism of frictional heterogeneity, or even form asperities rather than barriers. In addition to halting rupture through geometric discontinuity, debated possibilities include frictionally strengthening the interface so it cannot break and frictionally weakening the interface so it cannot accumulate strain. In a thorough discussion of this issue, Wang and Bilek (2014) note that many previous models focused solely on frictional heterogeneity and erroneously ignored the structural effects. They argue that geometric discontinuity is the dominant factor, ultimately leading to weakening and fault creep. Analysis of the 2015 Gorkha (Nepal) earthquake indicates that the rupture was limited on all sides by structural ramps (Hubbard et al., 2016; Qiu et al., 2016), supporting the idea that geometric discontinuity alone is sufficient (though perhaps not strictly necessary) to produce a rupture barrier. A further possibility is that dewatering of fracture zones increases the pore fluid pressure, promoting interseismic creep; this was suggested by Tilmann et al. (2010) and Meltzner et al. (2012) for Simeulue and the Batu Islands as well as by Moreno et al. (2014) for the Mocha FZ, among others. More generally, the presence of fluids along the subduction interface likely inhibits the propagation of large seismic ruptures by reducing the effective normal stress, allowing creep to prevent the buildup of seismic slip potential; see Bilek and Lay (2018) for additional review of this effect and other factors influencing megathrust rupture segmentation.

As discussed throughout section 2, there is also significant evidence that concentrated upper plate deformation is linked to megathrust barrier regions, either as the product (as is likely in South America) or the cause (as is possible in Cascadia) of megathrust fault behavior. Upper plate structures have the potential to influence rupture segmentation through the same set of mechanisms as lower plate structures (e.g. geometric discontinuity, change in frictional properties, fluid flow), but the relationships are more challenging to study since the relevant features are less easily identifiable than the prominent, typically linear subducting features. Most upper plate studies have been local or regional since each study site typically involves analysis of a large amount of geologic data. A few global analyses have been done comparing the slip distributions of major 20th-century subduction earthquakes to gravity and bathymetric anomalies in the upper plate. Song and Simons (2003) argued that forearc gravity lows are controlled by long-term shear traction while Wells et al. (2003) hypothesized that forearc bathymetric basins indicate subduction erosion. Thus, both basins and gravity lows can be interpreted as the result of persistent strongly-coupled asperities on the megathrust interface below. The asperities identified in both studies are largely consistent with our catalog, but it was clear even from the more limited set of ruptures they considered that not all fault asperities correspond to distinct basins, that some neighboring basin-defined asperities might rarely or never rupture independently of each other, and that boundaries between basins (basement highs) do not necessarily correspond to barriers (and for those that do, there is no clear indicator of whether the barrier is persistent or merely frequent). More recently, Bassett and Watts (2015a, b) produced gravity-anomaly-based global maps of both subducting plate features and forearc structure, noting many examples where subducting features and along-strike forearc discontinuities correspond with apparent rupture barriers, though again they found the relationship was not one-to-one. Many of these correlations were noted by earlier studies and are discussed above, though a more comprehensive comparison between our catalog of barriers and their maps may be warranted in the future. In summary, subducting relief and along-strike forearc discontinuities are both reasonable (though imperfect) proxies for rupture barriers, with larger features more likely to indicate persistent barriers.

The distribution of interseismic coupling, as determined from the few available decades of instrumental geodesy, is also commonly used as a proxy to identify asperities (locked regions) and barriers (creeping regions). In addition to areas of steady interseismic creep, areas with transient slow slip events are now being recognized for their reduced strain accumulation and seismic potential (e.g., Rolandone et al., 2018). Many of the barriers we identify do indeed show reduced strain accumulation according to recent geodesy. However, as observed in the Sumatran case, the strain accumulation rate may not be steady over the entire interseismic period and the recent instrumentally recorded period may or may not be representative of long-term trends. Thus, recent interseismic coupling must be considered in conjunction with long-

term earthquake chronologies and/or paleogeodesy and should never be the sole factor used to predict fault rupture segmentation.

Numerous researchers, beginning with Ruff and Kanamori (1980), have approached subduction earthquake size forecasting from the opposite direction: rather than studying rupture barriers, they have sought correlations between maximum earthquake size (M_{max}) and physical factors such as plate convergence rate, subducting plate age or buoyancy, dip angle, sediment thickness, and others. Such studies often have inappropriately coarse resolution, reducing subduction zones thousands of kilometers long to single data points, and many proposed correlations have since been contradicted by more recent earthquakes. A recent global analysis with higher spatial resolution found at best weak correlations between M_{max} and a wide variety of physical parameters, but the authors did identify a few factors, generally related to wide seismogenic zones, high normal stress, and low interface curvature, that seem to be requirements for M > 8.5 earthquakes (Schellart and Rawlinson, 2013). This is perhaps unsurprising since these characteristics essentially represent the absence of interface heterogeneities (which as discussed above, tend to inhibit rupture). Bletery et al. (2016) further explored the connection with interface curvature, hypothesizing that mega-ruptures require large areas with homogeneous shear strength (and thus little curvature). Also, Scholl et al. (2015) did find a significant correlation between great earthquakes and subducting sediment >1 km thick, after accounting for a bias that the majority of trenches have sediments <1 km thick. Schellart and Rawlinson (2013) did not make this correction and were also testing for a linear relationship between sediment thickness and magnitude, rather than testing for the effect of a threshold sediment thickness. An interface smoothing effect at >1 km sediment thickness is consistent with the independent finding that relief >1 km disrupts rupture propagation. Along similar lines, van Rijsingen et al. (2018) found that $M_W \geq 7.5$ megathrust earthquakes since 1900 preferentially initiated in areas of moderate seafloor roughness but that rupture areas (especially of the largest events) were preferentially located in areas of smooth seafloor.

In summary, there is significant evidence that wide, smooth, flat, homogenous subduction interfaces are conducive to forming asperities that rupture in great earthquakes. However, even these more comprehensive studies are difficult to relate directly to our analysis. This is partly because, as is typical, they rely heavily on the instrumental and recent historical records, ignoring older historical or paleoseismic evidence of rare larger ruptures. More importantly, despite the higher resolution, these studies tend not to illuminate individual barriers between neighboring asperities: for example, the entire South American subduction zone is found capable of great to giant earthquakes, despite the general scientific consensus that rupture in a single 6000-km-long event, ~5 times the length of the 1960 Valdivia rupture, is vanishingly unlikely. Even if a fault interface is generally wide and smooth, a single narrow discontinuity (perhaps not captured at the scale employed) may be enough to functionally limit rupture length. While the identification of seismogenic zone width and interface smoothness as controlling parameters on segmentation is consistent with the existing suite of observations on subduction zones, it would be ideal for a future study to investigate the specific correlation between these parameters and the locations of likely rupture barriers in our catalog.

A note of caution is necessary about attempts to define rupture segmentation based on the width of the seismogenic zone (SZ). Numerous researchers have attempted to define the extent of the SZ in various subduction zones worldwide, and in theory it is a worthwhile endeavor since the area of the SZ defines the seismogenic potential and locations where the width of the zone narrows may function as rupture barriers. However, like several other terms we discuss in this review, the "seismogenic zone" has been defined differently by various researchers (Wang and Tréhu, 2016). Our interest lies in the zone that ruptures in large to great earthquakes, which is correlated with (but is not necessarily identical to) the interseismically coupled zone and/or the mechanically velocity-weakening zone. The zone of instrumentally recorded small to moderate earthquakes (i.e. background seismicity) is potentially a very poor proxy for that of large to great earthquakes: for example, the Cascadia subduction zone currently has very little background seismicity but clearly ruptured in great earthquakes in the past. Therefore, "seismogenic zones" based on background seismicity are scarcely relevant to rupture segmentation, and even those based on interseismic coupling or inferred interface mechanics may have limited utility. As an illustrative example, Krabbenhoeft et al. (2010) map the "seismogenic zone" of the Sunda Megathrust based on geomorphology of the accretionary prism, validated by other geophysical data which are also merely potential proxies for the SZ. Their first-order interpretation of a wider SZ along Sumatra than along Java is credible, but none of the along-strike rupture barriers we note along the Sumatran margin are at all evident in their data, and the shallow region updip of their defined SZ is known to rupture during both tsunami earthquakes (e.g. 2010) and full-width events (e.g. 2004).

Finally, a common weakness of virtually all past studies of either M_{max} or segmentation mechanisms is that they exclusively examine correlations between fault features and the locations and endpoints of recent historical and instrumentally recorded earthquake ruptures. The latter dataset generally represents (at most) one rupture cycle and may or may not be representative of long-term patterns over many cycles. As noted by Corbi et al. (2017b), the short observational time period results in a bias toward the most frequent rupture mode (e.g., only those faults with very frequent large earthquakes will have their M_{max} accurately represented). We suggest that future such studies can be improved by focusing on the locations identified as persistent or frequent rupture barriers over many cycles.

Physics-based dynamic numerical models and analog models of earthquake rupture and recurrence over many earthquake cycles are able to reproduce persistent and frequent barriers and generally support our observation-based inferences. Kaneko et al. (2010), inspired in large part by the Sumatra example, modeled a barrier region as a velocity-strengthening patch and found that the persistency of the barrier depended on its size and frictional properties. They also noted that narrow barrier regions between asperities naturally lead to rupture cascades, since the rupture of one asperity easily increases stress on the neighboring asperity. These observations have been corroborated by analog models (Corbi et al., 2017a; Rosenau et al., 2019). Noda and Lapusta (2013) modeled barrier zones and the shallow megathrust domain as "conditionally stable" areas capable of both interseismic creep and coseismic rupture, reproducing the infrequent but occasional rupture of these regions in comparison to neighboring rate-weakening asperities. Numerical models (e.g., Tal and Hager, 2018), analog models (e.g., van Rijsingen et al., 2019), and laboratory rock experiments (e.g., Goebel et al., 2017) have all demonstrated that increasing fault roughness results in smaller, more frequent ruptures and eventually aseismic slip. Dynamic rupture models have supported the observation that larger fault stepovers and bends are more likely to serve as barriers to rupture (e.g., Lozos et al., 2011). Romanet et al. (2018) found that a fault stepover alone (with pure rate-weakening rheology on both fault segments) can induce diverse slip behavior including slow slip events, which would reinforce a geometric rupture barrier.

3. Cycles, supercycles, and clusters

We now move on to the review of earthquake recurrence patterns. As with segmentation, discussion of rupture recurrence and cyclicity also suffers from terminological confusion. Temporal clustering of earthquakes is a behavior that has often been proposed and debated, but it remains difficult to precisely define what qualifies as a cluster. In general, we identify clusters when the time intervals between two or more earthquakes (rupturing the same or nearby asperities) are significantly shorter than the typical recurrence interval on a given fault. However, rather than a sharp boundary, there is a continuum of decreasing confidence in our identification of a cluster as the intra-cluster time interval increases from less than 1% of the RI up to ~30% of the RI. If typical RIs are >100 years and the events occurred hours apart, few would argue it was a random coincidence, but if they occurred 25 years apart the significance of the clustering becomes more ambiguous. Depending on where clusters fall along this continuum, we describe them as "tightly," "moderately," or "weakly" clustered.

Related to clustering is the term "supercycle," originated by Grant and Sieh (1994) to describe the phenomenon in which "the cycle terminates in several events rather than just a single large earthquake." In that case, apparent clusters of paleoseismic events (separated by longer quiescent periods) at a single site on the San Andreas Fault were interpreted as successive ruptures of the same fault segment. The term did not catch on at the time and was next applied to the Mentawai case (Sieh et al., 2008). However, the Mentawai supercycles are crucially different than the proposed San Andreas behavior, in that each of the events in a Mentawai cluster are unique. While there is overlap, each event dominantly ruptures a different part of the fault plane. The term "supercycle" was subsequently applied to the 2011 Tohoku giant earthquake, yet the latter is a third, distinct case: multiple fault segments or asperities that more commonly rupture independently, in the Tohoku case ruptured together in a single rare, larger event. The Tohoku case had the additional wrinkle of involving large amounts of slip on the shallow domain of the megathrust interface, a region that had not ruptured recently and may have a much longer, semi-independent RI. In the wake of the Tohoku event, Goldfinger et al. (2013a) made the crucial point that long paleoseismic records are necessary to capture the full range of fault behavior, but swept together all four of these distinct phenomena (clustered similar ruptures, clustered complementary ruptures, rare multi-asperity linkage, and superimposed RIs of different lengths) under the blanket titular "Superquakes and Supercycles." Since then, the usage of the term has proliferated with numerous authors applying "supercycle" to any of the above phenomena on either megathrusts or terrestrial faults (many such papers are discussed elsewhere in this review).

Any given fault may exhibit several or all of these types of behavior, and they may well be interrelated, but it is worth being more precise with classification as these types have different implications for both seismic hazard and fault mechanics. As an example of the ongoing terminology confusion, Herrendörfer et al. (2015) defined a supercycle as "a long-term cluster of differently-sized megathrust earthquakes, leading up to the final complete failure of a subduction zone segment," which seems to describe an unspecified type of temporal clustering involving rare larger events. (However, since temporal clustering does not seem to be a required feature in their models—smaller events are distributed throughout their supercycle periods rather than concentrated at the end—-perhaps they meant "series" rather than "cluster.") Herrendörfer et al. then attempted to draw a connection between their definition of supercycle behavior and width of the megathrust seismogenic zone, pointing out that observations of megathrust supercycle behavior (in Sumatra, Japan, Chile, Ecuador, and Cascadia) appear to correlate with wide seismic zones and building numerical models to explore this connection further.

However, the six observation cases Herrendörfer et al. cites, all of which were termed "supercycles" in the papers they reference, represent several different types of behavior, none of which necessarily match the behavior produced by the Herrendörfer et al. model. The Mentawai segment of the Sumatran Sunda megathrust exhibits temporally clustered complementary ruptures but has no evidence for rare rupture of the entire segment. The cited studies of Hokkaido, Chile, and Ecuador report evidence for relatively rare large events that rupture multiple along-strike asperities (Chlieh et al., 2014; Cisternas et al., 2005; Métois et al., 2014; Nanayama et al., 2003); temporal clustering may also occur in these areas but was not part of the "supercycle" behavior described in those papers. Interpretation of the Cascadia turbidite record suggests several different "families" of earthquakes that involve rupture of different lengths of the margin (Goldfinger et al., 2012, 2017), but the longest "full-margin" ruptures appear to be the dominant mode, occurring more frequently than the other types, and the putative "clustering" is not strong (Cascadia is discussed in more detail below in section 3.4). Furthermore, the rare large events in all of these cases involve joining asperities along strike, whereas the Herrendörfer et al. model is based solely on varying frictional properties along dip and has no along-strike dimension. The 2011 Tohoku rupture, the most recent "superevent" on the Japan Trench, involved unusually large amounts of shallow slip, indicating depth-dependent behavior variability that could relate to the Herrendörfer et al. model, but even that case crucially involved multiple along-strike asperities in addition to the shallow megathrust domain. While the Herrendörfer et al. model can be evaluated on its own merits (see section 3.8), its ability to explain "supercycle" behavior on real subduction zones may be much more limited than the authors suggest. A more careful classification of the observed behavior might have led to a very different model of "supercycles," perhaps focusing on along-strike variability or exploring distinct mechanisms for each type of observed behavior.

We divide cycle behavior into four major classes (Fig. 7) that have distinct implications for seismic hazard and fault mechanics: 1) quasi-periodic similar ruptures, 2) clustered similar ruptures, 3) clustered complementary ruptures, and 4) superimposed cycles. Case (1) is the most easily understood, as the fault segment is likely homogenous, behaves as a single asperity, and is subject to a simple cycle of strain accumulation and release. It is likely that each event releases all the available potential energy in the system. Although it will not be possible to precisely predict when an earthquake will occur, the hazard will predictably increase as a function of the elapsed time since the last rupture. In case (2), clustered similar ruptures indicate periods of accelerated strain release, in which each earthquake releases only part of the available potential energy. The occurrence of one rupture actually increases the probability of a second rupture on that same fault segment, such that earthquake hazard will be high during a cluster period and low otherwise. Case (3), also called a rupture cascade, is analogous to case (1) in terms of energy implications except that strain is released in a series of earthquakes rather than a single event. Neighboring asperities may have similar RIs but are capable of independent rupture (separated from each other by persistent or frequent barriers). The occurrence of one earthquake decreases the hazard within its own rupture area but heightens it in neighboring areas. Other descriptive terms that have been used to indicate case (3) include "serial ruptures" (Atwater and Griggs, 2012) and

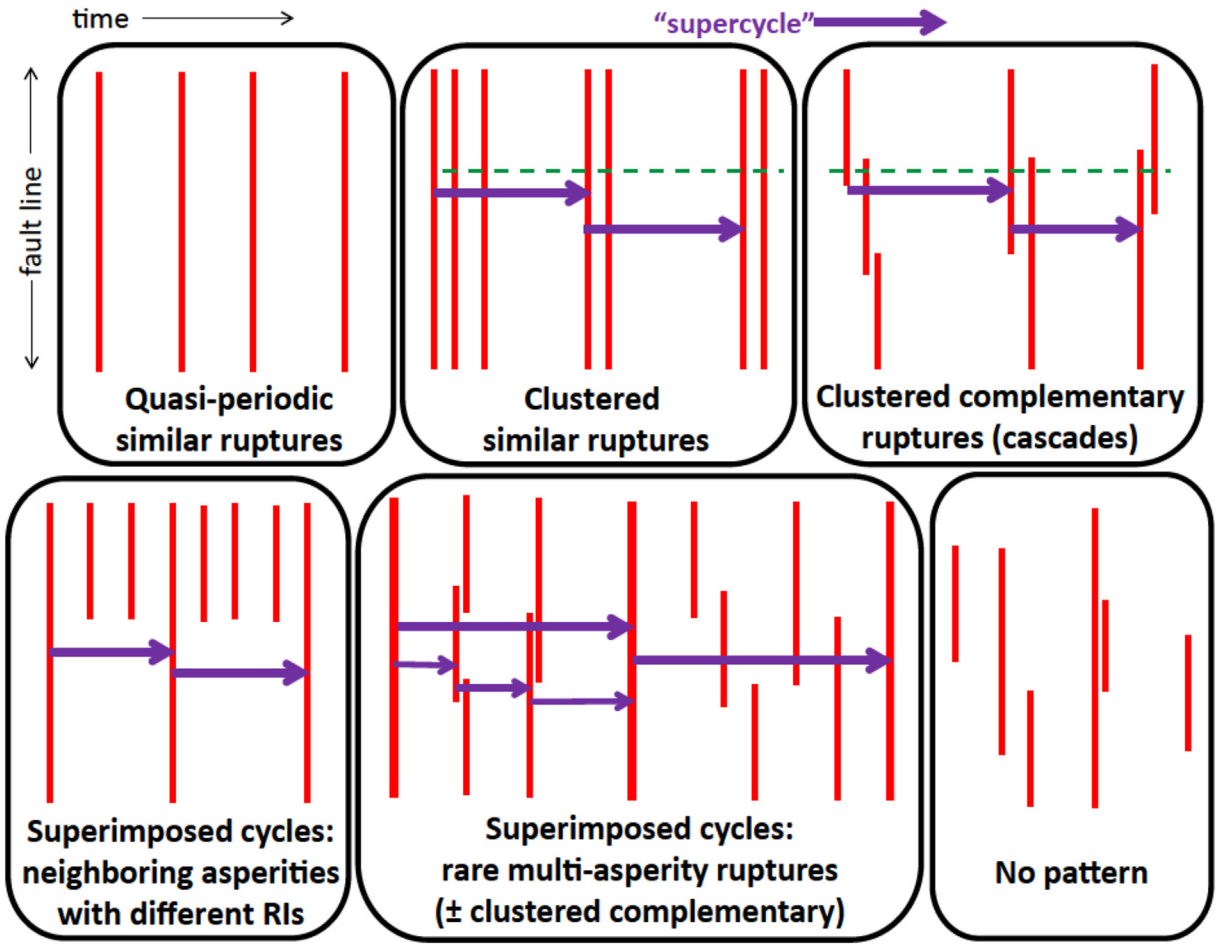

Fig. 7. Types of rupture recurrence patterns. Each pattern is defined by relative temporal and spatial scales and may be expressed over a wide variety of absolute scales: for example, earthquake clusters may span hours to centuries and the intervals between them may span decades to millennia, but a cluster is defined as a group of earthquakes occurring within a time span much shorter than the average RI for that section of fault. The term "supercycle" has been applied to several distinct cases (indicated by purple arrows) that have differing implications for fault mechanics and earthquake hazard. Superimposed cycles in the form of rare multi-asperity ruptures may have piecemeal rupture cascades nested within (one type of supercycle within another). Long earthquake chronologies at multiple sites are required to reveal these patterns: a single site, even with a long record, located at the green dashed line would fail to distinguish between clustered complementary and clustered similar ruptures.

"earthquake synchrony" across multiple faults or fault segments (Benedetti et al., 2013).

Superimposed cycles (case 4) occur when there are two or more families of events that involve the same fault, indicating that hazards in the region will depend on both cycles. This case involves two or more neighboring asperities with different RIs, and/or rare multi-asperity rupture (two common styles shown on Fig. 7). On megathrust faults, this behavior is often produced by a longer RI for the shallowest asperities, designated domain A by Lay et al. (2012) and Kanamori (2014). These asperities may rupture individually in rare "tsunami earthquakes" (Polet and Kanamori, 2000) or as part of rare full-width events (such as the 2011 Tohoku and 2004 Aceh–Andaman ruptures). It is possible that most or all rare multi-asperity ruptures are controlled by long-RI asperities, but this is difficult to assess without knowing rupture areas extremely precisely.

Earthquake recurrence behavior that does not appear to fit one of these recognizable patterns is more difficult to understand and anticipate, perhaps dominated by ephemeral barriers, fluctuating fault stress, and other more chaotic effects. As a reference for the following sections, the rupture history diagrams for the Sumatran Sunda Megathrust, South American subduction zone, and Japanese subduction zones are reproduced in Fig. 8 with cascades highlighted by red shaded ellipses and recurrence cycles shown by arrows.

3.1. Sunda Megathrust

Each of the three master segments we previously identified has distinct patterns of rupture recurrence (Figs. 3 and 8). The behavior of the Aceh–Andaman segment is the least well constrained, due to its apparently much longer RI of great to giant earthquakes and the lack of microatoll data from the Andaman and Nicobar Islands. It is clear that both segment-spanning rupture and piecemeal smaller ruptures are possible, as both have occurred during the historical period. However, it is unlikely that the aggregated piecemeal ruptures (even allowing for additional events that may be missing from the historical record) came close to equaling the 2004 rupture. It is more likely that great to giant events are the dominant rupture mode, with certain asperities occasionally producing smaller independent earthquakes during the intervening periods (a form of superimposed cycle). Coral microatoll records on northern Simeulue Island indicate that the penultimate great to giant earthquake occurred c. 1450 C.E., with an earlier event c. 1394 C.E. (Meltzner et al., 2010). Less precisely dated archaeological, paleotsunami, and turbidite records are consistent with that

interpretation (Daly et al., 2019; Jankaew et al., 2008; Monecke et al., 2008; Patton et al., 2015; Sieh et al., 2015), though none of these data precisely constrain the northern extent of either rupture.

The long-term average length and regularity of the RI of such events remains uncertain. Turbidite records along the trench off the coast of Aceh suggest that the long-term average RI of significant earthquakes in this region is only ~160 years and the ~500 year intervals between the most recent few events are unusual (Patton et al., 2015). Intriguingly, there appear to be phases (such as the current era) during which the RIs are several hundred years long, and others during which the RIs are <150 years long (this was called "supercycle behavior" by the authors). RI length remains relatively steady during each millennial-scale phase.

Another long-term geologic record has been discovered in the form of tsunami deposits preserved in a cave on the coast of Aceh (Rubin et al., 2017). Unfortunately the most recent 2400 years of deposits were scoured away by the 2004 and earlier tsunamis, but the remaining record extends to 7400 years B.P. The cave records one tsunami deposit between 7400 and 6600 B.P. (before the beginning of the turbidite record) and five between 6600 and 5200 B.P. (during which there were also five turbidites—a long-RI phase). This part of the cave record also agrees well with other nearby paleotsunami studies (Kelsey et al., 2015). However, there follows a ~2150-year gap in the cave record without tsunami deposits, during which time 13 turbidites were deposited. This comparison suggests that megathrust earthquakes probably continued during this period, but did not produce large tsunamis (or at least did not produce deposits preserved in this cave). Subsequently, four tsunami deposits were laid down in the cave within a very short hundred-year time span (indicating either a cascade of neighboring complementary ruptures, or repeated rupture of the same asperity), followed by the final preserved prehistoric tsunami deposit at 2900 B.P. It is conceivable that these five events correspond to the five imprecisely dated turbidites that occurred within the same time span, though there is nothing in the turbidite record to suggest the quick succession of events required by the cave chronology.

In summary, discrepancies between the cave and turbidite records indicate that possibly neither is presenting a complete picture of megathrust earthquake recurrence. The cave record is likely sensitive only to rupture of the shallow domain of the megathrust, and may be missing ruptures centered deeper on the interface that did not produce large tsunamis (akin to the 2007 Mentawai earthquake, Borrero et al., 2009). It is also not possible to determine the source rupture areas from a single paleotsunami study site. Conversely, the turbidite record is sensitive to any strong seismic shaking and could include large non-subduction events. Furthermore, both of these records sample only the proximal Aceh section of the megathrust, leaving the long-term earthquake chronology of the Nicobar and Andaman sections far more poorly constrained.

The Nias segment potentially has the simplest behavior of the three, though its continuous record is limited to ~250 years. The two well established great earthquake ruptures, in 2005 and 1861, both spanned the length of the segment and had very similar deformation patterns (Meltzner et al., 2015). The rupture area of the historical 1843 earthquake is less well established, but it is clear from the coral records that it was a much smaller event than the others and may have occurred along an upper-plate splay fault. It is not yet known whether earlier ruptures in c. 1422 and possibly in c. 1580 were similar to 1861 and 2005 or whether successive RIs are similar or variable in length, as corals dating earlier than the 1800s have yet to be investigated on Nias, but the available data are consistent with quasi-periodic similar ruptures being the dominant mode of strain release. Given its short length relative to many other master segments, the Nias segment may be composed of fewer asperities and have commensurately fewer potential rupture modes. However, there is some additional behavior variability along dip, as evidenced by the 1907 likely shallow megathrust rupture (Kanamori et al., 2010; Martin et al., 2019) and the 2010 deep rupture (U.S. Geological Survey, 2010).

Longer coral records above the Mentawai segment indicate that it exhibits rupture cascades approximately every 200 years (Philibosian et al., 2017). Each known cascade evolved uniquely, but all included at least two great earthquake ruptures, one centered in the northwest and the other in the southeast (within the ongoing cascade that began in 2007, the northwestern great earthquake has yet to occur, and is expected in the near future if the model is correct). As discussed in section 2.1.1, the two great earthquakes and others within a given cascade often overlap beneath the central Mentawai Islands. However, detailed analysis of the rupture areas of each event during the 17th-century cascade indicates that the smaller events dominantly ruptured different asperities (Philibosian et al., 2017), as has so far also been the case for the ongoing cascade. Therefore, while they might appear so as one-dimensionally depicted ruptures, the Mentawai events are not clustered similar ruptures, but are moderately to weakly clustered complementary ruptures. The clusters have varied in duration from 36 to ~100 years.

The shallow domain of the Mentawai megathrust has a semi-independent rupture cycle which is superimposed upon the ~200-year cycle that dominates at intermediate depths. A shallow "tsunami earthquake" occurred off the Pagai Islands in 2010 (e.g., Hill et al., 2012), with a similar (but not identical) predecessor in c. 1314 (Philibosian et al., 2012). A discontinuous series of coral microatoll records extending back 2500 years suggests that shallow domain earthquakes in this area may occur every ~1000 years, and deformation trends elsewhere in the Mentawai Islands hint that other sections of the shallow megathrust may also accumulate and release tectonic strain (Philibosian et al., 2012, 2017). It is also possible that the shallow domain sometimes ruptures along with the more typical intermediate-depth seismogenic zone (domain B of Lay et al., 2012): the 1797 and 1833 earthquakes both produced significant tsunamis (Natawidjaja et al., 2006), which would likely require the participation of the shallow megathrust. However, the recent 2007–2008 ruptures did not involve the shallow domain and produced only small tsunamis (Borrero et al., 2009; Konca et al., 2008). It is not possible to determine from coral records alone whether earlier Mentawai ruptures included the shallow megathrust, but lack of contemporaneous tsunami reports suggests that the 17th-century events did not (Philibosian et al., 2017). Thus, the shallow-domain superimposed cycle produces rare events, but these are not necessarily full-width "superquakes."

At a broader scale, the tight temporal clustering of the three M > 8 and seven M 7–8 ruptures that occurred along the Sumatra–Andaman Sunda Megathrust between 2000 and 2010 (within a span of time that is 7% or less of a typical recurrence interval on any one segment) is unlikely to be coincidental. These 10 events form a cascade that spans all three master segments, leaving only the northwestern Mentawai segment as a significant seismic gap. Due to data gaps, it is unclear whether any of the previous events during the past 700 years formed multi-segment cascades. It is likely that all three segments ruptured (from south to north) between 1350 and 1450, forming a loose but possibly still interrelated series.

3.2. South America

The ten segments we delineated earlier exhibit a range of earthquake cycle behavior (Figs. 4 and 8). While almost all have had at least one end-to-end rupture in recorded history, most have also

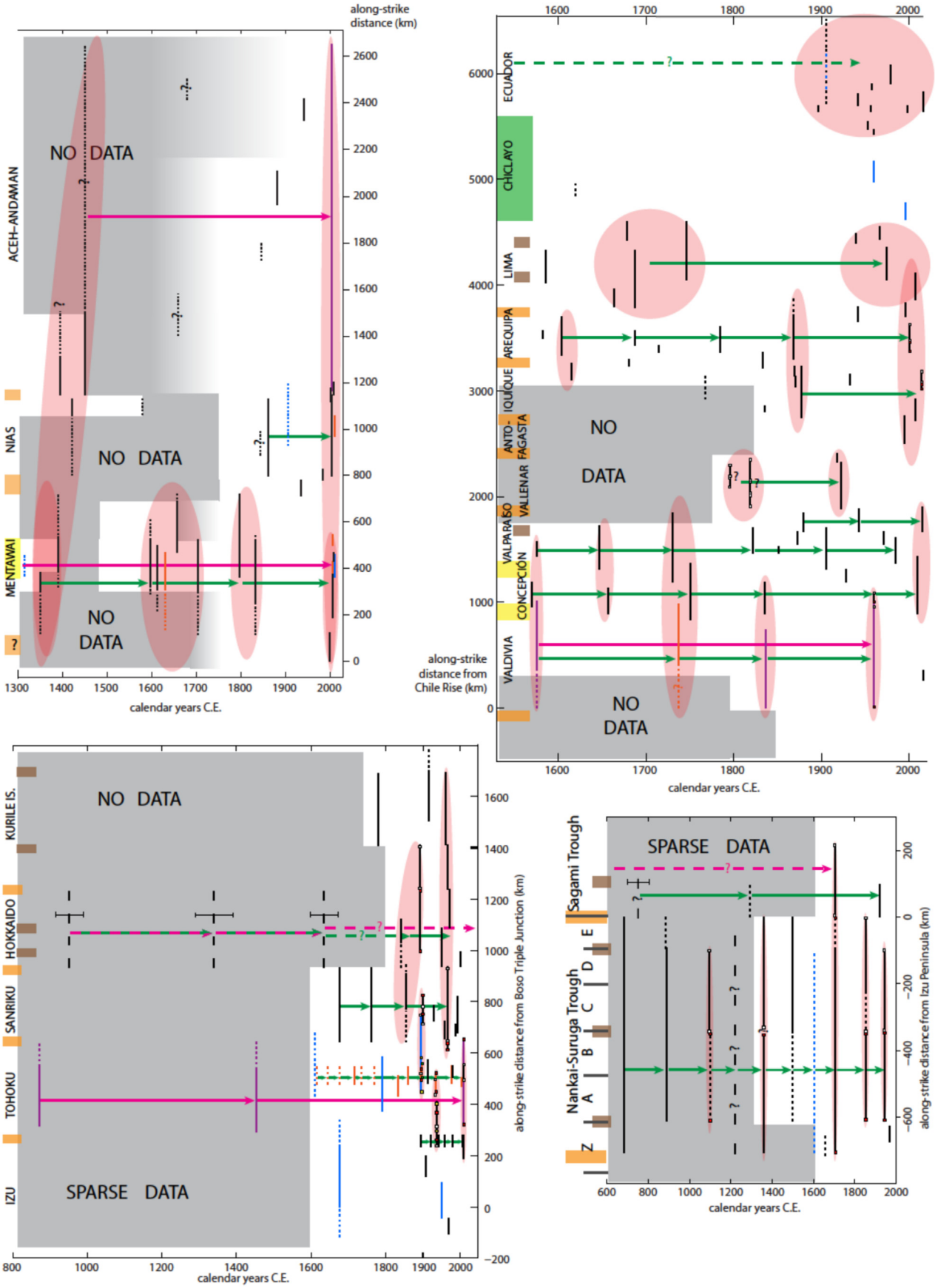

Fig. 8. Earthquake recurrence patterns observed along the Sumatran Sunda Megathrust, South American subduction zone, Nankai-Suruga-Sagami Trough, and Japan-Kurile Trench (clockwise from upper left). A version of this figure with year labels for each earthquake rupture is given in Figure S4. Rupture symbols as on Figs. 3–5; segment names and colored bars indicating barriers are shown at the far left of each plot. Red shaded ellipses indicate rupture cascades (narrower when the events are more tightly temporally clustered). Arrows indicate quasi-periodic recurrence of single events or rupture cascades, colored magenta in the case of a longer cycle superimposed on a shorter (green) cycle. If only a single arrow is shown along a particular horizontal line, data are consistent with quasi-periodic recurrence but the record is too short to confirm this. Arrows are dashed when the cycle appears to be longer than the period of record.

had rupture modes in which a series of clustered complementary events rupture the entire segment. We will discuss each segment in turn.

In the Ecuador–Colombia area, there have been five large to great megathrust earthquakes since 1900. The first and largest event, in 1906, has typically been estimated to have ruptured ~500 km along strike (the entire Ecuador segment), while later events in 1942, 1958, 1979, and 2016 seemingly reactivated parts of the 1906 rupture area, suggesting that there are at least two possible rupture styles (Nocquet et al., 2016). Recent reanalysis of tsunami and shaking intensity records have led some researchers to conclude that the 1906 rupture was more limited in extent than previously thought, with slip either concentrated updip (Yoshimoto et al., 2017) or to the north (Yamanaka et al., 2017) of the subsequent smaller ruptures (dotted rupture line on Fig. 4 reflects this uncertainty). Prior to 1906, there are no historical records of great megathrust earthquakes in the area since the time of European settlement in the 1500s. Migeon et al. (2016) identified turbidite deposits that may correspond to the 20th-century events in a single seafloor sediment core off the Ecuadorean coast. Based on their stratigraphy and estimated sediment accumulation rates, the youngest seismically-triggered turbidite prior to 1906 was emplaced 250–300 years earlier, an unusually long interval—the average interval between the seismic turbidites they identified was less than 100 years. This supports the interpretation that the lack of historical megathrust earthquake records before 1906 truly represents quiescence. Migeon et al. (2016) further note that turbidites similar to the 1906 turbidite were emplaced ~600 years earlier, suggesting a longer RI for 1906-type ruptures, but the ability to distinguish longer and shorter megathrust ruptures based on a single core is questionable.

The earlier models of the 1906 event as a 500-km homogeneous rupture present challenges for understanding the cycle behavior of the Ecuador segment. While it is not surprising that a segment would have both single and piecewise rupture modes, it is strange that most of the 1906 rupture area would rupture again within about a century, given that the entire segment had been quiescent for ~300 years before 1906. This scenario requires significant seismic potential to remain despite the huge 1906 rupture, or a post-1906 increase in interface coupling leading to a much shorter rupture RI. In contrast, the newer more detailed models suggest that the subsequent smaller ruptures filled in areas with reduced or zero slip in 1906, in which case they could be considered moderately clustered complementary ruptures (distributed over ~100 years of a 300+ year recurrence interval).

From the Carnegie Ridge south to the Mendaña Fracture Zone, along the northern coast of Peru (which we call the Chiclayo segment), there have been no definite historical subduction earthquakes other than two shallow tsunami earthquakes in 1960 and 1996 (Bilek, 2010). Two other M~7.5 earthquakes in the 1950s in far northern Peru are considered to be subduction interface events by Villegas-Lanza et al. (2016). A potential, though probably moderately-sized subduction event in 1619 is the only other disruption in ~450 years of quiescence (Dorbath et al., 1990). Such a long quiescent period could indicate either a very long-period recurrence of very large earthquakes, or that the plate interface is freely slipping and not accumulating any strain. Recent analysis of the GPS velocity field suggests that this entire segment is indeed freely slipping (Nocquet et al., 2014), though poor model resolution near the trench permits very shallow coupling which may indicate tsunami earthquake asperities (Villegas-Lanza et al., 2016). Akin to the central creeping segment of the San Andreas Fault, this is a major anomaly in an otherwise extremely seismically active plate boundary.

Continuing south, the behavior of the Lima segment appears somewhat similar to the Mentawai segment, with moderately temporally clustered ruptures that are largely complementary but with significant overlap. There are two historical rupture sequences, one between 1664 and 1746 and the other between 1940 and 2007, each involving four separate earthquakes (Bilek, 2010; Dorbath et al., 1990). The cascades have similar durations (82 and 67 years) and are separated by 200 years of quiescence. In another similarity to the Mentawai case, the two rupture sequences are quite distinct: the earlier cascade appears to have involved longer ruptures with significant overlap, whereas in the recent cascade the segment has been “mosaicked” by smaller, mostly complementary ruptures. The earliest recorded earthquake on the Lima segment, in 1586, occurred less than 80 years before the beginning of the 1664–1746 sequence (Dorbath et al., 1990). As Lima has continuous records since its founding in 1535, it is fairly certain that no other major earthquakes happened in the area for ~50 years prior to the 1586 event, so it does not appear to be part of an earlier cluster. The 1586 event seems to be an isolated partial rupture of the Lima segment, perhaps a rare occurrence.

South of the Nazca Ridge, the Arequipa segment has had fairly regular ruptures approximately every 100 years, but a closer inspection suggests significant variability in rupture extent: the 1604 and 1868 earthquakes were very large and involved rupture of the entire segment, while a pair in 1687 and 1715 and a single event in 1784 were seemingly less extensive (Dorbath et al., 1990; Okal et al., 2006). The most recent ruptures, a pair separated by 10 days in 2001, clearly involved only about half the segment (Bilek, 2010; Okal et al., 2006). We can surmise that the Arequipa segment is made up of multiple distinct asperities, some of which have longer rupture RIs and move only during very large, full-segment ruptures: a case of superimposed cycles involving rare multi-asperity ruptures. If the historical rupture lengths are accurate, it should not be surprising if there is no further rupture of the Arequipa segment for a century, even though the 2001 earthquakes did not release as much strain as the preceding 1868 earthquake.

Due to the shorter period of written history in the Atacama Desert of northern Chile, only one or two earthquake cycles are recorded for the Iquique, Antofagasta, and Vallenar segments, so we cannot be confident that the historical record captures the full range of fault behavior and we also cannot rigorously assess RIs. Nevertheless, it is possible to make valuable observations. The available data are consistent with ~150 year RIs on the Iquique segment, with the two most recent rupture sequences exhibiting different modes: full segment rupture in 1877 (preceded by smaller M ~7.5 ruptures a few years earlier; Comte and Pardo, 1991), and piecemeal rupture (three M > 7.7 events) with little overlap in 2007–2014 (so far; additional ruptures are expected in order to equal the 1877 event; Bilek, 2010; Hayes et al., 2014). It is also notable that rupture cascades on the Arequipa and Iquique segments appear to be coordinated: both segments ruptured completely within 10 years in 1868–1877 and most parts have ruptured again in the 20+ years since 1996, though a few gaps remain. The 2007 Pisco and 1995 Antofagasta earthquakes, extending north and south into the Lima and Antofagasta segments, respectively, may also be related to the recent Arequipa–Iquique cascade, though no Lima or Antofagasta segment event was coordinated with the 1868–1877 cascade.

The Antofagasta segment has had only one complete rupture in recorded history (a single M_w 8.1 event in 1995), with no M > 7.5 earthquakes for at least 150 years prior. It is the shortest of the 10 segments we define and is thus perhaps less likely to exhibit piecemeal rupture cascades. However, it did produce several M 7–7.5 earthquakes during the 20th century (not shown on Fig. 4, which is limited to M > 7.5 events). The Iquique segment also

produced numerous M 7–7.5 events in the late 19th and throughout the 20th centuries (Comte and Pardo, 1991; Saillard et al., 2017). Since they are too small to have generated tsunamis, it is not certain that all of these were megathrust events, and the record is not complete for earthquakes in this magnitude range in most other areas and pre-instrumental time periods. Nevertheless, it is likely that these two segments have many small asperities that are capable of rupturing independently.

The historical record includes at least two complete ruptures of the Vallenar segment, just over a century apart, dominated by M > 8 events in 1819 and 1922. However, both of these events were preceded by smaller ruptures, forming cascades. There were two ruptures of somewhat indeterminate size in 1796 as well as two smaller (but still notable) earthquakes a week before the largest 1819 event, and the 1922 event was preceded by a 1918 rupture towards the north end of the segment (Beck et al., 1998). Also, the 1922 event had three pulses of moment release, suggesting that this segment has three major asperities, some of which may have ruptured separately in 1796 and 1819 (Beck et al., 1998). (As mentioned in section 2.2.2, it is possible that the subduction of the Copiapó seamounts is related to this asperity fragmentation.) Now, nearly a century has elapsed since the last rupture on the Vallenar segment, longer than any other South American megathrust segment (other than the creeping Chiclayo segment). If the historically recorded hundred-year interval is typical of the Vallenar segment, it is very likely that it will rupture again soon. Past behavior suggests the rupture will likely involve more than one M > 7.5 earthquake, though most of the strain may be released by a single M > 8 event.

Moving into central and southern Chile, 450-year histories resume for the Valparaíso, Concepción, and Valdivia segments. All three appear to have relatively regular RIs, though the earthquakes are by no means identical. The south-central portion of the Valparaíso segment has had a large rupture every ~70–90 years, but records suggest the rupture length has varied significantly, ranging between the entire ~700-km segment in 1730 and a ~200 km asperity in 1985 (Beck et al., 1998; Carvajal et al., 2017a). Due to lack of significant coastal settlement at the time, it is unknown whether the earliest (16th-century) historical events produced tsunamis, so their assignment to the megathrust is less certain (Cisternas et al., 2012). Meanwhile, during the last 150 years the northern (Illapel) and north-central (near Valparaíso) portions of the segment have ruptured independently, potentially governed by similar RIs but without obvious coordination with the south-central ruptures. The boundary between the north and south-central parts of the Valparaíso segment is associated with the Juan Fernandez seamounts, which, as discussed in section 2.2, may frequently (but not always) arrest rupture propagation.

Similarly to the Valparaíso segment, the Concepción segment has had fairly regular ruptures (every 85–95 years) of varying lengths, though most extended over at least half the 600-km-long segment (Beck et al., 1998; Melnick et al., 2009). The 1928 Talca earthquake was the exception to this, involving only the northernmost ~100 km. The remaining slip deficit in that cycle was likely released (at least in part) by the 1960 M8+ Concepción earthquake, which occurred the day before the Valdivia M9.5 earthquake (Cifuentes, 1989) and, while a great earthquake in its own right, has been eclipsed in the literature by its giant successor. The occurrence of the 1939 Chillán earthquake inland from Concepción, while not a typical subduction event, may also have affected the penultimate Concepción cycle. These disruptions apparently did not extend to the most recent cycle, when the entire segment ruptured during the 2010 Maule earthquake (e.g., Yue et al., 2014). As discussed in section 2.2, both ends of the Concepción segment appear to be more diffuse than most other segment boundaries, with wide boundary zones that can link with either adjoining segment. This behavior is at least partially responsible for the variability in rupture length on both the Concepción and Valparaíso segments.

The Valdivia segment is the longest of those we have delineated, defined by the giant 1960 rupture and its predecessors. Most analyses of the historical record suggest that its ruptures have all been single events separated by ~100–160 years, though the sparse settlement of southern Chile in earlier history leaves open the possibility of missing events (Kelleher, 1972). It is important to note that not all the Valdivia segment earthquakes were necessarily comparable to the giant 1960 event, contrary to what is suggested by many graphical depictions (e.g., Melnick et al., 2009). Cisternas et al. (2005, 2017) infer from geologic and historical records that the recurrence time of 1960-sized events is actually close to 300 years, with the most recent comparable event occurring in 1575. They suggest that the more recent 1737 event likely occurred deeper on the fault interface and may have been limited to the northern half of the master segment, while the 1837 event involved broad rupture but was likely limited to the southern part. The tsunami and ground deformation for both events were seemingly lesser than for 1960. Based on lacustrine paleoseismic records near Valdivia, Moernaut et al. (2014) concur with Cisternas et al. and further suggest that the southern half of the segment might have ruptured separately after the northern part ruptured in 1737 event. Their suggestion is based on very sparse reports of earthquakes in the 1740s in southern Chile mentioned in the historical compilation by Lomnitz (2004), but it is also possible that these were merely aftershocks of the 1737 event rather than major megathrust ruptures in their own right. A synthesis of paleoseismic data along the Valdivia segment (extending to 5000 years B.P.) supports the hypothesis that full-segment ruptures occur every ~300 years, with one or two smaller events akin to 1837 or 1737 often occurring within these intervals (Moernaut et al., 2018). One site exhibits a strong bimodality in RI of tsunami deposits, illustrating that multiple rupture modes are at work (Kempf et al., 2019). Overall, the available data suggest that some form of superimposed cycle affects the Valdivia segment, with certain asperities (separated along strike and/or along dip) having longer RIs than others.

While there is no solid historical evidence for internal rupture cascades within the Valdivia, Concepción, or Valparaíso segments, they do present another example of cascades involving multiple segments. Past earthquakes on these three segments have frequently been tightly correlated in time (Melnick et al., 2009), though in the last cycles they seem to have drifted out of phase. Based on geodetic observations surrounding the 2010 Maule and 2015 Illapel earthquakes, Melnick et al. (2017) propose a mechanism for such cascades in which the rotational elastic response to one large earthquake instigates a “super-interseismic period” during which the strain accumulation rate is increased in neighboring areas. Intriguingly, the effects of this mechanism (in contrast to near-field stress transfer) are strongest some distance away from the edges of the first rupture, potentially explaining the ~200-km gap between the Maule and Illapel rupture areas as well as similar gaps between successive ruptures in past cascades. Unlike near-field stress transfer, this mechanism would incite rupture cascades only on dip-slip faults.

3.3. Japan

3.3.1. Nankai-Sagami Trough

Due to several internal frequent barriers, both the Nankai and Sagami master segments have multiple rupture modes (Figs. 5 and 8). With more extensive historical records and a shorter RI, the

behavior of the Nankai Trough can be more confidently characterized. During the past 600 years (for which the historical record of Nankai great earthquakes is likely complete), the central A-B (Nankai) and C-D (Tonankai) asperities have ruptured every ~100–150 years, either together in a single event or separately in a closely-timed doublet (just 32 hours apart in 1854, separated by a few years in other cases). The frequency of historically known earthquakes is lower before 1400 C.E. with RIs >200 years. Ishibashi (2004) noted that the historical records are sufficiently sparse to permit missing earthquakes in this period and specifically suggested a missing event within the longest (262-year) hiatus between known historical earthquakes, in the 1200s. A review of all available paleoseismic data does support the hypothesis that a Nankai subduction earthquake occurred in the 1200s, but there is little or no evidence of additional events within the other two ~200-year periods of 887–1096 and 684–887 (Garrett et al., 2016). Therefore, at least one of the 200-year interseismic intervals is probably real, and the full range of RI variability is ~100–200 years. This range also accommodates the additional wrinkle that the 1605 event is considered a tsunami earthquake (e.g., Garrett et al., 2016; Ishibashi, 2004), and as such would probably not have ruptured the interface at intermediate depths (though strain could have been released through aseismic slip). Some researchers have recently suggested that the 1605 event may have actually occurred in 1614, or that it might have been sourced from the Izu-Bonin trench rather than the Nankai Trough (Fujino et al., 2018; Fujiwara et al., 2020 and references therein), further confirming that this event should not be counted when assessing the recurrence intervals of typical Nankai Trough ruptures. However, in comparison to even the shorter RIs, the rupture cascades have been spectacularly tightly temporally clustered. There have been at least three doublets (1944/1946, 1854/1854, and 1096/1099), and the 1361 earthquake was also potentially a doublet: though a single large event is suggested by geological observations (Garrett et al., 2016), historical records suggest two events a few days apart (Ishibashi, 2004).

The behavior of the marginal Z (Hyuga-nada) and E (Tokai) asperities presents a conundrum: they appear to sometimes, but not always, rupture along with their respective neighboring Nankai and Tonankai asperities. This variability is particularly unequivocal for the Tokai asperity, illustrated by comparing the most recent and best-documented Tonankai earthquakes of 1944 and 1854. This discrepancy was noticed early on by Ando (1975), leading to speculation that the Tokai asperity was likely to rupture independently in the near future to fill the seismic gap. However, there is no evidence (paleoseismic or historical) that the Tokai asperity has ever ruptured individually. It appears more likely that the Tokai asperity simply has a longer (and perhaps more erratic) RI than the Nankai and Tonankai asperities, or that slip is sometimes accommodated aseismically.

Parts of the Hyuga-nada asperity, however, did rupture individually in a M_w 7.5 earthquake in 1968 (Yagi et al., 1998) and a slightly larger event centered farther southwest in 1662 (Nakata et al., 2012). The 1968 event could be considered part of the 20th-century cascade, but there is no candidate earthquake that could have filled in the Z segment the 19th century, and the 1662 event was not clearly correlated with other Nankai Trough ruptures. Even with the participation of individual smaller ruptures, it still seems that the Hyuga-nada asperity, like the Tokai asperity, also has longer and more irregular RIs than the Nankai and Tonankai asperities. There has also been significant documented postseismic slow slip on the Hyuga-nada megathrust interface (Yagi et al., 2001), and episodic slow slip events have occurred below the Bungo Channel near the Z/A boundary (Hirose and Obara, 2005). If a significant amount of plate convergence is typically accommodated by slow slip in this region, that may explain the irregularity and lower frequency of seismic slip.

It should be noted that while along-strike extent of Nankai Trough ruptures is relatively well constrained, along-dip extent is more equivocal. Comparisons of inland shaking intensity and estimated tsunami size suggest that there may have been significant variations in depth extent of past ruptures (e.g., Fujino et al., 2018; Fujiwara et al., 2020; Seno, 2012). Thus, there may be additional superimposed cycles related to less frequent rupture of the shallowest (domain A) and/or deepest (domain C) parts of the megathrust, though it is likely that most events other than the 1605/1614 tsunami earthquake involved the intermediate domain B.

Based on historical records alone, it is difficult to say more about the Sagami Trough than 1) at least two rupture modes are possible, and 2) RIs are probably >300 years on average. Paleoseismic data are necessary to go further. As both the historical 1923 Taisho and 1703 Genroku earthquakes were associated with marine terrace formation, paleoseismic earthquake chronologies have dominantly been based on flights of terraces and beach ridges, suggesting average RIs of ~400 years for Taisho-type events and 1000–3000 years for Genroku-type events (Komori et al., 2017; Shishikura, 2014). However, these estimates are based on *a priori* assumptions that there is a one-to-one correspondence between large terraces and Genroku-type events, and between small terraces and Taisho-type events. It is conceivable that major subduction earthquakes (particularly tsunami earthquakes centered far from shore) could sometimes occur without forming terraces, that terraces could sometimes form due to climatic effects rather than tectonic uplift, that coseismically uplifted terraces could be erased by erosion, and that the observed terraces could have been formed by earthquake ruptures that are different from both the 1923 and 1703 events (Komori et al., 2017; Sato et al., 2016; Shishikura, 2014). Nevertheless, the simplest model that explains the available data is that of a superimposed cycle: an asperity west of the Boso Peninsula that ruptures every 1000+ years along with the eastern asperity, while the eastern asperity ruptures every ~400 years, usually independently. One additional feature of note is the temporal proximity of the 1703 Genroku earthquake (Sagami Trough full rupture) to the 1707 Nankai Trough full rupture. It is possibly a coincidence, especially since there is no obvious correlation between Nankai Trough events and any of the three most recent Taisho-type Sagami events: 1923, 1293 (historical + geological), and 700–800 C.E. (geological). However, it is intriguing to speculate that rare, large Genroku-type events might be capable of triggering Nankai Trough events.

3.3.2. *Japan-Kurile Trench*

As the RIs of the largest events are longer than the historical period along the Japan-Kurile trench, our analysis of rupture patterns is more tenuous in this region than in others. Nevertheless, the common themes of rupture cascades and superimposed cycles of larger and smaller events are still evident in the data (Figs. 5 and 8). All three of the master segments we delineate exhibit multiple rupture modes. One important note is that, throughout this region, older records (both historical and geological) preserve only the larger events: as examples, only the “outsized” tsunamis are preserved in the Sendai plain sediment archives (e.g., Sawai et al., 2012), Miyagi-oki earthquakes are not confidently identified before the 19th century (Earthquake Research Committee, 2011), and the repeating Ibaraki-oki earthquakes are known only from the instrumental period (Mochizuki et al., 2008). Therefore, it cannot be proven that recently-observed patterns of smaller events necessarily extended millennia into the past. However, neither is there any reason to believe they did not.

The 2011 Tohoku-oki rupture area (which covers most of the Tohoku-oki master segment) contains at least three asperities,

adjacent along dip, that had previously ruptured individually (Fig. 5): the nearshore Miyagi-oki asperity with its well-documented ~40-year RI, the shallow subduction domain which produced tsunami earthquakes in 1896–7, 1793, and possibly 1611, and the region in between which had prior ruptures in 1915, 1981, and two days before the giant 2011 Tohoku-oki earthquake. The RI of earthquakes similar to the 2011 Tohoku-oki event is estimated to be 500–800 years based on analysis of paleotsunami deposits (Sawai et al., 2012). The 869 Jogan earthquake and tsunami has become generally recognized as a likely predecessor (e.g., Namegaya and Satake, 2014), and another event in 1454 has more recently been added to the list (Sawai et al., 2015). While both of these historical events are estimated to have extended at least 200–300 km along strike, it is currently unknown whether they were truly as extensive (particularly in terms of shallow slip) as the 2011 event, due to the limited spatial extent of historical records and tsunami deposit preservation (Namegaya and Satake, 2014; Sawai et al., 2015). It is unquestionable, however, that they were far larger than any other historical events in the Tohoku-oki region.

Adjacent to the 2011 rupture area, a cluster of three M > 7.5 megathrust earthquakes occurred off Fukushima in 1938, with potentially overlapping source areas (two large normal faulting events were also part of this cluster). It is impossible to analyze a rupture recurrence pattern for these asperities as there have been no other historical ruptures of a comparable size, indicating quiescence for at least 400 and likely as long as 800 years (Abe, 1977; Hatori, 1976). It is possible, however, that the Fukushima-oki asperities ruptured as part of 2011-type events in the past. In summary, while the precise similarity of past events is uncertain, the behavior of the Tohoku-oki master segment can be understood as a patchwork of small asperities, some rupturing regularly or irregularly in cycles of decades to a century, others rupturing only in large, rare events that link many asperities. On the scale of a century or two the behavior appears chaotic, but on longer time scales the superimposed cycles emerge.

The Sanriku(-oki) master segment has essentially complete ruptures much more frequently: some or all of the well-documented 1968 rupture area is generally thought to have been the source of tsunamigenic earthquakes in 1677, 1763, and 1856, making for fairly regular 100-year intervals (Aida, 1977; Earthquake Research Committee, 2011; Hatori, 1975b; Satake, 2015). However, other rupture modes also exist: the 1968 source area has been modeled as a pair of asperities, and several smaller ruptures of the southern asperity have occurred during the 20th century (Yamanaka and Kikuchi, 2004). It is likely that additional single-asperity ruptures occurred prior to the 20th century but were insufficiently noteworthy to appear in historical documents. This behavior is actually quite analogous to the Tohoku-oki segment, though scaled down in both space and time.

As detailed in section 2.3.2, the Hokkaido(-oki) master segment and adjacent Kurile Trench to the north has fully ruptured twice historically, both times in cascades. The mid-20th-century cascade also potentially includes the adjacent 1968 rupture on the Sanriku-oki segment to the south. However, longer multi-asperity ruptures also occur along Hokkaido, known from paleotsunami deposits. Interestingly, the most recent of these larger events occurred in the early 1600s (constrained by volcanic ash from historical eruptions) and should have produced a tsunami on the Sanriku coast. It has been suggested that the 1611 Keicho Sanriku tsunami, commonly interpreted as the result of a shallow domain "tsunami earthquake" along the Japan Trench, actually originated from the Kurile Trench (Minoura et al., 2013; Okamura and Namegaya, 2011). Ironically, the long-term average RI of full-master-segment ruptures (~400 years, with significant variability) is better constrained than the RI of piecemeal ruptures like those that have occurred in historical times, because tsunami deposits from the smaller ruptures may be sparse or absent on the Hokkaido coast (Sawai et al., 2009). There are two plausible interpretations of the observations. If the historical behavior is typical but evidence has not been preserved, complete rupture of the Hokkaido-oki master segment occurs every ~100 years, about three-fourths of the time in a piecemeal cascade and one-fourth of the time in a single event. Alternatively, if the historical behavior is actually uncommon, complete rupture occurs every ~400 years, usually as a single event but occasionally as a piecemeal cascade.

3.4. Cascadia

Based on the Goldfinger et al. (2012, 2017) interpretation of the Holocene turbidite record, the Cascadia megathrust exhibits a form of superimposed cycles, in which longer full-margin ruptures are interspersed with shorter events (Fig. 6, left). However, the proposed behavior is unusual in comparison to most other fault systems we discuss, in that rupture of the entire master segment appears to be the most common behavior, and that virtually all of the proposed ruptures have the same southern endpoint but extend northward to varying degrees. Thus, only the southernmost asperity ruptures independently of the others, and the rupture frequency of each sub-segment decreases northward. In their updated analysis, Goldfinger et al. (2017) do propose that the northern asperities (offshore Washington state) may have ruptured independently once or twice, but this does not appear to be common. Based on comparisons with terrestrial data, Atwater and Griggs (2012) and Hutchinson and Clague (2017) both argue that the penultimate full-margin event in the Goldfinger et al. chronology (T2) was also limited to northern Cascadia or was perhaps two ruptures separated by a gap, rather than being a single contiguous full-margin rupture.

If the Goldfinger et al. interpretation is correct, the Cascadia megathrust is the only major fault system in our analysis which does not exhibit rupture cascades. This apparent anomaly warrants extra scrutiny of the interpretation of the paleoseismic data. As noted by Atwater and Griggs (2012), geologic evidence (even including tree rings) generally cannot distinguish between single long ruptures and tightly temporally clustered non-overlapping complementary ruptures, and only the historical tsunami records from Japan brought confidence that the most recent full-margin rupture, in the year 1700, was a single event (Atwater et al., 2005). Some terrestrial evidence, such as a pair of tsunami deposits separated by only a few decades of deposition (Nelson et al., 2006), is consistent with rupture cascades although it does not conclusively demonstrate their existence. Ultimately, the strength of the interpretation that Cascadia typically experiences single full-margin ruptures rather than rupture cascades hinges on how confidently the synchronicity of turbidites in different cores can be established. As discussed in section 1.2, the accuracy of the turbidite correlation techniques employed by Goldfinger et al. is debated (Atwater and Griggs, 2012; Atwater et al., 2014), and the techniques have not yet been validated against a historical record of subduction earthquakes that includes rupture cascades. The final evaluation of whether the Cascadia megathrust is truly an outlier in terms of rupture cascades may thus depend on future turbidite research in South America or Japan.

Largely independently of the above issues, Goldfinger et al. (2012) also argued that the full-margin ruptures of the Cascadia megathrust are temporally clustered. However, the "clusters" span ~2000 years on average while the gaps between clusters average only about 1000 years long. Thus, the Cascadia behavior might be better described as occasionally "skipping" a full-margin rupture than by "clustering," since the latter term suggests acceleration of

tectonic strain release within a relatively brief period. It is also noteworthy that the unusually long intervals between full-margin ruptures appear to contain more frequent and longer partial-margin ruptures, leaving only the northernmost asperities apparently un-ruptured. It is worth considering that perhaps strain on that section of the megathrust was released aseismically during these intervals, which would leave no trace in the turbidite record. If that is the case, Cascadia behavior can be understood under a model of quasi-periodic strain accumulation and release. Furthermore, in their updated analysis, Goldfinger et al. (2017) noted that several of these gap-filling partial-margin ruptures were longer than previously thought, reaching close to the full length and making the clusters far less pronounced. Regardless, the Cascadia events are not an ideal example of clustered similar ruptures.

Patterns of ETS recurrence make for an interesting study in their own right and, due to their much shorter RIs, numerous complete cycles are already recorded in detail and the chronology expands further every year (Fig. 6, right). Although largely beyond the scope of this review, in the future these rich records can perhaps provide some insight into the longer-term patterns of earthquake recurrence. The eight ETS segments in Cascadia identified by Boyarko et al. (2015) each have varying RIs and degrees of regularity, with the longest segment (between Seattle and Vancouver) notably strongly periodic. ETS cascades are also apparent, in which distinct ETS events occur simultaneously or in close succession on different segments. These features are not limited to Cascadia ETS, as ETS segments along the Nankai Trough likewise each have characteristic RIs and have also hosted multi-segment ETS cascades (Obara, 2010). It is possible that the mechanisms governing these patterns are similar to those responsible for analogous patterns in earthquake recurrence.

3.5. Other subduction zones

Rupture cascades are apparent during the 200-year recorded history of the Middle America subduction zone. As examples, eight $M > 7.5$ earthquakes occurred along various parts of the margin within a span of 6 years between 1898 and 1904, and several neighboring earthquake doublets have occurred within even shorter periods (Astiz and Kanamori, 1984). However, many asperities involved in these cascades have also had isolated ruptures. While RIs for frequently-rupturing individual asperities can be estimated, the historical earthquake chronology is too short to assess the overall abundance or frequency of cascades.

The near-complete rupture of the entire Alaska-Aleutian margin during the 20th century is clearly a cascade, since the five M_w 8+ events occurred within a span of 27 years while RIs of great earthquakes along this margin are generally thought to be several hundred years (Wesson et al., 2007). Certain asperities (particularly in the Aleutians) appear to have more frequent independent ruptures, but most have ruptured only once in recorded history, and paleoseismic data is as of yet insufficient to assess recurrence over much of the margin. A recent review of coastal paleoseismic data throughout the more thoroughly studied 1964 rupture area concluded that there has been significant variability among earthquakes during the preceding 4000 years, with none of the previous events exactly resembling the 1964 rupture (Shennan et al., 2016). With RIs of >500 years for Prince William Sound subduction earthquakes, an even broader network of sites with extremely long paleoseismic histories would be required to truly assess the variety and frequency of rupture patterns. Thus, we rely largely on faults with shorter RIs in building our catalog.

3.6. Non-subduction examples

Rupture cascades unquestionably occur on the North Anatolian Fault, as evidenced by the 20th-century cascade that has been a favorite of earthquake scientists for decades (Barka, 1996). Observation of how this sequence had progressed allowed the anticipation of the 1999 Izmit earthquake, as well as the speculation that such cascades had also occurred in the more distant past (Stein et al., 1997). A more recent review combining paleoseismic evidence and historical records suggests that other cascades have occurred, but that they are not always as coordinated or complete as the spectacular 20th-century example (Fraser et al., 2010). Each of the three segments defined by Fraser et al. appears to exhibit distinct recurrence behavior. The western segment, around the Sea of Marmara, typically has short ruptures with more frequent and irregular recurrence. Magnitude estimates based on historical data alone suggest that M 7.5+ events generally do not occur on the western segment, whereas such longer ruptures are more typical of the central and eastern segment (Bohnhoff et al., 2016). The central segment ruptures fairly regularly, about every 450 years, with each complete rupture potentially composed of several earthquakes (Fraser et al., 2010; Rockwell and Biasi, 2017). The eastern segment seems to be composed of at least two asperities that may rupture individually or together, with full ruptures at potentially longer intervals (Fraser et al., 2012), a case of superimposed cycles.

On the Dead Sea Fault, there is substantial evidence of rupture cascades from historical data; for instance, an apparently mostly southward-cascading flurry of ruptures that spanned the 12th century (Marco and Klinger, 2014). From historical records alone, it is known that multiple major earthquakes have occasionally occurred within the same year, from hours to months apart, and distinct macroseismal areas suggest they involved different parts of the fault rather than being aftershocks (Agnon, 2014; Ambraseys, 2009; Marco and Klinger, 2014). Clustering is also evident in paleoseismic records. For example, at one site in the central Jordan Valley, paleoseismic data combined with archaeological and historical data suggest that during the last several thousand years, ruptures have happened in pairs with 1000+ years between pairs and 300–500 years between earthquakes in a pair (Ferry et al., 2011). However, it is not clear whether the entire Jordan Valley section ruptured during each of these earthquakes (which would be clustered similar ruptures), or whether they are more akin to the Mentawai case (clustered complementary ruptures with an overlap zone). Lefevre et al. (2018) integrated paleoseismic and historical records for the portion of the DSF south of Lebanon and proposed that clustered complementary ruptures have ruptured the entire fault several times within the last few millennia. Based on a compilation of historical events, Zohar (2020) noted evidence of alternating activity between the northern and southern DSF and that clustering appears more common in the northern region. However, he assigned rough rupture length categories based on estimated magnitude, acknowledging that the precise rupture extent of most events is not well constrained. As a whole, RIs on the DSF do appear to be more variable than on the North Anatolian Fault and most of the megathrust faults that we review, though without precise rupture extent for each event it is difficult to assess the true recurrence pattern.

Additional recent or historical examples of rupture cascades can be found along many other terrestrial faults, though there are generally insufficient data to evaluate the long-term prevalence of such behavior. Much of the Kunlun Fault in China has ruptured within the last century in a series of five major earthquakes, an obvious cascade given that RIs are estimated to be hundreds of years or more (e.g., Li et al., 2005; Lin et al., 2006; Lin and Guo, 2008). The sequence is consistent with static stress triggering

(Xie et al., 2014). Paleoseismic data are as yet insufficient to begin speculating about whether similar cascades have occurred there in the past. The East Anatolian Fault (EAF) in Turkey (which connects the NAF and the DSF) hosted a flurry of earthquakes during the 19th century, including three with M > 7, and had long quiescent periods before and since (Ambraseys, 1989). Only a few researchers have remarked on the EAF cascade. There have been very few paleoseismic studies along the EAF so RIs and the prevalence of cascades are as of yet largely unknown, but based on historical records the RIs are likely several hundred years. As an example of a rupture cascade on a broader fault network, four large to great earthquakes occurred in Mongolia within a span of 52 years (1905–1957), along faults that have likely RIs in the thousands of years. Chéry et al. (2001) hypothesized that postseismic stress transfer might be responsible for triggering earthquakes across the broadly distributed Mongolian fault systems. Such sequences are not limited to strike-slip faults: seven individual surface-rupturing earthquakes above M 6.5 occurred on a network of Basin and Range normal faults in west-central Nevada between 1915 and 1954, including three more closely associated pairs separated by one year, 1.5 months, and 4 min, respectively (Bell et al., 1999; Hodgkinson et al., 1996; Wallace et al., 1984). Rupture recurrence intervals of any one section of these faults are in the thousands of years, and the rupture sequence is consistent with static stress triggering. Historical records suggest numerous rupture cascades on various individual and networked strike-slip and thrust faults in Iran, with one confirmed 20th-century example (Berberian and Yeats, 1999). RIs for these faults are generally unknown and likely vary, but cascades are nevertheless identifiable based on the long periods of historical quiescence separating comparatively brief periods of activity.

Quasi-periodic recurrence and rupture cascades are both clearly evident in the instrumental records of earthquakes on certain oceanic transform faults. As with segmentation, the most spectacular example is the Gofar-Discovery transform which hosts ~10 distinct seismogenic asperities, each with highly periodic earthquake RIs of ~5 years (Boettcher and McGuire, 2009; Froment et al., 2014; McGuire, 2008; Wolfson-Schwehr et al., 2014). These ruptures are organized into repeating cascades in which multiple asperities along the length of the transform system rupture (roughly in east to west order) over a period of ~2 years, less than half the typical RI. There is also at least one case where a particular segment ruptured in two events during one cycle and in a single event in another (McGuire, 2008), a potential expression of a superimposed cycle. It should be noted, however, that while all earthquakes in each repeating sequence are sourced roughly from the same fault area, there is substantial variation in earthquake magnitude, suggesting that the rupture areas overlap significantly but are not identical (McGuire, 2008). The Blanco, Clipperton, Siqueiros, Eltanin, and Charlie-Gibbs transforms also exhibit quasi-periodic recurrence of similar but varying magnitude ruptures (Aderhold and Abercrombie, 2016; Boettcher and McGuire, 2009; McGuire, 2008; Sykes and Ekström, 2012). Synchronization between events on neighboring asperities (cascading behavior) is apparent, though less well studied, in the Blanco and Eltanin records (Boettcher and McGuire, 2009; Sykes and Ekström, 2012). As oceanic transforms represent some of the simplest fault systems in the world, with slip concentrated on a single structure with little or no branching or interaction with other faults, the prevalence of quasi-periodic recurrence and rupture cascades supports our interpretation that these behaviors represent the natural "base state" of fault systems. It is physically reasonable that slower-slipping and more complex fault networks are more likely to deviate from these basic behaviors.

3.7. Do clustered similar ruptures occur?

Clusters have often been identified in earthquake chronologies from single paleoseismic sites, e.g. Grant and Sieh (1994); Sieh et al. (1989); Weldon et al. (2004) for the San Andreas fault. These apparent clusters have often become less pronounced or significant in later analyses (Akçiz et al., 2010; Scharer et al., 2010, 2011), but furthermore, with only one site it is hard to distinguish between overlap zones between neighboring complementary ruptures and clustered similar ruptures, or to identify smaller events that might have only a local effect. Earthquake RIs have generally been calculated for a single site and then used with the implicit or explicit assumption that all earthquakes recorded at that site represent rupture of the same fault segment. This assumption may be erroneous: if a RI were calculated based on a single site in the central Mentawai Islands, researchers might conclude that earthquakes on the Mentawai segment were highly aperiodic and that future behavior was difficult to anticipate. However, with the broader context of dozens of sites, the supercycle pattern emerges and the fault behavior becomes much more comprehensible—-while there is overlap in rupture area, the ruptures are largely complementary. The concept of a quasi-periodic earthquake cycle can still be applied, but the culmination of each cycle is made up of multiple complementary earthquakes rather than a single earthquake.

Although many paleoseismic studies have reported clusters, there are few that can confidently be attributed to clustered similar ruptures as opposed to overlapping complementary ruptures. There is fairly strong evidence of similar-event clusters (or at least pulses of faster scarp exhumation) on slow-slipping normal faults in central Italy, based on event chronologies at multiple sites on a single fault system (Schlagenhauf et al., 2011). The authors called these "supercycles." Benedetti et al. (2013) expanded the earlier study to several other nearby faults and found evidence for clustering on those as well, though as only a single paleoseismic site was developed on each of these other faults, the possibility of "false clustering" due to sites being located in overlap zones of neighboring ruptures cannot be entirely excluded. Benedetti et al. also point out that this fault system appears to display "earthquake synchrony," in which multiple neighboring faults rupture within a relatively short period. The recent cascade of ruptures on neighboring faults including the 1997 Colfiorito, 2009 L'Aquila, and 2016 Amatrice/Mt. Vettore earthquakes (Falcucci et al., 2018; Wedmore et al., 2017) appears to be a modern-day example, and previous likely cascades can be identified in the historical record (Verdecchia et al., 2018). However, "earthquake synchrony" (i.e. rupture cascade) behavior should be considered independently of whether clustered similar ruptures occur. While successive ruptures overlapped to some extent during the 2016 sequence, detailed slip models show that each earthquake dominantly ruptured different asperities and that structural discontinuities (fault intersections) formed barriers that limited rupture propagation (Walters et al., 2018), more consistent with our model of clustered complementary ruptures than with the clustered similar ruptures inferred from prehistoric fault exhumation rates.

Even if the paleoseismic data do truly represent clustered similar ruptures, it is not clear that the central Italian case is a good analog for behavior of major plate boundary faults. One might expect more erratic behavior in that tectonic environment, with numerous sub-parallel slow-slipping faults that can readily influence each other through static stress changes (Wedmore et al., 2017). A comparison among long single-site earthquake chronologies on various strike-slip faults suggests that RIs are generally more consistent on fast-slipping faults and more variable on slow-slipping faults (Yuan et al., 2018). Among potential clustered similar

ruptures on plate boundary faults, one of the most striking is on the Jordan Gorge section of the Dead Sea Fault (relatively slow-slipping), which records two lone events in the second millennium C.E. and seven in the first (Wechsler et al., 2014). Nevertheless, it is also possible to explain the data if some of the clustered events are actually "tail ends" of ruptures that dominantly extended either north or south of the site, a hypothesis espoused in an updated study of the same site that focused on slip-per-event (Wechsler et al., 2018). Another candidate is the El Asnam fault in Algeria, which could be called a plate boundary fault although it is relatively slow-slipping and is part of a larger fault network. Ratzov et al. (2015) argued that the El Asnam fault has clustered similar ruptures (to which they applied the term "supercycles"), based on turbidite paleoseismology that supported earlier trenching studies by Meghraoui et al. (1988). However, only one of the terrestrial sites has a long enough complete record to suggest clustering, so overlap of neighboring complementary ruptures at that site is still a plausible alternate explanation. As the turbidite source areas are not proximal to the El Asnam fault and there are other potential triggering faults, regional earthquake synchrony rather than repeated El Asnam ruptures would also explain the data. With a high-resolution turbidite record spanning the entire Holocene and numerous sampling sites along the entire plate boundary (Goldfinger et al., 2012, 2017), the Cascadia megathrust is one of the best environments to search for temporal clustering. As discussed above, the observed record is not strongly clustered and the arguable weak clustering would apply only to the northern asperities.

Because of the stringent data precision, quantity, and spatial distribution requirements for positive identification of clustered similar ruptures, and the many faults that exhibit some evidence for such behavior, one could argue that clustered similar ruptures may be common but are not apparent with current paleoseismic data limitations. Such may indeed be the case, but it is important to note that most long single-site paleoseismic records are more consistent with quasi-periodic than random recurrence (Williams et al., 2019), and some of the longest and most complete paleoseismic records preclude clustered similar ruptures. Based on turbidite paleoseismology in small lakes and ponds, the Alpine Fault in New Zealand exhibits highly non-clustered, quasi-periodic behavior (Howarth et al., 2014, 2018). As there are no historical ruptures and the dating uncertainty is multidecadal, segmentation and length of individual ruptures cannot be strongly established: the strong, similar periodicity established at multiple sites is consistent with either quasi-periodic long ruptures or temporally clustered non-overlapping shorter ruptures. However, the possibility of clustered similar ruptures can be fairly confidently excluded for the Alpine Fault.

3.8. Mechanisms and models of clustering and cyclicity

Gradual strain accumulation and release when a strength threshold is exceeded has long been the underlying mechanism assumed for quasi-periodic similar earthquakes. Many fault segments in our survey exhibit behavior consistent with such a mechanism, though the heterogeneity inherent in large-scale natural systems generally precludes precise periodicity and exact repetition. Clustered complementary ruptures can be understood as being driven by this same simple mechanism, with the addition of a variety of secondary processes. Structural barriers, discussed in detail in section 2, naturally lead to supercycles because multiple ruptures are required to release stress on the whole fault. If the barriers between asperities are relatively narrow, one rupture may easily hasten another via direct Coulomb stress transfer, leading to temporal clustering (considered in the literature as the likely mechanism behind many rupture cascades in our catalog). Frequent barriers that are occasionally traversed produce a superimposed cycle with rare multi-asperity ruptures. As mentioned in section 2.7, these cycle behaviors and relationships with barriers have been demonstrated in numerical and analog models of subduction zones (Corbi et al., 2017a; Kaneko et al., 2010). However, the effects of static stress transfer appear to diminish significantly within a year (Nandan et al., 2016) and the area of effect is fairly proximal to the fault, so clusters that are more broadly temporally or spatially distributed may require a different mechanism. Poroelastic effects, postseismic afterslip, and viscoelastic relaxation are possibilities for earthquake-triggering stress transfer over longer time periods of years to decades; viscoelastic processes may furthermore transfer stress over longer distances of up to thousands of kilometers (Freed, 2005). Each of these has been invoked as a likely mechanism for one or more specific rupture cascades in our catalog (e.g., Ando and Imanishi, 2011; DeVries et al., 2016; Hughes et al., 2010). The super-interseismic phase identified by Melnick et al. (2017) provides yet another mechanism to transfer stress over longer periods and across wider barriers (on dip-slip faults only).

Dynamic stress transfer (through seismic waves) has been observed to trigger earthquakes at very long, potentially global distances. While the direct effect of the passage of the wave train is even more temporally limited than static stress transfer (minutes), delays of up to several weeks have been commonly observed (Freed, 2005). It is likely that static or dynamic stress changes commonly instigate slower processes such as fluid flow or aseismic slip transients, which may then go on to trigger seismic rupture (potentially even years or decades later). In addition to affecting structurally segmented faults, any of these triggering mechanisms may also lead to clustered complementary ruptures in the case of ephemeral barriers that are linked to stress state rather than fault structure. Finally, Scholz (2010) noted that neighboring faults with similar RIs that can affect each other by means of Coulomb stress transfer may naturally develop synchronized rupture cycles. It has even been proposed that earthquake recurrence could be weakly synchronized on a global scale, either self-synchronized via dynamic triggering of slow slip or due to a global forcing effect such as slight changes in Earth's rotation (Bendick and Bilham, 2017; Sammis and Smith, 2013).

It appears from our analysis that clustered similar ruptures may be rare on major fast-slipping plate boundary faults. Where they do occur, one possibility is that earthquakes may appear clustered if slip is accommodated through aseismic creep during intervening periods between "clusters." Biemiller and Lavier (2017) modeled this process for normal faults by simulating a mixture of velocity-strengthening and velocity-weakening material in fault zones, causing the fault to occasionally switch between aseismic and seismic behavior regimes. Real-world examples of such "regime change" are suggested by certain microatoll records above the Nias segment of the Sunda megathrust (Meltzner et al., 2012, 2015). Some of the observed changes in interseismic deformation rate have been inferred to result from temporal changes in coupling (Tsang et al., 2015a), but these changes could also be explained by long-duration slow-slip events (e.g., Tsang et al., 2015b). No evidence for clustering has yet been found on the Nias segment, but if no large megathrust rupture occurred between c. 1580 and 1861, it would suggest that some inter-event times are nearly twice as long as others.

If, however, it can be demonstrated that fault slip (and not merely seismicity) is concentrated in time, this implies either variability in fault strength over time (permitting more frequent ruptures during some periods) or variability in fault loading rate over time. Having observed clustering at multi-millennial scales on the slow-slipping Garlock fault in California, Dolan et al. (2016)

hypothesized that strength and loading rate could be affected by particularly large ruptures or groups of ruptures, leading to longer-term cycles of strength fluctuation or stress transfer between faults. Kenner and Simons (2005) model postseismic reloading of a fault (through aseismic slip in the transition zone) as a mechanism for clustering. This effect would be most significant in tectonic regimes where deformation rates are slow and earthquake RIs are long, as is indeed the case for many of the examples noted in section 3.7.

Herrendörfer et al. (2015) propose a model in which wider megathrust seismogenic zones lead to a type of supercycle behavior which is perhaps best described as a superimposed cycle: smaller events occur near the down-dip edge of the modeled locked zone throughout the intervals between large ruptures of the entire fault. This occurs because ruptures are unable to propagate into the center of the locked zone until stress concentrations have been transferred there from below. Their model is potentially applicable to superimposed cycles along dip in subduction zones, such as the Tohoku case. However, as discussed in section 3, this mechanism cannot readily be related to any type of supercycle behavior along strike, and many aspects of the model, such as the scale of the fault width and stress drop and the crack-like mega-ruptures, are not physically reasonable.

Independently of the mechanism proposed by Herrendörfer et al., a wider seismogenic zone may indeed permit more behavior complexity simply because there is more room for heterogeneity and multiple asperities. A simpler mechanism to produce superimposed cycles is variability in fault strength or frictional properties between neighboring asperities, such that one ruptures more frequently than another (demonstrated in numerical models by Kato, 2016). This is particularly likely given that superimposed cycles are often related to longer RIs for shallow megathrust asperities (domain A): the longer and potentially less regular rupture cycles of shallow asperities are likely due to the distinct mechanical properties of the accretionary prism. These properties originally led many researchers to assume that shallow megathrust regions could never rupture seismically (e.g., Byrne et al., 1988). A growing collection of worldwide examples indicates that shallow rupture on thrust faults is not uncommon and may be universally possible (Hubbard et al., 2015); nevertheless, this type of region likely does accumulate less seismic potential and is less prone to dynamic rupture than domains B and C. Additionally, numerical modeling indicates that stress heterogeneities resulting from fault-bend folds naturally give rise to superimposed cycles of various rupture "families" under certain frictional conditions (Sathiakumar et al., 2020), and that a broad spectrum of recurrence behavior including various types of superimposed cycles can be induced merely by varying frictional properties on a homogeneous single-asperity flat strike-slip or dip-slip fault (Barbot, 2019). As noted above, rare multi-asperity ruptures along strike can be produced in a subduction setting by an appropriate asperity/barrier size ratio (Corbi et al., 2017a). Kato (2016) also observed that earthquake RIs in his two-asperity model became more variable when the frictional parameters were transitional between promoting seismic and aseismic slip. It should be noted that while numerical models provide some hints as to which physical parameters influence RI, *a priori* determination of RI from physical parameters is generally not feasible (Bizzarri and Crupi, 2014) and must still be done based on earthquake chronologies for each individual fault.

Ye et al. (2018) observed that rupture complexity (as measured by excess radiated energy) of megathrust earthquakes varies from region to region but is relatively consistent within regions, suggesting that complexity is largely controlled by persistent geological factors rather than ephemeral stress state. They propose that rupture modes are primarily influenced by two parameters: relative asperity/barrier size and fault interface roughness within asperities. In their framework, fault segments that behave as single asperities are generally smooth and produce large, homogenous ruptures with little variability. For more heterogeneous fault segments with multiple asperities, the variability depends on the asperity roughness: ruptures of individual asperities occur in both cases, but rupture of a rough asperity is more likely to trigger neighboring asperities, leading to more frequent multi-asperity ruptures. Rupture of a smooth asperity generates less excess radiated energy and is thus is more likely to remain confined. This framework potentially explains the different rupture modes observed on various megathrust segments in our survey, and could easily extend to non-subduction environments.

4. Conclusions & implications for earthquake science and seismic hazard analysis

In this review, we have catalogued the rupture behavior of all plate boundary faults for which existing data are sufficient to assess segmentation and cycle patterns. We conclude the following:

(1) It is necessary to be as precise as possible with the terminology relating to earthquake recurrence: "cluster," "segment," and "supercycle" have all become ambiguous terms which may be employed and interpreted differently by different researchers. We suggest that the term "segment" should not be used for purely geographically defined fault sections, that authors always specify whether they are referring to structural or rupture segmentation, and that they use more specific descriptive terms such as "clustered similar ruptures," "rupture cascades," and "superimposed cycles."

(2) Fault behavior cannot be fully constrained by a sparse distribution of sites or sites with short paleoseismic records. A dense network of sites with records spanning many cycles is required. Furthermore, radiometric age control alone is typically insufficiently precise to distinguish between some common behavior patterns; it is necessary to apply additional constraints from history, stratigraphy, or slip magnitude.

(3) Researchers should be aware of the variety of cycle behavior that is well documented and seek to recognize these patterns as more data emerge:
   - o Persistent and frequent barriers, rupture cascades, superimposed cycles, and quasi-periodic recurrence are common features of most major faults (Table 2). However, the earthquakes in a given quasi-periodic sequence often vary substantially in magnitude/rupture area, even on ultra-simple oceanic transforms.
   - o Barrier regions accommodate slip through reduced interseismic coupling, slow slip events, and/or smaller more localized ruptures. They are frequently associated with structural features such as subducting seafloor relief or fault trace discontinuities, but the correspondence is generally not sufficiently straightforward to confidently identify barrier regions *a priori.*
   - o Clustered similar ruptures do not appear to be common, but broad overlap zones between neighboring master segments do occur. Earthquake chronologies at sites within these zones may have the appearance of clustered similar ruptures.
   - o On megathrust faults, the shallow asperities (domain A) often have a longer and possibly more erratic rupture cycle, superimposed on the usually shorter and more regular cycle of domain B. These regions may rupture individually,

producing "tsunami earthquakes," or along with domain B in full-width "superquakes."

(4) It is advisable to assess the data in detail and recognize the specific type (or multiple potential types) of behavior before performing earthquake hazard assessment or modeling segmentation or cycle mechanisms, because the different types of behavior we observe have differing implications for both hazard and mechanisms.

While faults with long RIs and no historical earthquakes do not make good primary examples for this catalog, it is instructive to note that relevant information may still be gleaned when they are approached in the framework we suggest. Even if specific rupture patterns cannot be positively identified, it may be possible to rule out certain possibilities. Fittingly, the Wasatch Fault in Utah, which inspired early hypotheses of earthquake recurrence (Gilbert, 1884), has become one of the best-studied faults in this category, with ~20 paleoseismic sites extending thousands of years along its ~200 km length. A comprehensive analysis of earthquake chronologies at these sites indicated that the most precisely dated ruptures were largely confined within individual structurally defined segments, while for less precisely dated events with overlapping ages, multi-segment ruptures could not be ruled out (DuRoss et al., 2016). Thus, the primary structural segment boundaries are at least frequent barriers and potentially persistent barriers. Lesser fault discontinuities are probably not persistent barriers but may be frequent barriers. RIs for each segment are fairly steady and similar, between 1100 and 1300 years, and the similarity of ages between some events on neighboring segments suggests rupture cascades and/or rare multi-segment ruptures. There is little or no evidence for strongly clustered similar ruptures. Wasatch researchers recognize the importance of gathering paleoseismic data specifically at structural segment boundaries that are likely rupture barriers (Bennett et al., 2018).

The Wasatch analysis also illustrates that slip profiles of individual events may help to confirm the location of rupture barriers, although they are far from perfect indicators especially on normal faults (DuRoss et al., 2016). An along-strike minimum in long-term uplift rate matches a more minor step-over rather than a primary segment boundary (Jewell and Bruhn, 2013). Those authors argue that some ruptures must therefore traverse the primary segment boundary and it cannot be a persistent barrier. However, it is also possible that slip in the boundary region "catches up" via the tail ends of ruptures from both sides, via slow slip, or via smaller events that are centered in the boundary region, all of which demonstrably occur in boundary zones on our catalog faults. Documentation of such behavior is admittedly less common in non-subduction environments, though this could simply be due to lack of data. The ongoing expanding understanding of Wasatch Fault behavior is vital for accurately characterizing hazards to the adjacent metropolitan area of Salt Lake City.

While we have focused on the relatively small number of faults with particularly long, complete earthquake chronologies (Fig. 1), the insights revealed and approaches defined in this review illuminate paths forward for assessing the behavior of any fault. Most subduction zones are candidates for turbidite paleoseismology and those in warm waters have the potential for coral microatoll studies. Terrestrial faults in regions with long historical records, such as those in south and east Asia and the Middle East, might well become contributors to the behavior catalog in the future with the ongoing expansion of paleoseismic studies in those regions. Although most of the terrestrial faults shown in Fig. 1 have at most one historical rupture and little or no paleoseismic data as of yet, the framework outlined in this review provides helpful context even for very limited information. We hope that approaching fault studies with knowledge of the common earthquake rupture patterns identified in this review will be beneficial to earthquake science and hazard analysis worldwide.

Credit author statement

Belle Philibosian: Conceptualization, Investigation, Writing-Original draft preparation. **Aron J. Meltzner:** Investigation, Writing- Reviewing and Editing.

Declaration of competing interest

None.

Acknowledgments

We first wish to thank Tim Horscroft and the other editors of *Quaternary Science Reviews* for inviting us to contribute this manuscript. We are also very grateful for thorough manuscript reviews by Brian Atwater, Kate Scharer, and two anonymous reviewers as well as additional supplemental review by Steve DeLong and Suzanne Hecker, which led to many improvements. Discussions with and comments from numerous other earthquake scientists also shaped this paper, including particularly helpful conversations with Jay Patton, Tom Rockwell, Jeff McGuire, David Schwartz, and Aaron Wech. This work would not have been possible without the decades of groundbreaking research on Sumatran coral microatolls led by Kerry Sieh, who has also been a primary mentor to both authors. During the majority of her work on this manuscript, Belle Philibosian was supported by a U.S. Geological Survey Mendenhall Postdoctoral Fellowship. Aron Meltzner was supported by the National Research Foundation Singapore under its NRF Fellowship scheme (Award NRF-NRFF11-2019-0008), and by the Earth Observatory of Singapore through its funding from the National Research Foundation Singapore and the Singapore Ministry of Education under the Research Centres of Excellence initiative. This is Earth Observatory of Singapore contribution no. 260.

Appendix A. Supplementary data

Supplementary data to this article can be found online at https://doi.org/10.1016/j.quascirev.2020.106390.

References

Abe, K., 1977. Tectonic implications of the large Shioya-oki earthquakes of 1938. Tectonophysics 41, 269–289. https://doi.org/10.1016/0040-1951(77)90136-6.

Abercrombie, R.E., Antolik, M., Ekström, G., 2003. The June 2000 Mw 7.9 earthquakes south of Sumatra: deformation in the India-Australia plate. J. Geophys. Res. 108 https://doi.org/10.1029/2001JB000674.

Aderhold, K., Abercrombie, R.E., 2016. The 2015 Mw 7.1 earthquake on the Charlie-Gibbs transform fault: repeating earthquakes and multimodal slip on a slow oceanic transform. Geophys. Res. Lett. 43, 6119–6128. https://doi.org/10.1002/2016GL068802.

Agnon, A., 2014. Pre-instrumental earthquakes along the Dead Sea rift. In: Garfunkel, Z., Ben-Avraham, Z., Kagan, E. (Eds.), Dead Sea Transform Fault System: Reviews. Springer Netherlands, pp. 207–261.

Aida, I., 1977. Simulations of large tsunamis occurring in the past off the coast of the Sanriku district [in Japanese with English abstract]. Bull. Earthq. Res. Inst. 52, 71–101. http://hdl.handle.net/2261/12623.

Akçiz, S.O., Grant Ludwig, L., Arrowsmith, J.R., Zielke, O., 2010. Century-long average time intervals between earthquake ruptures of the San Andreas fault in the Carrizo Plain, California. Geology 38, 787–790. https://doi.org/10.1130/G30995.1.

Aki, K., 1979. Characterization of barriers on an earthquake fault. J. Geophys. Res. 84, 6140–6148. https://doi.org/10.1029/JB084iB11p06140.

Allen, C.R., 1975. Geological criteria for evaluating seismicity. Geol. Soc. Am. Bull. 86, 1041–1057. https://doi.org/10.1130/0016-7606(1975)86<1041:GCFES>2.0.CO;2.

Amante, C., Eakins, B.W., 2009. ETOPO1 1 Arc-Minute Global Relief Model:

Procedures, Data Sources and Analysis. National Geophysical Data Center, NOAA. https://doi.org/10.7289/V5C8276M. NOAA Technical Memorandum NESDIS NGDC-24.
Ambraseys, N.N., 1989. Temporary seismic quiescence: SE Turkey. Geophys. J. Int. 96, 311–331. https://doi.org/10.1111/j.1365-246X.1989.tb04453.x.
Ambraseys, N.N., 2009. Earthquakes in the Mediterranean and Middle East. Cambridge University Press, Cambridge, UK.
Ando, M., 1975. Source mechanisms and tectonic significance of historical earthquakes along the Nankai Trough. Tectonophysics 27, 119–140. https://doi.org/10.1016/0040-1951(75)90102-X.
Ando, R., Imanishi, K., 2011. Possibility of Mw 9.0 mainshock triggered by diffusional propagation of after-slip from Mw 7.3 foreshock. Earth Planets Space 63. https://doi.org/10.5047/eps.2011.05.016. Article no. 47.
Astiz, L., Kanamori, H., 1984. An earthquake doublet in Ometepec, Guerrero, Mexico. Phys. Earth Planet. In. 34, 24–45. https://doi.org/10.1016/0031-9201(84)90082-7.
Atwater, B.F., Carson, B., Griggs, G.B., Johnson, H.P., Salmi, M.S., 2014. Rethinking turbidite paleoseismology along the Cascadia subduction zone. Geology 42, 827–830. https://doi.org/10.1130/G35902.1.
Atwater, B.F., Griggs, G.B., 2012. Deep-sea Turbidites as Guides to Holocene Earthquake History at the Cascadia Subduction Zone—Alternative Views for a Seismic-Hazard Workshop. U.S. Geological Survey Open-File Report, 2012–1043.
Atwater, B.F., Musumi-Rokkaku, S., Satake, K., Tsuji, Y., Ueda, K., Yamaguchi, D.K., 2005. The Orphan Tsunami of 1700: Japanese Clues to a Parent Earthquake in North America. U.S. Geological Survey, Reston, Va. and University of Washington Press, Seattle, Wash. https://doi.org/10.3133/pp1707.
Barbot, S., 2019. Slow-slip, slow earthquakes, period-two cycles, full and partial ruptures, and deterministic chaos in a single asperity fault. Tectonophysics 768. https://doi.org/10.1016/j.tecto.2019.228171. Article 228171.
Barka, A.A., 1996. Slip distribution along the North Anatolian Fault associated with the large earthquakes of the period 1939 to 1967. Bull. Seismol. Soc. Am. 86, 1238–1254.
Barnhart, W.D., Murray, J.P., Briggs, R.W., Gomez, F., Miles, C.P.J., Svarc, J., Riquelme, S., Stressler, B.J., 2016. Coseismic slip and early afterslip of the 2015 Illapel, Chile, earthquake: implications for frictional heterogeneity and coastal uplift. J. Geophys. Res. 121, 6172–6191. https://doi.org/10.1002/2016JB013124.
Barrientos, S., Ward, S.N., 1990. The 1960 Chile earthquake: inversion for slip distribution from surface deformation. Geophys. J. Int. 103, 589–598. https://doi.org/10.1111/j.1365-246X.1990.tb05673.x.
Barrientos, S.E., 2007. Earthquakes in Chile. In: Moreno, T., Gibbons, W. (Eds.), The Geology of Chile. The Geological Society, London, U.K., pp. 263–287
Bassett, D., Sandwell, D.T., Fialko, Y., Watts, A.B., 2016. Upper-plate controls on coseismic slip in the 2011 magnitude 9.0 Tohoku-oki earthquake. Nature 531, 92–96. https://doi.org/10.1038/nature16945.
Bassett, D., Watts, A.B., 2015a. Gravity anomalies, crustal structure, and seismicity at subduction zones: 1. Seafloor roughness and subducting relief. G-cubed 16, 1508–1540. https://doi.org/10.1002/2014GC005684.
Bassett, D., Watts, A.B., 2015b. Gravity anomalies, crustal structure, and seismicity at subduction zones: 2. Interrelationships between fore-arc structure and seismogenic behavior. G-cubed 16, 1541–1576. https://doi.org/10.1002/2014GC005685.
Beck, S., Barrientos, S., Kausel, E., Reyes, M., 1998. Source characteristics of historic earthquakes along the central Chile subduction zone. J. S. Am. Earth Sci. 11, 115–129. https://doi.org/10.1016/S0895-9811(98)00005-4.
Bell, J.W., dePolo, C.M., Ramelli, A.R., Sarna-Wojcicki, A.M., Meyer, C.E., 1999. Surface faulting and paleoseismic history of the 1932 Cedar Mountain earthquake area, west-central Nevada, and implications for modern tectonics of the Walker Lane. Geol. Soc. Am. Bull. 111, 791–807. https://doi.org/10.1130/0016-7606(1999)111<0791:SFAPHO>2.3.CO;2.
Bendick, R., Bilham, R., 2017. Do weak global stresses synchronize earthquakes? Geophys. Res. Lett. 44, 8320–8327. https://doi.org/10.1002/2017GL074934.
Benedetti, L., Manighetti, I., Gaudemer, Y., Finkel, R., Malavieille, J., Pou, K., Arnold, M., Aumaitre, G., Bourles, D., Keddadouche, K., 2013. Earthquake synchrony and clustering on Fucino Faults (central Italy) as revealed from in situ ^{36}Cl exposure dating. J. Geophys. Res. Solid Earth 118, 4948–4974. https://doi.org/10.1002/jgrb.50299.
Bennett, S.E.K., DuRoss, C.B., Gold, R.D., Briggs, R.W., Personius, S.F., Reitman, N.G., Devore, J.R., Hiscock, A.I., Mahan, S.A., Gray, H.J., Gunnarson, S., Stephenson, W.J., Pettinger, E., Odum, J.K., 2018. Paleoseismic results from the Alpine site, Wasatch Fault zone: timing and displacement data for six Holocene earthquakes at the Salt Lake City–Provo segment boundary. Bull. Seismol. Soc. Am. 108, 3202–3224. https://doi.org/10.1785/0120160358.
Berberian, M., Yeats, R.S., 1999. Patterns of historical earthquake rupture in the Iranian plateau. Bull. Seismol. Soc. Am. 89, 120–139.
Bernhardt, A., Melnick, D., Hebbeln, D., Lückge, A., Strecker, M.R., 2015. Turbidite paleoseismology along the active continental margin of Chile – feasible or not? Quat. Sci. Rev. 120, 71–92. https://doi.org/10.1016/j.quascirev.2015.04.001.
Biasi, G., Weldon, R.J., 2009. San Andreas Fault rupture scenarios from multiple paleoseismic records: stringing pearls. Bull. Seismol. Soc. Am. 99, 471–498. https://doi.org/10.1785/0120080287.
Biasi, G.P., Wesnousky, S.G., 2017. Bends and ends of surface ruptures. Bull. Seismol. Soc. Am. 107, 2543–2560. https://doi.org/10.1785/0120160292.
Biemiller, J., Lavier, L., 2017. Earthquake supercycles as part of a spectrum of normal fault slip styles. J. Geophys. Res. Solid Earth 122, 3221–3240. https://doi.org/10.1002/2016JB013666.
Bilek, S.L., 2010. Seismicity along the South American subduction zone: review of large earthquakes, tsunamis, and subduction zone complexity. Tectonophysics 495, 2–14. https://doi.org/10.1016/j.tecto.2009.02.037.
Bilek, S.L., Lay, T., 2018. Subduction zone megathrust earthquakes. Geosphere 14, 1468–1500. https://doi.org/10.1130/GES01608.1.
Bilham, R., Engdahl, R., Feldl, N., Satyabala, S.P., 2005. Partial and complete rupture of the Indo-Andaman Plate boundary 1847-2004. Seismol Res. Lett. 76, 299–311. https://doi.org/10.1785/gssrl.76.3.299.
Bird, P., 2003. An updated digital model of plate boundaries. G-cubed 4. https://doi.org/10.1029/2001GC000252.
Bird, P., Kagan, Y.Y., Jackson, D.D., 2002. Plate tectonics and earthquake potential of spreading ridges and oceanic transform faults. In: Stein, S., Freymueller, J.T. (Eds.), Plate Boundary Zones, pp. 203–218.
Bizzarri, A., Crupi, P., 2014. Linking the recurrence time of earthquakes to source parameters: a dream or a real possibility? Pure Appl. Geophys. 171, 2537–2553. https://doi.org/10.1007/s00024-013-0743-1.
Bletery, Q., Thomas, A.M., Rempel, A.W., Karlstrom, L., Sladen, A., De Barros, L., 2016. Mega-earthquakes rupture flat megathrusts. Science 354, 1027–1031. https://doi.org/10.1126/science.aag0482.
Blumberg, S., Lamy, f., Arz, H.W., Echtler, H.P., Wiedicke, M., Haug, G.H., Oncken, O., 2008. Turbiditic trench deposits at the South-Chilean active margin: a Pleistocene-Holocene record of climate and tectonics. Earth Planet Sci. Lett. 268, 526–539. https://doi.org/10.1016/j.epsl.2008.02.007.
Boettcher, M.S., McGuire, J.J., 2009. Scaling relations for seismic cycles on mid-ocean ridge transform faults. Geophys. Res. Lett. 36 https://doi.org/10.1029/2009GL040115.
Bohnhoff, M., Martinez-Garzon, P., Bulut, F., Stierle, E., Ben-Zion, Y., 2016. Maximum earthquake magnitudes along different sections of the North Anatolian fault zone. Tectonophysics 674, 147–165. https://doi.org/10.1016/j.tecto.2016.02.028.
Borrero, J.C., Weiss, R., Okal, E., Hidayat, R., Suranto, Arcas, D., Titov, V.V., 2009. The tsunami of September 12, 2007, Bengkulu Province, Sumatra, Indonesia: post-tsunami field survey and numerical modeling. Geophys. J. Int. 178, 180–194. https://doi.org/10.1111/j.1365-246X.2008.04058.x.
Boyarko, D.C., Brudzinski, M.R., Porritt, R.W., Allen, R.M., Tréhu, A.M., 2015. Automated detection and location of tectonic tremor along the entire Cascadia margin from 2005 to 2011. Earth Planet Sci. Lett. 430, 160–170. https://doi.org/10.1016/j.epsl.2015.06.026.
Briggs, R.W., Engelhart, S.E., Nelson, A.R., Dura, T., Kemp, A.C., Haeussler, P.J., Corbett, D.R., Angster, S.J., Bradley, L.-A., 2014. Uplift and subsidence reveal a nonpersistent megathrust rupture boundary (Sitkinak Island, Alaska). Geophys. Res. Lett. 41, 2289–2296. https://doi.org/10.1002/2014GL059380.
Briggs, R.W., Sieh, K., Amidon, W.H., Galetzka, J., Prayudi, D., Suprihanto, I., Sastra, N., Suwargadi, B., Natawidjaja, D., Farr, T.G., 2008. Persistent elastic behavior above a megathrust rupture patch: Nias island, West Sumatra. J. Geophys. Res. 113 https://doi.org/10.1029/2008JB005684. Article B12406.
Briggs, R.W., Sieh, K., Meltzner, A.J., Natawidjaja, D., Galetzka, J., Suwargadi, B., Hsu, Y., Simons, M., Hananto, N., Suprihanto, I., Prayudi, D., Avouac, J.-P., Prawirodirdjo, L., Bock, Y., 2006. Deformation and slip along the Sunda megathrust in the great 2005 Nias-Simeulue earthquake. Science 311, 1897–1901. https://doi.org/10.1126/science.1122602.
Brudzinski, M.R., Allen, R.M., 2007. Segmentation in episodic tremor and slip all along Cascadia. Geology 35, 907–910. https://doi.org/10.1130/G23740A.1.
Byrne, D.E., Davis, D.M., Sykes, L.R., 1988. Loci and maximum size of thrust earthquakes and the mechanics of the shallow region of subduction zones. Tectonics 7, 833–857. https://doi.org/10.1029/TC007i004p00833.
Carena, S., 2011. Subducting-plate topography and nucleation of great and giant earthquakes along the South American trench. Seismol Res. Lett. 82, 629–637. https://doi.org/10.1785/gssrl.82.5.629.
Carvajal, M., Cisternas, M., Catalan, P.A., 2017a. Source of the 1730 Chilean earthquake from historical records: implications for the future tsunami hazard on the coast of Metropolitan Chile. J. Geophys. Res. 122, 3648–3660. https://doi.org/10.1002/2017JB014063.
Carvajal, M., Cisternas, M., Gubler, A., Catalán, P.A., Winckler, P., Wesson, R.L., 2017b. Reexamination of the magnitudes for the 1906 and 1922 Chilean earthquakes using Japanese tsunami amplitudes: implications for source depth constraints. J. Geophys. Res. Solid Earth 122, 4–17. https://doi.org/10.1002/2016JB013269.
Castillo-Aja, R., Ramírez-Herrera, M.T., 2016. Updated tsunami catalog for the Jalisco–Colima coast, Mexico, using data from historical archives. Seismol Res. Lett. 88, 144–158. https://doi.org/10.1785/0220160133.
Chéry, J., Carretier, S., Ritz, J.-F., 2001. Postseismic stress transfer explains time clustering of large earthquakes in Mongolia. Earth Planet Sci. Lett. 194, 277–286. https://doi.org/10.1016/S0012-821X(01)00552-0.
Chlieh, M., Avouac, J.-P., Sieh, K., Natawidjaja, D., Galetzka, J., 2008. Heterogeneous coupling of the Sumatran megathrust constrained by geodetic and paleogeodetic measurements. J. Geophys. Res. 113 https://doi.org/10.1029/2007JB004981. Article B05305.
Chlieh, M., Mothes, P.A., Nocquet, J.M., Jarrin, P., Charvis, P., Cisneros, D., Font, Y., Collot, J.Y., Villegas-Lanza, J.C., Rolandone, F., Vallee, M., Regnier, M., Segovia, M., Martin, X., Yepes, H., 2014. Distribution of discrete seismic asperities and aseismic slip along the Ecuadorian megathrust. Earth Planet Sci. Lett. 400, 292–301. https://doi.org/10.1016/j.epsl.2014.05.027.
Cifuentes, I.L., 1989. The 1960 Chilean earthquakes. J. Geophys. Res. 94, 665–680. https://doi.org/10.1029/JB094iB01p00665.
Cisternas, M., Atwater, B.F., Torrejon, F., Sawai, Y., Machuca, G., Lagos, M., Eipert, A.,

Youlton, C., Salgado, I., Kamataki, T., Shishikura, M., Rajendran, C.P., Malik, J., Husni, M., 2005. Predecessors of the giant 1960 Chile earthquake. Nature 437, 404–407. https://doi.org/10.1038/nature03943.
Cisternas, M., Carvajal, M., Wesson, R., Ely, L.L., Gorigoitia, N., 2017. Exploring the historical earthquakes preceding the giant 1960 Chile earthquake in a time-dependent seismogenic zone. Bull. Seismol. Soc. Am. 107, 2664–2675. https://doi.org/10.1785/0120170103.
Cisternas, M., Torrejón, F., Gorigoitia, N., 2012. Amending and complicating Chile's seismic catalog with the Santiago earthquake of 7 August 1580. J. S. Am. Earth Sci. 33, 102–109. https://doi.org/10.1016/j.jsames.2011.09.002.
Clark, K.J., Cochran, U.A., Berryman, K.R., Biasi, G., Villamor, P., Bartholomew, T., Litchfield, N., Pantosti, D., Marco, S., Van Dissen, R., Turner, G., Hemphill-Haley, M., 2013. Deriving a long paleoseismic record from a shallow-water Holocene basin next to the Alpine Fault, New Zealand. Geol. Soc. Am. Bull. 125, 811–832. https://doi.org/10.1130/B30693.1.
Clark, M.M., Grantz, A., Rubin, M., 1972. Holocene activity of the Coyote Creek fault as recorded in sediments of Lake Cahuilla. In: The Borrego Mountain Earthquake of April 9, 1968. U.S. Geological Survey Professional Paper 787, pp. 112–180.
Comte, D., Pardo, M., 1991. Reappraisal of great historical earthquakes in the Northern Chile and Southern Peru seismic gaps. Nat. Hazards 4, 23–44. https://doi.org/10.1007/BF00126557.
Contreras-Reyes, E., Carrizo, D., 2011. Control of high oceanic features and subduction channel on earthquake ruptures along the Chile-Peru subduction zone. Phys. Earth Planet. In. 186, 49–58. https://doi.org/10.1016/j.pepi.2011.03.002.
Corbi, F., Funiciello, F., Brizzi, S., Lallemand, S., Rosenau, M., 2017a. Control of asperities size and spacing on seismic behavior of subduction megathrusts. Geophys. Res. Lett. 44, 8227–8235. https://doi.org/10.1002/2017GL074182.
Corbi, F., Herrendörfer, R., Funiciello, F., van Dinther, Y., 2017b. Controls of seismogenic zone width and subduction velocity on interplate seismicity: insights from analog and numerical models. Geophys. Res. Lett. 44, 6082–6091. https://doi.org/10.1002/2016GL072415.
Cummins, P.R., Baba, T., Kodaira, S., Kaneda, Y., 2002. The 1946 Nankai earthquake and segmentation of the Nankai Trough. Phys. Earth Planet. In. 132, 75–87. https://doi.org/10.1016/S0031-9201(02)00045-6.
Daly, P., Sieh, K., Seng, T.Y., McKinnon, E.E., Parnell, A.C., Ardiansyah, Feener, R.M., Ismail, N., Nizamuddin, Majewski, J., 2019. Archaeological evidence that a late 14th-century tsunami devastated the coast of northern Sumatra and redirected history. Proc. Natl. Acad. Sci. Unit. States Am. 116, 11679–11686. https://doi.org/10.1073/pnas.1902241116.
Das, S., Aki, K., 1977. Fault plane with barriers: a versatile earthquake model. J. Geophys. Res. 82, 5658–5670. https://doi.org/10.1029/JB082i036p05658.
DeVries, P.M.R., Krastev, P.G., Meade, B.J., 2016. Geodetically constrained models of viscoelastic stress transfer and earthquake triggering along the North Anatolian fault. G-cubed 17, 2700–2716. https://doi.org/10.1002/2016GC006313.
Dolan, J.F., McAuliffe, L.J., Rhodes, E.J., McGill, S.F., Zinke, R., 2016. Extreme multi-millennial slip rate variations on the Garlock fault, California: strain supercycles, potentially time-variable fault strength, and implications for system-level earthquake occurrence. Earth Planet Sci. Lett. 446, 123–136. https://doi.org/10.1016/j.epsl.2016.04.011.
Dorbath, L., Cisternas, A., Dorbath, C., 1990. Assessment of the size of large and great historical earthquakes in Peru. Bull. Seismol. Soc. Am. 80, 551–576.
Dura, T., Horton, B.P., Cisternas, M., Ely, L.L., Hong, I., Nelson, A.R., Wesson, R.L., Pilarczyk, J.E., Parnell, A.C., Nikitina, D., 2017. Subduction zone slip variability during the last millennium, south-central Chile. Quat. Sci. Rev. 175, 112–137. https://doi.org/10.1016/j.quascirev.2017.08.023.
DuRoss, C.B., Personius, S.F., Crone, A.J., Olig, S.S., Hylland, M.D., Lund, W.R., Schwartz, D.P., 2016. Fault segmentation: new concepts from the Wasatch Fault zone, Utah, USA. J. Geophys. Res. Solid Earth 121. https://doi.org/10.1002/2015JB012519.
Earthquake Research Committee, 2004. Long-term evaluation of earthquake activity along the Kuril trench (second edition) [in Japanese]. Earthquake Research Promotion Headquarters. http://www.jishin.go.jp/main/chousa/kaikou_pdf/chishima2.pdf.
Earthquake Research Committee, 2011. Long-term evaluation of earthquake activity from off Sanriku to off Boso (second edition) [in Japanese]. Earthquake Research Promotion Headquarters. https://www.jishin.go.jp/main/chousa/kaikou_pdf/sanriku_boso_4.pdf.
Falcucci, E., Gori, S., Bignami, C., Pietrantonio, G., Melini, D., Moro, M., Saroli, M., Galadini, F., 2018. The Campotosto seismic gap in between the 2009 and 2016–2017 seismic sequences of central Italy and the role of inherited lithospheric faults in regional seismotectonic settings. Tectonics 37, 2425–2445. https://doi.org/10.1029/2017TC004844.
Ferry, M., Meghraoui, M., Abou Karaki, N., Al-Taj, M., Khalil, L., 2011. Episodic behavior of the Jordan Valley section of the Dead Sea Fault inferred from a 14-ka-long integrated catalog of large earthquakes. Bull. Seismol. Soc. Am. 101, 39–67. https://doi.org/10.1785/0120100097.
Fraser, J., Vanneste, K., Hubert-Ferrari, A., 2010. Recent behavior of the North Anatolian Fault: insights from an integrated paleoseismological data set. J. Geophys. Res. Solid Earth 115. https://doi.org/10.1029/2009jb006982.
Fraser, J.G., Hubert-Ferrari, A., Verbeeck, K., Garcia-Moreno, D., Avsar, U., Maricq, N., Coudijzer, A., Vlamynck, N., Vanneste, K., 2012. A 3000-year record of surface-rupturing earthquakes at Gunalan: variable fault-rupture lengths along the 1939 Erzincan earthquake-rupture segment of the North Anatolian Fault, Turkey. Ann. Geophys. 55, 895–927. https://doi.org/10.4401/ag-4884.
Freed, A.M., 2005. Earthquake triggering by static, dynamic, and postseismic stress transfer. Annu. Rev. Earth Planet Sci. 33, 335–367. https://doi.org/10.1146/annurev.earth.33.092203.122505.
Froment, B., McGuire, J.J., van der Hilst, R.D., Gouédard, P., Roland, E.C., Zhang, H., Collins, J.A., 2014. Imaging along-strike variations in mechanical properties of the Gofar transform fault, East Pacific Rise. J. Geophys. Res. Solid Earth 119, 7175–7194. https://doi.org/10.1002/2014JB011270.
Fujino, S., Kimura, H., Komatsubara, J., Matsumoto, D., Namegaya, Y., Sawai, Y., Shishikura, M., 2018. Stratigraphic evidence of historical and prehistoric tsunamis on the Pacific coast of central Japan: implications for the variable recurrence of tsunamis in the Nankai Trough. Quat. Sci. Rev. 201, 147–161. https://doi.org/10.1016/j.quascirev.2018.09.026.
Fujiwara, O., Aoshima, A., Irizuki, T., Ono, E., Obrochta, S.P., Sampei, Y., Sato, Y., Takahashi, A., 2020. Tsunami deposits refine great earthquake rupture extent and recurrence over the past 1300 years along the Nankai and Tokai fault segments of the Nankai Trough, Japan. Quat. Sci. Rev. 227 https://doi.org/10.1016/j.quascirev.2019.105999.
Fujiwara, O., Hirakawa, K., Irizuki, T., Hasegawa, S., Hase, Y., Uchida, J., 2010. Millennium-scale recurrent uplift inferred from beach deposits bordering the eastern Nankai Trough, Omaezaki area, central Japan. Isl. Arc 19, 374–388. https://doi.org/10.1111/j.1440-1738.2010.00729.x.
Fukao, Y., Furumoto, M., 1979. Stress drops, wave spectra and recurrence intervals of great earthquakes - implications of the Etorofu earthquake of 1958 November 6. Geophys. J. Roy. Astron. Soc. 57, 23–40. https://doi.org/10.1111/j.1365-246X.1979.tb03769.x.
Garrett, E., Fujiwara, O., Garrett, P., Heyvaert, V.M.A., Shishikura, M., Yokoyama, Y., Hubert-Ferrari, A., Brückner, H., Nakamura, A., De Batist, M., the QuakeRecNankai team, 2016. A systematic review of geological evidence for Holocene earthquakes and tsunamis along the Nankai-Suruga Trough, Japan. Earth Sci. Rev. 159, 337–357. https://doi.org/10.1016/j.earscirev.2016.06.011.
Garrett, E., Fujiwara, O., Riedesel, S., Walstra, J., Deforce, K., Yokoyama, Y., Schmidt, S., Brückner, H., de Batist, M., Heyvaert, V.M.A., the QuakeRecNankai team, 2018. Historical Nankai-Suruga megathrust earthquakes recorded by tsunami and terrestrial mass movement deposits on the Shirasuka coastal lowlands, Shizuoka Prefecture, Japan. Holocene 28. https://doi.org/10.1177/0959683617752844.
Gilbert, G.K., 1884. A theory of the earthquakes of the Great Basin, with a practical application [from the Salt Lake Tribune of Sept. 30, 1883]. American Journal of Science ser 3 (27), 49–53. https://doi.org/10.2475/ajs.s3-27.157.49.
Goebel, T.H.W., Kwiatek, G., Becker, T.W., Brodsky, E.E., Dresen, G., 2017. What allows seismic events to grow big?: insights from b-value and fault roughness analysis in laboratory stick-slip experiments. Geology 45, 815–818. https://doi.org/10.1130/G39147.1.
Goes, S.D.B., 1996. Irregular recurrence of large earthquakes: an analysis of historic and paleoseismic catalogs. J. Geophys. Res. 101, 5739–5749. https://doi.org/10.1029/95JB03044.
Goldfinger, C., Galer, S., Beeson, J., Hamilton, T., Black, B., Romsos, C., Patton, J., Nelson, C.H., Hausmann, R., Morey, A., 2017. The importance of site selection, sediment supply, and hydrodynamics: a case study of submarine paleoseismology on the northern Cascadia margin, Washington USA. Mar. Geol. 384 (4–17), 25–46. https://doi.org/10.1016/j.margeo.2016.06.008.
Goldfinger, C., Ikeda, Y., Yeats, R.S., Ren, J., 2013a. Superquakes and supercycles. Seismol Res. Lett. 84, 24–32. https://doi.org/10.1785/0220110135.
Goldfinger, C., Morey, A.E., Black, B., Beeson, J., Nelson, C.H., Patton, J., 2013b. Spatially limited mud turbidites on the Cascadia margin: segmented earthquake ruptures? Nat. Hazards Earth Syst. Sci. 13, 2109–2146. https://doi.org/10.5194/nhess-13-2109-201.
Goldfinger, C., Nelson, C.H., Morey, A., Johnson, J.E., Gutierrez-Pastor, J., Eriksson, A.T., Karabanov, E., Patton, J., Gracia, E., Enkin, R., Dallimore, A., Dunhill, G., Vallier, T., 2012. Turbidite Event History: Methods and Implications for Holocene Paleoseismicity of the Cascadia Subduction Zone. U.S. Geological Survey Professional Paper 1661-F.
Goldfinger, C., Patton, J.R., Van Daele, M., Moernaut, J., Nelson, C.H., de Batist, M., Morey, A.E., 2014. Can turbidites be used to reconstruct a paleoearthquake record for the central Sumatran margin?: COMMENT. Geology 42, e344. https://doi.org/10.1130/G35558C.1.
Grant, L.B., Sieh, K., 1994. Paleoseismic evidence of clustered earthquakes on the San Andreas Fault in the Carrizo Plain, California. J. Geophys. Res. 99, 6819–6841. https://doi.org/10.1029/94JB00125.
Gulick, S.P., Austin Jr., J.A., McNeill, L.C., Bangs, N.L.B., Martin, K.M., Henstock, T.J., Bull, J.M., Dean, S., Djajadihardja, Y.S., Permana, H., 2011. Updip rupture of the 2004 Sumatra earthquake extended by thick indurated sediments. Nat. Geosci. 4, 453–456. https://doi.org/10.1038/ngeo1176.
Hartleb, R.D., Dolan, J.F., Akyüz, H.S., Dawson, T.E., Tucker, A.Z., Yerli, B., Rockwell, T.K., Toraman, E., Çakir, Z., Dikbaş, A., Altunel, E., 2002. Surface rupture and slip distribution along the Karadere segment of the 17 August 1999 İzmit and the western section of the 12 November 1999 Düzce, Turkey, earthquakes. Bull. Seismol. Soc. Am. 92, 67–78. https://doi.org/10.1785/0120000829.
Hatori, T., 1975a. Sources of tsunamis generated off Boso Peninsula [in Japanese with English abstract]. Bull. Earthq. Res. Inst. 50, 83–91. http://hdl.handle.net/2261/12588.
Hatori, T., 1975b. Tsunami magnitude and wave source regions of historical Sanriku tsunamis in northeast Japan [in Japanese with English abstract]. Bull. Earthq. Res. Inst. 50, 397–414. http://hdl.handle.net/2261/12604.

Hatori, T., 1976. Source mechanisms of tsunamis associated with the Fukushima-oki earthquake swarm in 1938 [in Japanese with English abstract]. J. Seismol. Soc. Japan (Zisin 2) 29, 179–190. https://doi.org/10.4294/zisin1948.29.2_179.
Hatori, T., 1987. Distributions of seismic intensity and tsunami of the 1793 Miyagi-oki earthquake, northeastern Japan [in Japanese with English abstract]. Bull. Earthq. Res. Inst. 62, 297–309. http://hdl.handle.net/2261/12992.
Hayes, G.P., Herman, M.W., Barnhart, W.D., Furlong, K.P., Riquelme, S., Benz, H.M., Bergman, E., Barrientos, S., Earle, P.S., Samsonov, S., 2014. Continuing megathrust earthquake potential in Chile after the 2014 Iquique earthquake. Nature 512, 295–298. https://doi.org/10.1038/nature13677.
Henstock, T.J., McNeill, L.C., Bull, J.M., Cook, B.J., Gulick, S.P.S., Austin Jr., J.A., Permana, H., Djajadihardja, Y.S., 2016. Downgoing plate topography stopped rupture in the AD 2005 Sumatra earthquake. Geology 44, 71–74. https://doi.org/10.1130/g37258.1.
Herrendörfer, R., van Dinther, Y., Gerya, T., Dalguer, L.A., 2015. Earthquake supercycle in subduction zones controlled by the width of the seismogenic zone. Nat. Geosci. 8, 471–474. https://doi.org/10.1038/ngeo2427.
Hill, E.M., Borrero, J.C., Huang, Z., Qiu, Q., Banerjee, P., Natawidjaja, D.H., Elosegui, P., Fritz, H.M., Suwargadi, B.W., Pranantyo, I.R., Li, L., Macpherson, K.A., Skanavis, V., Synolakis, C.E., Sieh, K., 2012. The 2010 M_w 7.8 Mentawai earthquake: very shallow source of a rare tsunami earthquake determined from tsunami field survey and near-field GPS. J. Geophys. Res. 117 https://doi.org/10.1029/2012JB009159. Article B06402.
Hirata, K., Satake, K., Tanioka, Y., Hasegawa, Y., 2009. Variable tsunami sources and seismic gaps in the southernmost Kuril Trench: a review. Pure Appl. Geophys. 166, 77–96. https://doi.org/10.1007/s00024-008-0432-7.
Hirose, H., Obara, K., 2005. Repeating short- and long-term slow slip events with deep tremor activity around the Bungo channel region, southwest Japan. Earth Planets Space 57, 961–972. https://doi.org/10.1186/BF03351875.
Hodgkinson, K.M., Stein, R.S., King, G.C.P., 1996. The 1954 Rainbow Mountain-Fairview Peak-Dixie Valley earthquakes: a triggered normal faulting sequence. J. Geophys. Res. 101, 25459–25471. https://doi.org/10.1029/96JB01302.
Hok, S., Fukuyama, E., Hashimoto, C., 2011. Dynamic rupture scenarios of anticipated Nankai-Tonankai earthquakes, southwest Japan. J. Geophys. Res. 116 https://doi.org/10.1029/2011JB008492. Article B12319.
Holtkamp, S., Brudzinski, M., 2014. Megathrust earthquake swarms indicate frictional changes which delimit large earthquake ruptures. Earth Planet Sci. Lett. 390, 234–243. https://doi.org/10.1016/j.epsl.2013.10.033.
Hori, T., 2006. Mechanisms of separation of rupture area and variation in time interval and size of great earthquakes along the Nankai Trough, southwest Japan. J. Earth Simul. 5, 8–19.
Howarth, J.D., Cochran, U.A., Langridge, R.M., Clark, K., Fitzsimons, S.J., Berryman, K., Villamor, P., Strong, D.T., 2018. Past large earthquakes on the Alpine Fault: paleoseismological progress and future directions. N. Z. J. Geol. Geophys. 61, 309–328. https://doi.org/10.1080/00288306.2018.1464658.
Howarth, J.D., Fitzsimons, S.J., Norris, R.J., Jacobsen, G.E., 2014. Lake sediments record high intensity shaking that provides insight into the location and rupture length of large earthquakes on the Alpine Fault, New Zealand. Earth Planet Sci. Lett. 403, 340–351. https://doi.org/10.1016/j.epsl.2014.07.008.
Hubbard, J., Almeida, R., Foster, A., Sapkota, S.N., Bürgi, P., Tapponnier, P., 2016. Structural segmentation controlled the 2015 Mw 7.8 Gorkha earthquake rupture in Nepal. Geology 44, 639–642. https://doi.org/10.1130/G38077.1.
Hubbard, J., Barbot, S., Hill, E.M., Tapponnier, P., 2015. Coseismic slip on shallow decollement megathrusts; implications for seismic and tsunami hazard. Earth Sci. Rev. 141, 45–55. https://doi.org/10.1016/j.earscirev.2014.11.003.
Hughes, K.L.H., Masterlark, T., Mooney, W.D., 2010. Poroelastic stress-triggering of the 2005 M8.7 Nias earthquake by the 2004 M9.2 Sumatra–Andaman earthquake. Earth Planet Sci. Lett. 293, 289–299. https://doi.org/10.1016/j.epsl.2010.02.043.
Hutchinson, I., Clague, J., 2017. Were they all giants? Perspectives on late Holocene plate-boundary earthquakes at the northern end of the Cascadia subduction zone. Quat. Sci. Rev. 169, 29–49. https://doi.org/10.1016/j.quascirev.2017.05.015.
Hyodo, M., Hori, T., Kaneda, Y., 2016. A possible scenario for earlier occurrence of the next Nankai earthquake due to triggering by an earthquake at Hyuga-nada, off southwest Japan. Earth Planets Space 68. https://doi.org/10.1186/s40623-016-0384-6.
Ikehara, K., Kanamatsu, T., Nagahashi, Y., Strasser, M., Fink, H., Usami, K., Irino, T., Wefer, G., 2016. Documenting large earthquakes similar to the 2011 Tohoku-oki earthquake from sediments deposited in the Japan Trench over the past 1500 years. Earth Planet Sci. Lett. 445, 48–56. https://doi.org/10.1016/j.epsl.2016.04.009.
Ishibashi, K., 2004. Status of historical seismology in Japan. Ann. Geophys. 47, 339–368. https://doi.org/10.4401/ag-3305.
Jackson, D.D., Kagan, Y.Y., 1993. Reply [to "Comment on 'Seismic gap hypothesis: ten years after' by Y. Y. Kagan and D. D. Jackson"]. J. Geophys. Res. 98, 9917–9920. https://doi.org/10.1029/93JB00699.
Jacob, J., Dyment, J., Yatheesh, V., 2014. Revisiting the structure, age, and evolution of the Wharton Basin to better understand subduction under Indonesia. J. Geophys. Res. 119, 169–190. https://doi.org/10.1002/2013JB010285.
Jankaew, K., Atwater, B.F., Sawai, Y., Choowong, M., Charoentitirat, T., Martin, M.E., Prendergast, A., 2008. Medieval forewarning of the 2004 Indian Ocean tsunami in Thailand. Nature 455, 1228–1231. https://doi.org/10.1038/nature07373.
Jara-Muñoz, J., Melnick, D., Brill, D., Strecker, M.R., 2015. Segmentation of the 2010 Maule Chile earthquake rupture from a joint analysis of uplifted marine terraces and seismic-cycle deformation patterns. Quat. Sci. Rev. 113, 171–192. https://doi.org/10.1016/j.quascirev.2015.01.005.
Jewell, P.W., Bruhn, R.L., 2013. Evaluation of Wasatch Fault segmentation and slip rates using Lake Bonneville shorelines. J. Geophys. Res. 118, 2528–2543. https://doi.org/10.1002/jgrb.50174.
Kagan, Y.Y., Jackson, D.D., 1991. Seismic gap hypothesis: ten years after. J. Geophys. Res. 96, 21419–21431. https://doi.org/10.1029/91JB02210.
Kagan, Y.Y., Jackson, D.D., 1995. New seismic gap hypothesis: five years after. J. Geophys. Res. 100, 3943–3959. https://doi.org/10.1029/94JB03014.
Kanamori, H., 2014. The diversity of large earthquakes and its implications for hazard mitigation. Annu. Rev. Earth Planet Sci. 42, 7–26. https://doi.org/10.1146/annurev-earth-060313-055034.
Kanamori, H., Rivera, L., Lee, W.H.K., 2010. Historical seismograms for unravelling a mysterious earthquake: the 1907 Sumatra earthquake. Geophys. J. Int. 183, 358–374. https://doi.org/10.1111/j.1365-246X.2010.04731.x.
Kaneko, Y., Avouac, J.-P., Lapusta, N., 2010. Towards inferring earthquake patterns from geodetic observations of interseismic coupling. Nat. Geosci. 3, 363–369. https://doi.org/10.1038/ngeo843.
Kato, N., 2016. Earthquake cycles in a model of interacting fault patches: complex behavior at transition from seismic to aseismic slip. Bull. Seismol. Soc. Am. 106, 1772–1787. https://doi.org/10.1785/0120150185.
Kelleher, J., 1972. Rupture zones of large South American earthquakes and some predictions. J. Geophys. Res. 77, 2087–2103. https://doi.org/10.1029/JB077i011p02087.
Kelleher, J., McCann, W., 1976. Buoyant zones, great earthquakes, and unstable boundaries of subduction. J. Geophys. Res. 81, 4885–4896. https://doi.org/10.1029/JB081i026p04885.
Kelleher, J., Sykes, L.R., Oliver, J., 1973. Possible criteria for predicting earthquake locations and their application to major plate boundaries of the Pacific and the Caribbean. J. Geophys. Res. 78, 2547–2585. https://doi.org/10.1029/JB078i014p02547.
Kelsey, H.M., Bockheim, J.G., 1994. Coastal landscape evolution as a function of eustasy and surface uplift rate, Cascadia margin, southern Oregon. Geol. Soc. Am. Bull. 106, 840–854. https://doi.org/10.1130/0016-7606(1994)106<0840:CLEAAF>2.3.CO;2.
Kelsey, H.M., Engelhart, S.E., Pilarczyk, J.E., Horton, B.P., Rubin, C.M., Daryono, M.R., Ismail, N., Hawkes, A.D., Bernhardt, C.E., Cahill, N., 2015. Accommodation space, relative sea level, and the archiving of paleo-earthquakes along subduction zones. Geology 43, 675–678. https://doi.org/10.1130/G36706.1.
Kelsey, H.M., Ticknor, R.L., Bockheim, J.G., Mitchell, C.E., 1996. Quaternary upper plate deformation in coastal Oregon. Geol. Soc. Am. Bull. 108, 843–860. https://doi.org/10.1130/0016-7606(1996)108<0843:QUPDIC>2.3.CO;2.
Kemp, A.C., Cahill, N., Engelhart, S.E., Hawkes, A.D., Wang, K., 2018. Revising estimates of spatially variable subsidence during the A.D. 1700 Cascadia earthquake using a Bayesian foraminiferal transfer function. Bull. Seismol. Soc. Am. 108, 654–673. https://doi.org/10.1785/0120170269.
Kempf, P., Moernaut, J., de Batist, M., 2019. Bimodal recurrence pattern of tsunamis in South-Central Chile: a statistical exploration of paleotsunami data. Seismol Res. Lett. 90, 194–202. https://doi.org/10.1785/0220180204.
Kenner, S.J., Simons, M., 2005. Temporal clustering of major earthquakes along individual faults due to post-seismic reloading. Geophys. J. Int. 160, 179–194. https://doi.org/10.1111/j.1365-246X.2005.02460.x.
King, N.E., Thatcher, W., 1998. The coseismic slip distribution of the 1940 and 1979 Imperial Valley, California, earthquakes and their implications. J. Geophys. Res. 103, 18069–18086. https://doi.org/10.1029/98JB00575.
Kitamura, A., Seki, Y., Kitamura, Y., Haga, T., 2018. The discovery of emerged boring bivalves at Cape Omaezaki, Shizuoka, Japan: evidence for the 1361 CE Tokai earthquake along the Nankai Trough. Mar. Geol. 405, 114–119. https://doi.org/10.1016/j.margeo.2018.08.006.
Klinger, Y., Le Beon, M., Al-Qaryouti, M., 2015. 5000 yr of paleoseismicity along the southern Dead Sea fault. Geophys. J. Int. 202, 313–327. https://doi.org/10.1093/gji/ggv134.
Kodaira, S., Hori, T., Ito, A., Miura, S., Fujie, G., Park, J.-O., Baba, T., Sakaguchi, H., Kaneda, Y., 2006. A cause of rupture segmentation and synchronization in the Nankai Trough revealed by seismic imaging and numerical simulation. J. Geophys. Res. 111 https://doi.org/10.1029/2005JB004030.
Komori, J., Shishikura, M., Ando, R., Yokoyama, Y., Miyairi, Y., 2017. History of the great Kanto earthquakes inferred from the ages of Holocene marine terraces revealed by a comprehensive drilling survey. Earth Planet Sci. Lett. 471, 74–84. https://doi.org/10.1016/j.epsl.2017.04.044.
Konca, A.O., Avouac, J.-P., Sladen, A., Meltzner, A.J., Sieh, K., Fang, P., Li, Z., Galetzka, J., Genrich, J., Chlieh, M., Natawidjaja, D., Bock, Y., Fielding, E.J., Ji, C., Helmberger, D.V., 2008. Partial rupture of a locked patch of the Sumatra megathrust during the 2007 earthquake sequence. Nature 456, 631–635. https://doi.org/10.1038/nature07572.
Kopp, H., Weinrebe, W., Ladage, S., Barckhausen, U., Klaeschen, D., Flueh, E.R., Gaedicke, C., Djadjadihardja, Y., Grevemeyer, I., Krabbenhoeft, A., Papenberg, C., Zillmer, M., 2008. Lower slope morphology of the Sumatra trench system. Basin Res. 20, 519–529. https://doi.org/10.1111/j.1365-2117.2008.00381.x.
Krabbenhoeft, A., Weinrebe, R.W., Kopp, H., Flueh, E.R., Ladage, S., Papenberg, C., Planert, L., Djajadihardja, Y., 2010. Bathymetry of the Indonesian Sunda margin-relating morphological features of the upper plate slopes to the location and extent of the seismogenic zone. Nat. Hazards Earth Syst. Sci. 10, 1899–1911. https://doi.org/10.5194/nhess-10-1899-2010.
Kubo, H., Asano, K., Iwata, T., 2013. Source-rupture process of the 2011 Ibaraki-oki, Japan, earthquake (Mw 7.9) estimated from the joint inversion of strong-

motion and GPS data: relationship with seamount and Philippine Sea plate. Geophys. Res. Lett. 40, 3003–3007. https://doi.org/10.1002/grl.50558.
Kubota, T., Hino, R., Inazu, D., Ito, Y., Iinuma, T., Ohta, Y., Suzuki, S., Suzuki, K., 2017. Coseismic slip model of offshore moderate interplate earthquakes on March 9, 2011 in Tohoku using tsunami waveforms. Earth Planet Sci. Lett. 458, 241–251. https://doi.org/10.1016/j.epsl.2016.10.047.
Kuna, V.M., Nábělek, J.L., Braunmiller, J., 2019. Mode of slip and crust–mantle interaction at oceanic transform faults. Nat. Geosci. 12, 138–142. https://doi.org/10.1038/s41561-018-0287-1.
Landgrebe, T.C.W., Müller, R.D., 2015. Uncovering the relationship between subducting bathymetric ridges and volcanic chains with significant earthquakes using geophysical data mining. Aust. J. Earth Sci. 62, 171–180. https://doi.org/10.1080/08120099.2015.1003145.
Lange, D., Tilmann, F., Rietbrock, A., Collings, R., Natawidjaja, D.H., Suwargadi, B.W., Barton, P., Henstock, T., Ryberg, T., 2010. The fine structure of the subducted Investigator Fracture Zone in Western Sumatra as seen by local seismicity. Earth Planet Sci. Lett. 298, 47–56. https://doi.org/10.1016/j.epsl.2010.07.020.
Lay, T., Kanamori, H., 1981. An asperity model of large earthquake sequences. In: Simpson, D., Richards, P. (Eds.), Earthquake Prediction: an International Review. American Geophysical Union, Washington, D.C.
Lay, T., Kanamori, H., Ammon, C.J., Koper, K.D., Hutko, A.R., Ye, L., Yue, H., Rushing, T.M., 2012. Depth-varying rupture properties of subduction zone megathrust faults. J. Geophys. Res. 117 https://doi.org/10.1029/2011JB009133. Article B04311.
Lefevre, M., Klinger, Y., Al-Qaryouti, M., Le Béon, M., Moumani, K., 2018. Slip deficit and temporal clustering along the Dead Sea fault from paleoseismological investigations. Sci. Rep. 8 https://doi.org/10.1038/s41598-018-22627-9. Article 4511.
Leonard, L.J., Currie, C.A., Mazzotti, S., Hyndman, R.D., 2010. Rupture area and displacement of past Cascadia great earthquakes from coastal coseismic subsidence. Geol. Soc. Am. Bull. 122, 2079–2096. https://doi.org/10.1130/B30108.1.
Li, C.-F., He, Q.-L., Zhao, G.-G., 2005. Paleo-earthquake studies on the eastern section of the Kunlun fault. Acta Seismol. Sin. 18, 64–71. https://doi.org/10.1007/s11589-005-0007-y.
Li, D., Liu, Y., 2017. Modeling slow-slip segmentation in Cascadia subduction zone constrained by tremor locations and gravity anomalies. J. Geophys. Res. Solid Earth 122, 3138–3157. https://doi.org/10.1002/2016JB013778.
Lin, A., Guo, J., 2008. Nonuniform slip rate and millennial recurrence interval of large earthquakes along the eastern segment of the Kunlun Fault, northern Tibet. Bull. Seismol. Soc. Am. 98, 2866–2878. https://doi.org/10.1785/0120070193.
Lin, A., Guo, J., Kano, K., Awata, Y., 2006. Average slip rate and recurrence interval of large-magnitude earthquakes on the western segment of the strike-slip Kunlun fault, northern Tibet. Bull. Seismol. Soc. Am. 96, 1597–1611. https://doi.org/10.1785/0120050051.
Lomnitz, C., 2004. Major earthquakes of Chile: a historical survey, 1535-1960. Seismol Res. Lett. 75, 368–378. https://doi.org/10.1785/gssrl.75.3.368.
Lonsdale, P., 2005. Creation of the Cocos and Nazca plates by fission of the Farallon plate. Tectonophysics 404, 237–264. https://doi.org/10.1016/j.tecto.2005.05.011.
López, A.M., Okal, E.A., 2006. A seismological reassessment of the source of the 1946 Aleutian 'tsunami' earthquake. Geophys. J. Int. 165, 835–849. https://doi.org/10.1111/j.1365-246X.2006.02899.x.
Loveless, J.P., Meade, B.J., 2016. Two decades of spatiotemporal variations in subduction zone coupling offshore Japan. Earth Planet Sci. Lett. 436, 19–30. https://doi.org/10.1016/j.epsl.2015.12.033.
Lozos, J.C., Oglesby, D.D., Duan, B., Wesnousky, S.G., 2011. The effects of double fault bends on rupture propagation: a geometrical parameter study. Bull. Seismol. Soc. Am. 101, 385–398. https://doi.org/10.1785/0120100029.
Malik, J.N., Shishikura, M., Echigo, T., Ikeda, Y., Satake, K., Kayanne, H., Sawai, Y., Murty, C.V.R., Dikshit, O., 2011. Geologic evidence for two pre-2004 earthquakes during recent centuries near Port Blair, South Andaman Island, India. Geology 39, 559–562. https://doi.org/10.1130/G31707.1.
Marco, S., Klinger, Y., 2014. Review of on-fault palaeoseismic studies along the Dead Sea fault. In: Garfunkel, Z., Ben-Avraham, Z., Kagan, E. (Eds.), Dead Sea Transform Fault System: Reviews. Springer Netherlands, pp. 183–205.
Martin, S.S., Li, L., Okal, E.A., Morin, J., Tetteroo, A.E.G., Switzer, A.D., Sieh, K.E., 2019. Reassessment of the 1907 Sumatra "tsunami earthquake" based on macroseismic, seismological, and tsunami observations, and modeling. Pure Appl. Geophys. 176, 2831–2868. https://doi.org/10.1007/s00024-019-02134-2.
Matsu'ura, T., 2015. Late Quaternary uplift rate inferred from marine terraces, Muroto Peninsula, southwest Japan: forearc deformation in an oblique subduction zone. Geomorphology 234, 133–150. https://doi.org/10.1016/j.geomorph.2015.01.012.
McCann, W.R., Nishenko, S.P., Sykes, L.R., Krause, J., 1979. Seismic gaps and plate tectonics; seismic potential for major plate boundaries. Pure Appl. Geophys. 117, 1082–1147. https://doi.org/10.1007/BF00876211.
McGuire, J.J., 2008. Seismic cycles and earthquake predictability on East Pacific Rise transform faults. Bull. Seismol. Soc. Am. 93, 1067–1084. https://doi.org/10.1785/0120070154.
Meghraoui, M., Jaegy, R., Lammali, K., Albarède, F., 1988. Late Holocene earthquake sequences on the El Asnam (Algeria) thrust fault. Earth Planet Sci. Lett. 90, 187–203. https://doi.org/10.1016/0012-821X(88)90100-8.
Melnick, D., Bookhagen, B., Strecker, M.R., Echtler, H.P., 2009. Segmentation of megathrust rupture zones from fore-arc deformation patterns over hundreds to millions of years, Arauco peninsula, Chile. J. Geophys. Res. 114 https://doi.org/10.1029/2008JB005788.
Melnick, D., Moreno, M., Quinteros, J., Baez, J.C., Deng, Z., Li, S., Oncken, O., 2017. The super-interseismic phase of the megathrust earthquake cycle in Chile. Geophys. Res. Lett. 44, 784–791. https://doi.org/10.1002/2016GL071845.
Meltzner, A.J., Sieh, K., Chiang, H.-W., Shen, C.-C., Suwargadi, B.W., Natawidjaja, D.H., Philibosian, B., Briggs, R.W., 2012. Persistent termini of 2004- and 2005-like ruptures of the Sunda megathrust. J. Geophys. Res. 117 https://doi.org/10.1029/2011JB008888. Article B04405.
Meltzner, A.J., Sieh, K., Chiang, H.-W., Shen, C.-C., Suwargadi, B.W., Natawidjaja, D.H., Philibosian, B.E., Briggs, R.W., Galetzka, J., 2010. Coral evidence for earthquake recurrence and an A.D. 1390–1455 cluster at the south end of the 2004 Aceh-Andaman rupture. J. Geophys. Res. 115 https://doi.org/10.1029/2010JB007499. Article B10402.
Meltzner, A.J., Sieh, K., Chiang, H.-W., Wu, C.-C., Tsang, L.L.H., Shen, C.-C., Hill, E.M., Suwargadi, B.W., Natawidjaja, D.H., Philibosian, B., Briggs, R.W., 2015. Time-varying interseismic strain rates and similar seismic ruptures on the Nias–Simeulue patch of the Sunda megathrust. Quat. Sci. Rev. 122, 258–281. https://doi.org/10.1016/j.quascirev.2015.06.003.
Métois, M., Vigny, C., Socquet, A., Delorme, A., Morvan, S., Ortega, I., Valderas-Bermejo, M.-C., 2014. GPS-derived interseismic coupling on the subduction and seismic hazards in the Atacama region, Chile. Geophys. J. Int. 196, 644–655. https://doi.org/10.1093/gji/ggt418.
Migeon, S., Garibaldi, C., Ratzov, G., Schmidt, S., Collot, J.-Y., Zaragosi, S., Texier, L., 2016. Earthquake-triggered deposits in the subduction trench of the north Ecuador/south Colombia margin and their implication for paleoseismology. Mar. Geol. 384, 47–62. https://doi.org/10.1016/j.margeo.2016.09.008.
Milker, Y., Nelson, A.R., Horton, B.P., Engelhart, S.E., Bradley, L.-A., Witter, R.C., 2016. Differences in coastal subsidence in southern Oregon (USA) during at least six prehistoric megathrust earthquakes. Quat. Sci. Rev. 142, 143–163. https://doi.org/10.1016/j.quascirev.2016.04.017.
Minoura, K., Hirano, S., Yamada, T., 2013. Identification and possible recurrence of an oversized tsunami on the Pacific coast of northern Japan. Nat. Hazards 68, 631–643. https://doi.org/10.1007/s11069-013-0640-z.
Minoura, K., Imamura, F., Sugawara, D., Kono, Y., Iwashita, T., 2001. The 869 Jogan tsunami deposit and recurrence interval of large-scale tsunami on the Pacific coast of Northeast Japan. J. Nat. Disaster Sci. 23, 83–88.
Mochizuki, K., Yamada, T., Shinohara, M., Yamanaka, Y., Kanazawa, T., 2008. Weak interplate coupling by seamounts and repeating M ~ 7 earthquakes. Science 321, 1194–1197. https://doi.org/10.1126/science.1160250.
Moernaut, J., Van Daele, M., Fontjin, K., Heirman, K., Kempf, P., Pino, M., Valdebenito, G., Urrutia, R., Strasser, M., De Batist, M., 2018. Larger earthquakes recur more periodically: new insights in the megathrust earthquake cycle from lacustrine turbidite records in south-central Chile. Earth Planet Sci. Lett. 481, 9–19. https://doi.org/10.1016/j.epsl.2017.10.016.
Moernaut, J., Van Daele, M., Heirman, K., Fontjin, K., Strasser, M., Pino, M., Urrutia, R., De Batist, M., 2014. Lacustrine turbidites as a tool for quantitative earthquake reconstruction: new evidence for a variable rupture mode in south central Chile. J. Geophys. Res. 119, 1607–1633. https://doi.org/10.1002/2013JB010738.
Molnar, P., 1979. Earthquake recurrence intervals and plate tectonics. Bull. Seismol. Soc. Am. 69, 115–133.
Monecke, K., Finger, W., Klarer, D., Kongko, W., McAdoo, B.G., Moore, A.L., Sudrajat, S.U., 2008. A 1,000-year sediment record of tsunami recurrence in northern Sumatra. Nature 455, 1232–1234. https://doi.org/10.1038/nature07374.
Moore, D.E., Rymer, M.J., 2007. Talc-bearing serpentinite and the creeping section of the San Andreas fault. Nature 448, 795–797. https://doi.org/10.1038/nature06064.
Mora-Páez, H., Kellogg, J.N., Freymueller, J.T., Mencin, D., Fernandes, R.M.S., Diederix, H., LaFemina, P., Cardona-Piedrahita, L., Lizarazo, S., Peláez-Gaviria, J.-R., Díaz-Mila, F., Bohórquez-Orozcoa, O., Giraldo-Londoñoa, L., Corchuelo-Cuervoa, Y., 2019. Crustal deformation in the northern Andes – a new GPS velocity field. J. S. Am. Earth Sci. 89, 76–91. https://doi.org/10.1016/j.jsames.2018.11.002.
Moreno, M., Haberland, C., Oncken, O., Rietbrock, A., Angiboust, S., Heidbach, O., 2014. Locking of the Chile subduction zone controlled by fluid pressure before the 2010 earthquake. Nat. Geosci. 7, 292–296. https://doi.org/10.1038/NGEO2102.
Moreno, M., Melnick, D., Rosenau, M., Bolte, J., Klotz, J., Echtler, H., Baez, J., Bataille, K., Chen, J., Bevis, M., Hase, H., Oncken, O., 2011. Heterogeneous plate locking in the south-central Chile subduction zone; building up the next great earthquake. Earth Planet Sci. Lett. 305, 413–424. https://doi.org/10.1016/j.epsl.2011.03.025.
Morgan, P.M., Feng, L., Meltzner, A.J., Lindsey, E.O., Tsang, L.L.H., Hill, E.M., 2017. Sibling earthquakes generated within a persistent rupture barrier on the Sunda megathrust under Simeulue Island. Geophys. Res. Lett. 44, 2159–2166. https://doi.org/10.1002/2016GL071901.
Mueller, C.S., Briggs, R.W., Wesson, R.L., Petersen, M.D., 2015. Updating the USGS seismic hazard maps for Alaska. Quat. Sci. Rev. 113, 39–47. https://doi.org/10.1016/j.quascirev.2014.10.006.
Nakata, R., Hyodo, M., Hori, T., 2012. Numerical simulation of afterslips and slow slip events that occurred in the same area in Hyuga-nada of southwest Japan. Geophys. J. Int. 190, 1213–1220. https://doi.org/10.1111/j.1365-246X.2012.05552.x.
Namegaya, Y., Satake, K., 2014. Reexamination of the A.D. 869 Jogan earthquake size

from tsunami deposit distribution, simulated flow depth, and velocity. Geophys. Res. Lett. 41, 2297–2303. https://doi.org/10.1002/2013GL058678.
Nanayama, F., Furukawa, R., Shigeno, K., Makino, A., Soeda, Y., Igarashi, Y., 2007. Nine unusually large tsunami deposits from the past 4000 years at Kiritappu marsh along the southern Kuril Trench. Sediment. Geol. 200, 275–294. https://doi.org/10.1016/j.sedgeo.2007.01.008.
Nanayama, F., Satake, K., Furukawa, R., Shimokawa, K., Atwater, B.F., Shigeno, K., Yamaki, S., 2003. Unusually large earthquakes inferred from tsunami deposits along the Kuril trench. Nature 424, 660–663. https://doi.org/10.1038/nature01864.
Nandan, S., Ouillon, G., Woessner, J., Sornette, D., Wiemer, S., 2016. Systematic assessment of the static stress triggering hypothesis using interearthquake time statistics. J. Geophys. Res. Solid Earth 121, 1890–1909. https://doi.org/10.1002/2015jb012212.
Natawidjaja, D.H., Sieh, K., Chlieh, M., Galetzka, J., Suwargadi, B.W., Cheng, H., Edwards, R.L., Avouac, J.-P., Ward, S.N., 2006. Source parameters of the great Sumatran megathrust earthquakes of 1797 and 1833 inferred from coral microatolls. J. Geophys. Res. 111 https://doi.org/10.1029/2005JB004025. Article 6403.
Natawidjaja, D.H., Sieh, K., Ward, S.N., Cheng, H., Edwards, R.L., Galetzka, J., Suwargadi, B.W., 2004. Paleogeodetic records of seismic and aseismic subduction from central Sumatran microatolls, Indonesia. J. Geophys. Res. 109 https://doi.org/10.1029/2003JB002398. Article 4306.
Nelson, A.R., Kelsey, H.M., Witter, R.C., 2006. Great earthquakes of variable magnitude at the Cascadia subduction zone. Quat. Res. 65, 354–365. https://doi.org/10.1016/j.yqres.2006.02.009.
Newcomb, K.R., McCann, W.R., 1987. Seismic history and seismotectonics of the Sunda arc. J. Geophys. Res. 92, 421–439. https://doi.org/10.1029/JB092iB01p00421.
Nishenko, S.P., 1991. Circum-Pacific seismic potential: 1989–1999. Pure Appl. Geophys. 135, 169–259. https://doi.org/10.1007/BF00880240.
Nishenko, S.P., Jacob, K.H., 1990. Seismic potential of the Queen Charlotte-Alaska-Aleutian seismic zone. J. Geophys. Res. 95, 2511–2532. https://doi.org/10.1029/JB095iB03p02511.
Nishenko, S.P., Sykes, L.R., 1993. Comment on "Seismic gap hypothesis: ten years after" by Y. Y. Kagan and D. D. Jackson. J. Geophys. Res. 98, 9909–9916. https://doi.org/10.1029/93JB00101.
Nocquet, J.-M., Villegas-Lanza, J.C., Chlieh, M., Mothes, P.A., Rolandone, F., Jarrin, P., Cisneros, D., Alvarado, A., Audin, L., Bondoux, F., Martin, X., Font, Y., Régnier, M., Vallée, M., Tran, T., Beauval, C., Maguiña Mendoza, J.M., Martinez, W., Tavera, H., Yepes, H., 2014. Motion of continental slivers and creeping subduction in the northern Andes. Nat. Geosci. 7, 287–291. https://doi.org/10.1038/ngeo2099.
Nocquet, J.M., Jarrin, P., Vallée, M., Mothes, P.A., Grandin, R., Rolandone, F., Delouis, B., Yepes, H., Font, Y., Fuentes, D., Régnier, M., Laurendeau, A., Cisneros, D., Hernandez, S., Sladen, A., Singaucho, J.-C., Mora, H., Gomez, J., Montes, L., Charvis, P., 2016. Supercycle at the Ecuadorian subduction zone revealed after the 2016 Pedernales earthquake. Nat. Geosci. 10, 145–149. https://doi.org/10.1038/NGEO2864.
Noda, A., TuZino, T., Kanai, Y., Furukawa, R., Uchida, J., 2008. Paleoseismicity along the southern Kuril Trench deduced from submarine-fan turbidites. Mar. Geol. 254, 73–90. https://doi.org/10.1016/j.margeo.2008.05.015.
Noda, H., Lapusta, N., 2013. Stable creeping fault segments can become destructive as a result of dynamic weakening. Nature 493, 518–521. https://doi.org/10.1038/nature11703.
Obara, K., 2010. Phenomenology of deep slow earthquake family in southwest Japan: spatiotemporal characteristics and segmentation. J. Geophys. Res. Solid Earth 115. https://doi.org/10.1029/2008JB006048.
Okal, E.A., Borrero, J.C., Synolakis, C.E., 2006. Evaluation of tsunami risk from regional earthquakes at Pisco, Peru. Bull. Seismol. Soc. Am. 96, 1634–1648. https://doi.org/10.1785/0120050158.
Okamura, Y., Namegaya, Y., 2011. Reconsideration of the 17th century Kuril multi-segment earthquake [in Japanese with English abstract]. In: Annual Report on Active Fault and Paleoearthquake Researches, Geologic Survey of Japan, 11, pp. 15–20. https://www.gsj.jp/data/actfault-eq/h22seika/pdf/okamura.pdf.
Okuno, J., Nakada, M., Ishii, M., Miura, H., 2014. Vertical tectonic crustal movements along the Japanese coastlines inferred from late Quaternary and recent relative sea-level changes. Quat. Sci. Rev. 91, 42–61. https://doi.org/10.1016/j.quascirev.2014.03.010.
Okuwaki, R., Yagi, Y., 2017. Rupture process during the Mw 8.1 2017 Chiapas Mexico earthquake: shallow intraplate normal faulting by slab bending. Geophys. Res. Lett. 44, 11816–11823. https://doi.org/10.1002/2017GL075956.
Ota, Y., Omura, A., 1991. Late quaternary shorelines in the Japanese Islands. Quat. Res. 30, 175–186. https://doi.org/10.4116/jaqua.30.175.
Ozawa, S., Suito, H., Tobita, M., 2007. Occurrence of quasi-periodic slow-slip off the east coast of the Boso peninsula, Central Japan. Earth Planets Space 59, 1241–1245. https://doi.org/10.1186/BF03352072.
Patton, J.R., Goldfinger, C., Morey, A.E., Ikehara, K., Romsos, C., Stoner, J., Djadjadihardja, Y., Udrekh, Sri, A., Gaffar, E.Z., Vizcaino, A., 2015. A 6600 year earthquake history in the region of the 2004 Sumatra-Andaman subduction zone earthquake. Geosphere 11, 2067–2129. https://doi.org/10.1130/ges01066.1.
Paul, J., Rajendran, C.P., 2015. Short-term pre-2004 seismic subsidence near South Andaman: is this a precursor slow slip prior to a megathrust earthquake? Phys. Earth Planet. In. 248, 30–34. https://doi.org/10.1016/j.pepi.2015.08.006.
Paul, J., Rajendran, C.P., Lowry, A.R., Andrade, V., Rajendran, K., 2012. Andaman postseismic deformation observations: still slipping after all these years? Bull. Seismol. Soc. Am. 102, 343–351.
Philibosian, B., Sieh, K., Avouac, J.-P., Natawidjaja, D.H., Chiang, H.-W., Wu, C.-C., Perfettini, H., Shen, C.-C., Daryono, M.R., Suwargadi, B.W., 2014. Rupture and variable coupling behavior of the Mentawai segment of the Sunda megathrust during the supercycle culmination of 1797 to 1833. J. Geophys. Res. 119 https://doi.org/10.1002/2014JB011200.
Philibosian, B., Sieh, K., Avouac, J.-P., Natawidjaja, D.H., Chiang, H.-W., Wu, C.-C., Shen, C.-C., Daryono, M.R., Perfettini, H., Suwargadi, B.W., Lu, Y., Wang, X., 2017. Earthquake supercycles on the Mentawai segment of the Sunda megathrust in the seventeenth century and earlier. J. Geophys. Res. Solid Earth 122, 642–676. https://doi.org/10.1002/2016JB013560.
Philibosian, B., Sieh, K., Natawidjaja, D.H., Chiang, H.-W., Shen, C.-C., Suwargadi, B.W., Hill, E.M., Edwards, R.L., 2012. An ancient shallow slip event on the Mentawai segment of the Sunda megathrust, Sumatra. J. Geophys. Res. 117 https://doi.org/10.1029/2011JB009075. Article B05401.
Plafker, G., 1969. Tectonics of the March 27, 1964 Alaska Earthquake. U.S. Geological Survey Professional Paper 543-I.
Plafker, G., Rubin, M., 1978. Uplift history and earthquake recurrence as deduced from marine terraces on Middleton Island, Alaska. In: Isacks, B.L., Plafker, G. (Eds.), Proceedings of Conference VI: Methodology for Identifying Seismic Gaps and Soon-To-Break Gaps: Convened under Auspicies of National Earthquake Hazards Reduction Program, 25–27 May, 1978. U.S. Geological Survey Open-File Report 78–943, pp. 687–721.
Polet, J., Kanamori, H., 2000. Shallow subduction zone earthquakes and their tsunamigenic potential. Geophys. J. Int. 142, 684–702. https://doi.org/10.1046/j.1365-246x.2000.00205.x.
Porto, N.M., Fitzenz, D.D., 2016. An alternative segmentation model for the Alaskan Aleutian megathrust. Bull. Seismol. Soc. Am. 106, 1125–1132. https://doi.org/10.1785/0120150235.
Prawirodirdjo, L., McCaffrey, R., Chadwell, C.D., Bock, Y., Subarya, C., 2010. Geodetic observations of an earthquake cycle at the Sumatra subduction zone; role of interseismic strain segmentation. J. Geophys. Res. 115 https://doi.org/10.1029/2008JB006139. Article B03414.
Qiu, Q., Hill, E.M., Barbot, S., Hubbard, J., Feng, W., Lindsey, E.O., Feng, L., Dai, K., Samsonov, S.V., Tapponnier, P., 2016. The mechanism of partial rupture of a locked megathrust: the role of fault morphology. Geology 44, 875–878. https://doi.org/10.1130/G38178.1.
Rajendran, C.P., Rajendran, K., Anu, R., Earnest, A., Machado, T., Mohan, P.M., Freymueller, J.T., 2007. Crustal deformation and seismic history associated with the 2004 Indian Ocean earthquake; a perspective from the Andaman-Nicobar islands. Bull. Seismol. Soc. Am. 97, S174–S191. https://doi.org/10.1785/0120050630.
Rajendran, K., Rajendran, C.P., Earnest, A., Ravi Prasad, G.V., Dutta, K., Ray, D.K., Anu, R., 2008. Age estimates of coastal terraces in the Andaman and Nicobar Islands and their tectonic implications. Tectonophysics 455, 53–60. https://doi.org/10.1016/j.tecto.2008.05.004.
Ramírez-Herrera, M.T., Corona, N., Ruiz-Angulo, A., Melgar, D., Zavala-Hidalgo, J., 2018. The 8 September 2017 tsunami triggered by the Mw 8.2 intraplate earthquake, Chiapas, Mexico. Pure Appl. Geophys. 175, 25–34. https://doi.org/10.1007/s00024-017-1765-x.
Ratzov, G., Cattaneo, A., Babonneau, N., Deverchere, J., Yelles, K., Bracene, R., Courboulex, F., 2015. Holocene turbidites record earthquake supercycles at a slow-rate plate boundary. Geology 43, 331–334. https://doi.org/10.1130/G36170.1.
Reid, A., 2015. History and seismology in the ring of fire: punctuating the Indonesian past. In: Henley, D., Nordholt, H.S. (Eds.), Environment, Trade and Society in Southeast Asia: A Longue Durée Perspective. Brill, Leiden.
Reid, A., 2016. Two hitherto unknown Indonesian tsunamis of the seventeenth century: probabilities and context. J. Southeast Asian Stud. 47, 88–108. https://doi.org/10.1017/s002246341500048x.
Reid, H.F., 1910. The California Earthquake of April 18, 1906, Report of the State Earthquake Investigation Commission, Volume II: the Mechanics of the Earthquake. The Carnegie Institution of Washington.
Rikitake, T., 1976. Recurrence of great earthquakes at subduction zones. Tectonophysics 35, 335–362. https://doi.org/10.1016/0040-1951(76)90075-5.
Rivera, L., Sieh, K., Helmberger, D., Natawidjaja, D., 2002. A comparative study of the Sumatran subduction-zone earthquakes of 1935 and 1984. Bull. Seismol. Soc. Am. 92, 1721–1736. https://doi.org/10.1785/0120010106.
Robinson, D.P., Das, S., Watts, A.B., 2006. Earthquake rupture stalled by a subducting fracture zone. Science 312, 1203–1205. https://doi.org/10.1126/science.1125771.
Rockwell, T.K., Biasi, G., 2017. Paleoseismic interpretation of past earthquakes validated by long historical records argue for large scale regional or fault interaction (abstract presented at the Seismological Society of America Annual Meeting). Seismol Res. Lett. 88, 707.
Rolandone, F., Nocquet, J.M., Mothes, P.A., Jarrin, P., Vallee, M., Cubas, N., Hernandez, S., Plain, M., Vaca, S., Font, Y., 2018. Areas prone to slow slip events impede earthquake rupture propagation and promote afterslip. Sci. Adv. 4 https://doi.org/10.1126/sciadv.aao6596.
Rollins, J.C., Stein, R.S., 2010. Coulomb stress interactions among M $\geq$ 5.9 earthquakes in the Gorda deformation zone and on the Mendocino fault zone, Cascadia subduction zone, and northern San Andreas fault. J. Geophys. Res. Solid Earth 115. https://doi.org/10.1029/2009JB007117.
Romanet, P., Bhat, H.S., Jolivet, R., Madariaga, R., 2018. Fast and slow slip events emerge due to fault geometrical complexity. Geophys. Res. Lett. 45, 4809–4819. https://doi.org/10.1029/2018GL077579.

Rosenau, M., Horenko, I., Corbi, F., Rudolf, M., Kornhuber, R., Oncken, O., 2019. Synchronization of great subduction megathrust earthquakes: insights from scale model analysis. J. Geophys. Res. Solid Earth 124, 3646–3661. https://doi.org/10.1029/2018JB016597.

Rubin, C.M., Horton, B.P., Sieh, K., Pilarczyk, J.E., Daly, P., Ismail, N., Parnell, A.C., 2017. Highly variable recurrence of tsunamis in the 7,400 years before the 2004 Indian Ocean tsunami. Nat. Commun. 8 https://doi.org/10.1038/ncomms16019. Article 16019.

Ruff, L., Kanamori, H., 1980. Seismicity and the subduction process. Phys. Earth Planet. In. 23, 240–252. https://doi.org/10.1016/0031-9201(80)90117-X.

Saillard, M., Audin, L., Rousset, B., Avouac, J.-P., Chlieh, M., Hall, S.R., Husson, L., Farber, D.L., 2017. From the seismic cycle to long-term deformation: linking seismic coupling and Quaternary coastal geomorphology along the Andean megathrust. Tectonics 36, 241–256. https://doi.org/10.1002/2016TC004156.

Salman, R., Hill, E.M., Feng, L., Lindsey, E.O., Veedu, D.M., Barbot, S., Banerjee, P., Hermawan, I., Natawidjaja, D., 2017. Piecemeal rupture of the Mentawai patch, Sumatra: the 2008 Mw 7.2 North Pagai earthquake sequence. J. Geophys. Res. Solid Earth 122, 9404–9419. https://doi.org/10.1002/2017JB014341.

Sammis, C., Smith, S., 2013. Triggered tremor, phase-locking, and the global clustering of great earthquakes. Tectonophysics 589, 167–171. https://doi.org/10.1016/j.tecto.2012.12.021.

Satake, K., 2015. Geological and historical evidence of irregular recurrent earthquakes in Japan. Phil. Trans. Math. Phys. Eng. Sci. 373 https://doi.org/10.1098/rsta.2014.0375.

Satake, K., Nanayama, F., Yamaki, S., 2008. Fault models of unusual tsunami in the 17th century along the Kuril trench. Earth Planets Space 60, 925–935. https://doi.org/10.1186/BF03352848.

Sathiakumar, S., Barbot, S., Hubbard, J., 2020. Earthquake cycles in fault-bend folds. J. Geophys. Res. Solid Earth. https://doi.org/10.1029/2019JB018557.

Sato, T., Higuchi, H., Miyauchi, T., Endo, K., Tsumura, N., Ito, T., Noda, A., Matsu'ura, M., 2016. The source model and recurrence interval of Genroku-type Kanto earthquakes estimated from paleo-shoreline data. Earth Planets Space 68. https://doi.org/10.1186/s40623-016-0395-3. Article no. 17.

Sawai, Y., Fujii, Y., Fujiwara, O., Kamataki, T., Komatsubara, J., Okamura, Y., Satake, K., Shishikura, M., 2008a. Marine incursions of the past 1500 years and evidence of tsunamis at Suijin-numa, a coastal lake facing the Japan Trench. Holocene 18, 517–528. https://doi.org/10.1177/0959683608089206.

Sawai, Y., Kamataki, T., Shishikura, M., Nasu, H., Okamura, Y., Satake, K., Thomson, K.H., Matsumoto, D., Fujii, Y., Komatsubara, J., Aung, T.T., 2009. Aperiodic recurrence of geologically recorded tsunamis during the past 5500 years in eastern Hokkaido, Japan. J. Geophys. Res. 114 https://doi.org/10.1029/2007JB005503. Article B01319.

Sawai, Y., Namegaya, Y., Okamura, Y., Satake, K., Shishikura, M., 2012. Challenges of anticipating the 2011 Tohoku earthquake and tsunami using coastal geology. Geophys. Res. Lett. 39 https://doi.org/10.1029/2012GL053692. Article L21309.

Sawai, Y., Namegaya, Y., Tamura, T., Nakashima, R., Tanigawa, K., 2015. Shorter intervals between great earthquakes near Sendai: scour ponds and a sand layer attributable to A.D. 1454 overwash. Geophys. Res. Lett. 42, 4795–4800. https://doi.org/10.1002/2015GL064167.

Sawai, Y., Shishikura, M., Komatsubara, J., 2008b. A study on paleotsunami using hand corer in Sendai plain (Sendai city, Natori city, Iwanuma city, Watari town, Yamamoto town). Miyagi, Japan [in Japanese with English abstract]. In: Annual Report on Active Fault and Paleoearthquake Researches, Geologic Survey of Japan, 8, pp. 17–70. https://www.gsj.jp/data/actfault-eq/h19seika/pdf/02.sawai.pdf.

Sawai, Y., Shishikura, M., Okamura, Y., Matsu'ura, T., Komatsubara, J., Aung, T.T., 2007. Tsunami inundation history in Sendai Plain, inferred from tsunami deposits. Abstr. Progr. Geol. Soc. Am. 39, 158.

Scharer, K., Streig, A., 2018. The San Andreas Fault system: complexities along a major transform fault system and relation to earthquake hazards. In: Duarte, J. (Ed.), Transform Plate Boundaries and Fracture Zones. Elsevier.

Scharer, K.M., Biasi, G.P., Weldon, R.J., II, 2011. A reevaluation of the Pallett Creek earthquake chronology based on new AMS radiocarbon dates, San Andreas Fault, California. J. Geophys. Res. 116 https://doi.org/10.1029/2010JB008099. Article B12111.

Scharer, K.M., Biasi, G.P., Weldon, R.J., II Fumal, T.E., 2010. Quasi-periodic recurrence of large earthquakes on the southern San Andreas fault. Geology 38, 555–558. https://doi.org/10.1130/G30746.1.

Schellart, W.P., Rawlinson, N., 2013. Global correlations between maximum magnitudes of subduction zone interface thrust earthquakes and physical parameters of subduction zones. Phys. Earth Planet. In. 225, 41–67. https://doi.org/10.1016/j.pepi.2013.10.001.

Schlagenhauf, A., Manighetti, I., Benedetti, L., Gaudemer, Y., Finkel, R., Malavieille, J., Pou, K., 2011. Earthquake supercycles in Central Italy, inferred from ^{36}Cl exposure dating. Earth Planet Sci. Lett. 307, 487–500. https://doi.org/10.1016/j.epsl.2011.05.022.

Scholl, D.W., Kirby, S.H., von Huene, R., Ryan, H., Wells, R.E., Geist, E.L., 2015. Great (≥Mw8.0) megathrust earthquakes and the subduction of excess sediment and bathymetrically smooth seafloor. Geosphere 11, 236–265. https://doi.org/10.1130/ges01079.1.

Scholz, C.H., 2010. Large earthquake triggering, clustering, and the synchronization of faults. Bull. Seismol. Soc. Am. 100, 901–909. https://doi.org/10.1785/0120090309.

Schwartz, D.P., Coppersmith, K.J., 1984. Fault behavior and characteristic earthquakes: examples from the Wasatch and San Andreas fault zones. J. Geophys. Res. 89, 5681–5698. https://doi.org/10.1029/JB089iB07p05681.

Segall, P., Pollard, D.D., 1980. Mechanics of discontinuous faults. J. Geophys. Res. 85, 4337–4350. https://doi.org/10.1029/JB085iB08p04337.

Seno, T., 2012. Great earthquakes along the Nankai Trough - a new idea for their rupture mode and time series- [in Japanese with English abstract]. J. Seismol. Soc. Japan (Zisin 2) 64, 97–116. https://doi.org/10.4294/zisin.64.97.

Shennan, I., Barlow, N., Carver, G., Davies, F., Garrett, E., Hocking, E., 2014. Great tsunamigenic earthquakes during the past 1000 yr on the Alaska megathrust. Geology 42, 687–690. https://doi.org/10.1130/G35797.1.

Shennan, I., Bruhn, R., Plafker, G., 2009. Multi-segment earthquakes and tsunami potential of the Aleutian megathrust. Quat. Sci. Rev. 28, 7–13. https://doi.org/10.1016/j.quascirev.2008.09.016.

Shennan, I., Garrett, E., Barlow, N., 2016. Detection limits of tidal-wetland sequences to identify variable rupture modes of megathrust earthquakes. Quat. Sci. Rev. 150, 1–30. https://doi.org/10.1016/j.quascirev.2016.08.003.

Shimazaki, K., Kim, H.Y., Chiba, T., Satake, K., 2011. Geological evidence of recurrent great Kanto earthquakes at the Miura Peninsula, Japan. J. Geophys. Res. 116 https://doi.org/10.1029/2011JB008639.

Shimazaki, K., Nakata, T., 1980. Time-predictable recurrence model for large earthquakes. Geophys. Res. Lett. 7, 279–282. https://doi.org/10.1029/GL007i004p00279.

Shishikura, M., 2014. History of the paleo-earthquakes along the Sagami Trough, central Japan: review of coastal paleoseismological studies in the Kanto region. Episodes 37, 246–257. https://doi.org/10.18814/epiiugs/2014/v37i4/004.

Sieh, K., 1978. Prehistoric large earthquakes produced by slip on the San Andreas Fault at Pallett Creek, California. J. Geophys. Res. 83, 3907–3939. https://doi.org/10.1029/JB083iB08p03907.

Sieh, K., 1996. The repetition of large-earthquake ruptures. Proc. Natl. Acad. Sci. Unit. States Am. 93, 3764–3771. https://doi.org/10.1073/pnas.93.9.3764.

Sieh, K., Daly, P., Edwards McKinnon, E., Pilarczyk, J.E., Chiang, H.-W., Horton, B., Rubin, C.M., Shen, C.-C., Ismail, N., Vane, C.H., Feener, R.M., 2015. Penultimate predecessors of the 2004 Indian Ocean tsunami in Aceh, Sumatra: stratigraphic, archeological, and historical evidence. J. Geophys. Res. 120, 308–325. https://doi.org/10.1002/2014JB011538.

Sieh, K., Natawidjaja, D.H., Meltzner, A.J., Shen, C.-C., Cheng, H., Li, K.-S., Suwargadi, B.W., Galetzka, J., Philibosian, B., Edwards, R.L., 2008. Earthquake supercycles inferred from sea-level changes recorded in the corals of west Sumatra. Science 322, 1674–1678. https://doi.org/10.1126/science.1163589.

Sieh, K., Stuiver, M., Brillinger, D., 1989. A more precise chronology of earthquakes produced by the San Andreas Fault in Southern California. J. Geophys. Res. 94, 603–623. https://doi.org/10.1029/JB094iB01p00603.

Sieh, K., Ward, S.N., Natawidjaja, D., Suwargadi, B.W., 1999. Crustal deformation at the Sumatran subduction zone revealed by coral rings. Geophys. Res. Lett. 26, 3141–3144. https://doi.org/10.1029/1999GL005409.

Sims, J.D., 1975. Determining earthquake recurrence intervals from deformational structures in young lacustrine sediments. Tectonophysics 29, 141–152. https://doi.org/10.1016/0040-1951(75)90139-0.

Singh, S.C., Hananto, N., Mukti, M., Robinson, D.P., Das, S., Chauhan, A., Carton, H., Gratacos, B., Midnet, S., Djajadihardja, Y., Harjono, H., 2011. Aseismic zone and earthquake segmentation associated with a deep subducted seamount in Sumatra. Nat. Geosci. 4, 308–311. https://doi.org/10.1038/ngeo1119.

Som, S.K., Shivgotra, V., Saha, A., 2009. Coral microatoll as geodetic tool in North Andaman and Little Andaman, India. J. Earth Syst. Sci. 118, 157–162. https://doi.org/10.1007/s12040-009-0018-5.

Song, T.-R.A., Simons, M., 2003. Large trench-parallel gravity variations predict seismogenic behaviour in subduction zones. Science 301, 630–633. https://doi.org/10.1126/science.1085557.

Sparkes, R., Tilmann, F., Hovius, N., Hillier, J., 2010. Subducted seafloor relief stops rupture in South American great earthquakes: implications for rupture behaviour in the 2010 Maule, Chile earthquake. Earth Planet Sci. Lett. 298, 89–94. https://doi.org/10.1016/j.epsl.2010.07.029.

Stein, R.S., Barka, A.A., Dieterich, J.H., 1997. Progressive failure on the North Anatolian Fault since 1939 by earthquake stress triggering. Geophys. J. Int. 128, 594–604. https://doi.org/10.1111/j.1365-246X.1997.tb05321.x.

Styron, R., 2019. Global Earthquake Model Foundation Active Fault Database, GEMScienceTools/gem-Global-Active-Faults: First Release of 2019. https://doi.org/10.5281/zenodo.3376300 (Version 2019.0).

Suárez, G., Albini, P., 2009. Evidence for great tsunamigenic earthquakes (M 8.6) along the Mexican Subduction Zone. Bull. Seismol. Soc. Am. 99, 892–896. https://doi.org/10.1785/0120080201.

Sumner, E.J., Siti, M.I., McNeill, L.C., Talling, P.J., Henstock, T.J., Wynn, R.B., Djajadihardja, Y.S., Permana, H., 2013. Can turbidites be used to reconstruct a paleoearthquake record for the central Sumatran margin? Geology 41, 763–766. https://doi.org/10.1130/G34298.1.

Sumner, E.J., Siti, M.I., McNeill, L.C., Talling, P.J., Henstock, T.J., Wynn, R.B., Djajadihardja, Y.S., Permana, H., 2014. Can turbidites be used to reconstruct a paleoearthquake record for the central Sumatran margin?: REPLY. Geology 42, e353. https://doi.org/10.1130/G36161Y.1.

Sykes, L.R., Ekström, G., 2012. Earthquakes along Eltanin transform system, SE Pacific Ocean: fault segments characterized by strong and poor seismic coupling and implications for long-term earthquake prediction. Geophys. J. Int. 188, 421–434. https://doi.org/10.1111/j.1365-246X.2011.05284.x.

Takahashi, H., Hirata, K., 2003. The 2000 Nemuro-Hanto-Oki earthquake, off eastern Hokkaido, Japan, and the high intraslab seismic activity in the southwestern Kuril Trench. J. Geophys. Res. 108 https://doi.org/10.1029/2002JB001813.

Tal, Y., Hager, B.H., 2018. The slip behavior and source parameters for spontaneous slip events on rough faults subjected to slow tectonic loading. J. Geophys. Res. Solid Earth 123, 1810–1823. https://doi.org/10.1002/2017JB014737.
Tanioka, Y., Satake, K., 1996. Fault parameters of the 1896 Sanriku tsunami earthquake estimated from tsunami numerical modeling. Geophys. Res. Lett. 23, 1549–1552. https://doi.org/10.1029/96GL01479.
Taylor, F.W., Frohlich, C., Lecolle, J., Strecker, M.R., 1987. Analysis of partially emerged corals and reef terraces in the central Vanuatu Arc; comparison of contemporary coseismic and nonseismic with Quaternary vertical movements. J. Geophys. Res. 92, 4905–4933. https://doi.org/10.1029/JB092iB06p04905.
Thatcher, W., 1984. The earthquake deformation cycle, recurrence, and the time-predictable model. J. Geophys. Res. 89, 5674–5680. https://doi.org/10.1029/JB089iB07p05674.
Tilmann, F.J., Craig, T.J., Grevemeyer, I., Suwargadi, B., Kopp, H., Flueh, E., 2010. The updip seismic/aseismic transition of the Sumatra megathrust illuminated by aftershocks of the 2004 Aceh-Andaman and 2005 Nias events. Geophys. J. Int. 181, 1261–1274. https://doi.org/10.1111/j.1365-246X.2010.04597.x.
Tréhu, A.M., Blakely, R.J., Williams, M.C., 2012. Subducted seamounts and recent earthquakes beneath the central Cascadia forearc. Geology 40, 103–106. https://doi.org/10.1130/G32460.1.
Tsang, L.L.H., Meltzner, A.J., Hill, E.M., Freymueller, J.T., Sieh, K., 2015a. A paleogeodetic record of variable interseismic rates and megathrust coupling at Simeulue Island, Sumatra. Geophys. Res. Lett. 42, 10585–10594. https://doi.org/10.1002/2015GL066366.
Tsang, L.L.H., Meltzner, A.J., Philibosian, B., Hill, E.M., Freymueller, J.T., Sieh, K., 2015b. A 15 year slow-slip event on the Sunda megathrust offshore Sumatra. Geophys. Res. Lett. 42, 6630–6638. https://doi.org/10.1002/2015GL064928.
U.S. Geological Survey, 2010. M 7.8 - northern Sumatra, Indonesia finite fault. https://earthquake.usgs.gov/earthquakes/eventpage/usp000hat0/finite-fault.
van Rijsingen, E., Funiciello, F., Corbi, F., Lallemand, S., 2019. Rough subducting seafloor reduces interseismic coupling and mega-earthquake occurrence: insights from analogue models. Geophys. Res. Lett. 46, 3124–3132. https://doi.org/10.1029/2018GL081272.
van Rijsingen, E., Lallemand, S., Peyret, M., Arcay, D., Heuret, A., Funiciello, F., Corbi, F., 2018. How subduction interface roughness influences the occurrence of large interplate earthquakes. G-cubed 19, 2342–2370. https://doi.org/10.1029/2018GC007618.
Verdecchia, A., Pace, B., Visini, F., Scotti, O., Peruzza, L., Benedetti, L., 2018. The role of viscoelastic stress transfer in long-term earthquake cascades: insights after the central Italy 2016–2017 seismic sequence. Tectonics 37, 3411–3428. https://doi.org/10.1029/2018TC005110.
Victor, P., Sobiesiak, M., Glodny, J., Nielsen, S.N., Oncken, O., 2011. Long-term persistence of subduction earthquake segment boundaries: evidence from Mejillones Peninsula, northern Chile. J. Geophys. Res. 116 https://doi.org/10.1029/2010JB007771. Article B02402.
Villegas-Lanza, J.C., Chlieh, M., Cavalié, O., Tavera, H., Baby, P., Chire-Chira, J., Nocquet, J.-M., 2016. Active tectonics of Peru: heterogeneous interseismic coupling along the Nazca megathrust, rigid motion of the Peruvian Sliver, and Subandean shortening accommodation. J. Geophys. Res. Solid Earth 121, 7371–7394. https://doi.org/10.1002/2016JB013080.
Völker, D., Reichel, T., Wiedicke, M., Heubeck, C., 2008. Turbidites deposited on Southern Central Chilean seamounts: evidence for energetic turbidity currents. Mar. Geol. 251, 15–31. https://doi.org/10.1016/j.margeo.2008.01.008.
Wallace, R.E., 1970. Earthquake recurrence intervals on the San Andreas Fault. Geol. Soc. Am. Bull. 81, 2875–2890. https://doi.org/10.1130/0016-7606(1970)81[2875:ERIOTS]2.0.CO;2.
Wallace, R.E., Bonilla, M.G., Villalobos, H.A., 1984. Faulting Related to the 1915 Earthquakes in Pleasant Valley, Nevada. U.S. Geological Survey Professional Paper 1274-A, B.
Walters, R.J., Gregory, L.C., Wedmore, L.N.J., Craig, T.J., McCaffrey, K., Wilkinson, M., Chen, J., Li, Z., Elliott, J.R., Goodall, H., Iezzi, F., Livio, F., Michetti, A.M., Roberts, G., Vittori, E., 2018. Dual control of fault intersections on stop-start rupture in the 2016 Central Italy seismic sequence. Earth Planet Sci. Lett. 500, 1–14. https://doi.org/10.1016/j.epsl.2018.07.043.
Wang, K., Bilek, S.L., 2014. Fault creep caused by subduction of rough seafloor relief. Tectonophysics 610, 1–24. https://doi.org/10.1016/j.tecto.2013.11.024.
Wang, K., Tréhu, A.M., 2016. Some outstanding issues in the study of great megathrust earthquakes—the Cascadia example. J. Geodyn. 98, 1–18. https://doi.org/10.1016/j.jog.2016.03.010.
Wang, P.-L., Engelhart, S.E., Wang, K., Hawkes, A.D., Horton, B.P., Nelson, A.R., Witter, R.C., 2013. Heterogeneous rupture in the great Cascadia earthquake of 1700 inferred from coastal subsidence estimates. J. Geophys. Res. Solid Earth 118, 2460–2473. https://doi.org/10.1002/jgrb.50101.
Wech, A.G., 2010. Interactive tremor monitoring. Seismol Res. Lett. 81, 664–669. https://doi.org/10.1785/gssrl.81.4.664.
Wech, A.G., Bartlow, N.M., 2014. Slip rate and tremor genesis in Cascadia. Geophys. Res. Lett. 41, 392–398. https://doi.org/10.1002/2013GL058607.
Wechsler, N., Rockwell, T.K., Klinger, Y., 2018. Variable slip-rate and slip-per-event on a plate boundary fault: the Dead Sea fault in northern Israel. Tectonophysics 722, 210–226. https://doi.org/10.1016/j.tecto.2017.10.017.
Wechsler, N., Rockwell, T.K., Klinger, Y., Stepancikova, P., Kanari, M., Marco, S., Agnon, A., 2014. A paleoseismic record of earthquakes for the Dead Sea transform fault between the first and seventh centuries C.E.; nonperiodic behavior of a plate boundary fault. Bull. Seismol. Soc. Am. 104, 1329–1347. https://doi.org/10.1785/0120130304.
Wedmore, L.N.J., Walker, J.P.F., Roberts, G.P., Sammonds, P.R., McCaffrey, K.J.W., Cowie, P.A., 2017. A 667 year record of coseismic and interseismic Coulomb stress changes in central Italy reveals the role of fault interaction in controlling irregular earthquake recurrence intervals. J. Geophys. Res. Solid Earth 122, 5691–5711. https://doi.org/10.1002/2017JB014054.
Weldon, R., Scharer, K., Fumal, T., Biasi, G., 2004. Wrightwood and the earthquake cycle: what a long recurrence record tells us about how faults work. GSA Today (Geol. Soc. Am.) 14, 4–10.
Wells, R.E., Blakely, R.J., Sugiyama, Y., Scholl, D.W., Dinterman, P.A., 2003. Basin-centered asperities in great subduction zone earthquakes: a link between slip, subsidence and subduction erosion? J. Geophys. Res. 108 https://doi.org/10.1029/2002JB002072.
Wells, R.E., Blakely, R.J., Wech, A.G., McCrory, P.A., Michael, A., 2017. Cascadia subduction tremor muted by crustal faults. Geology 45, 515–518. https://doi.org/10.1130/G38835.1.
Wesnousky, S.G., 2006. Predicting the endpoints of earthquake ruptures. Nature 444, 358–360. https://doi.org/10.1038/nature05275.
Wesnousky, S.G., 2008. Displacement and geometrical characteristics of earthquake surface ruptures: issues and implications for seismic-hazard analysis and the process of earthquake rupture. Bull. Seismol. Soc. Am. 98, 1609–1632. https://doi.org/10.1785/0120070111.
Wesson, R.L., Boyd, O.S., Mueller, C.S., Bufe, C.G., Frankel, A.D., Petersen, M.D., 2007. Revision of Time-independent Probabilistic Seismic Hazard Maps for Alaska. U.S. Geological Survey Open-File. Report 2007-1043.
Williams, R.T., Davis, J.R., Goodwin, L.B., 2019. Do large earthquakes occur at regular intervals through time? A perspective from the geologic record. Geophys. Res. Lett. 46, 8074–8081. https://doi.org/10.1029/2019GL083291.
Wilson, D.S., 2002. The Juan de Fuca plate and slab: Isochron structure and Cenozoic plate motions. In: Kirby, S., Wang, K., Dunlop, S. (Eds.), The Cascadia Subduction Zone and Related Subduction Systems– Seismic Structure, Intraslab Earthquakes and Processes, and Earthquake Hazards. U.S. Geological Survey Open-File Report 02-328 and Geological Survey of Canada Open File 4350, pp. 9–12.
Witter, R.C., Briggs, R.W., Engelhart, S.E., Gelfenbaum, G., Koehler, R.D., Barnhart, W.D., 2014. Little late Holocene strain accumulation and release on the Aleutian megathrust below the Shumagin Islands, Alaska. Geophys. Res. Lett. 41, 2359–2367. https://doi.org/10.1002/2014GL059393.
Wolfson-Schwehr, M., Boettcher, M.S., McGuire, J.J., Collins, J.A., 2014. The relationship between seismicity and fault structure on the Discovery transform fault, East Pacific Rise. G-cubed 15, 3698–3712. https://doi.org/10.1002/2014GC005445.
Xie, C.D., Lei, X.L., Wu, X.P., Hu, X.L., 2014. Short- and long-term earthquake triggering along the strike-slip Kunlun fault, China: insights gained from the M-s 8.1 Kunlun earthquake and other modern large earthquakes. Tectonophysics 617, 114–125. https://doi.org/10.1016/j.tecto.2014.01.023.
Yagi, Y., Kikuchi, M., Sagiya, T., 2001. Co-seismic slip, post-seismic slip, and aftershocks associated with two large earthquakes in 1996 in Hyuga-nada, Japan. Earth Planets Space 53, 793–803. https://doi.org/10.1186/BF03351677.
Yagi, Y., Kikuchi, M., Yoshida, S., Yamanaka, Y., 1998. Source process of the Hyuganada earthquake of April 1, 1968 (Mjma 7.5), and relationship to the subsequent seismicity [in Japanese with English abstract]. J. Seismol. Soc. Japan (Zisin 2) 51, 139–148. https://doi.org/10.4294/zisin1948.51.1_139.
Yamamoto, Y., Obana, K., Takahashi, T., Nakanishi, A., Kodaira, S., Kaneda, Y., 2013. Imaging of the subducted Kyushu-Palau ridge in the Hyuga-nada region, western Nankai Trough subduction zone. Tectonophysics 589, 90–102. https://doi.org/10.1016/j.tecto.2012.12.028.
Yamamoto, Y., Obana, K., Takahashi, T., Nakanishi, A., Kodaira, S., Kaneda, Y., 2014. Seismicity and structural heterogeneities around the western Nankai Trough subduction zone, southwestern Japan. Earth Planet Sci. Lett. 396, 34–45. https://doi.org/10.1016/j.epsl.2014.04.006.
Yamamoto, Y., Takahashi, T., Kaiho, Y., Obana, K., Nakanishi, A., Kodaira, S., Kaneda, Y., 2017. Seismic structure off the Kii Peninsula, Japan, deduced from passive- and active-source seismographic data. Earth Planet Sci. Lett. 461, 163–175. https://doi.org/10.1016/j.epsl.2017.01.003.
Yamanaka, Y., Kikuchi, M., 2004. Asperity map along the subduction zone in northeastern Japan inferred from regional seismic data. J. Geophys. Res. 109 https://doi.org/10.1029/2003JB002683. Article B07307.
Yamanaka, Y., Tanioka, Y., Shiina, T., 2017. A long source area of the 1906 Colombia–Ecuador earthquake estimated from observed tsunami waveforms. Earth Planets Space 69. https://doi.org/10.1186/s40623-017-0750-z. Article 163.
Yamashita, Y., Shimizu, H., Goto, K., 2012. Small repeating earthquake activity, interplate quasi-static slip, and interplate coupling in the Hyuga-nada, southwestern Japan subduction zone. Geophys. Res. Lett. 39 https://doi.org/10.1029/2012GL051476.
Yanagisawa, H., Goto, K., Sugawara, D., Kanamaru, K., Iwamoto, N., Takamori, Y., 2016. Tsunami earthquake can occur elsewhere along the Japan Trench—historical and geological evidence for the 1677 earthquake and tsunami. J. Geophys. Res. 121, 3504–3516. https://doi.org/10.1002/2015JB012617.
Ye, L., Kanamori, H., Lay, T., 2018. Global variations of large megathrust earthquake rupture characteristics. Sci. Adv. 4, eaao4915 https://doi.org/10.1126/sciadv.aao4915.
Yepes, H., Audin, L., Alvarado, A., Beauval, C., Aguilar, J., Font, Y., Cotton, F., 2016. A new view for the geodynamics of Ecuador: implication in seismogenic source definition and seismic hazard assessment. Tectonics 35, 1249–1279. https://doi.org/10.1002/2015TC003941.
Yoshimoto, M., Kumagai, H., Acero, W., Ponce, G., Vásconez, F., Arrais, S., Ruiz, M.,

Alvarado, A., García, P.P., Dionicio, V., Chamorro, O., Maeda, Y., Nakano, M., 2017. Depth-dependent rupture mode along the Ecuador-Colombia subduction zone. Geophys. Res. Lett. 44, 2203–2210. https://doi.org/10.1002/2016GL071929.

Yuan, Z., Liu-Zeng, J., Wang, W., Weldon, R.J., Oskin, M.E., Shao, Y., Li, Z., Li, Z., Wang, P., Zhang, J., 2018. A 6000-year-long paleoseismologic record of earthquakes along the Xorkoli section of the Altyn Tagh fault, China. Earth Planet Sci. Lett. 497, 193–203. https://doi.org/10.1016/j.epsl.2018.06.008.

Yue, H., Lay, T., Rivera, L., An, C., Vigny, C., Tong, X., Baéz Soto, J.C., 2014. Localized fault slip to the trench in the 2010 Maule, Chile $M_w = 8.8$ earthquake from joint inversion of high-rate GPS, teleseismic body waves, InSAR, campaign GPS, and tsunami observations. J. Geophys. Res. 119, 7786–7804. https://doi.org/10.1002/2014JB011340.

Yule, D., 2009. The enigmatic San Gorgonio Pass. Geology 37, 191–192. https://doi.org/10.1130/focus022009.1.

Zachariasen, J., Sieh, K., Taylor, F.W., Edwards, R.L., Hantoro, W.S., 1999. Submergence and uplift associated with the giant 1833 Sumatran subduction earthquake: evidence from coral microatolls. J. Geophys. Res. 104, 895–919. https://doi.org/10.1029/1998JB900050.

Zachariasen, J., Sieh, K., Taylor, F.W., Hantoro, W.S., 2000. Modern vertical deformation above the Sumatran subduction zone: paleogeodetic insights from coral microatolls. Bull. Seismol. Soc. Am. 90, 897–913. https://doi.org/10.1785/0119980016.

Zielke, O., 2018. Earthquake recurrence and the resolution potential of tectonogeomorphic records. Bull. Seismol. Soc. Am. 108, 1399–1413. https://doi.org/10.1785/0120170241.

Zohar, M., 2020. Temporal and spatial patterns of seismic activity associated with the Dead Sea Transform (DST) during the past 3000 yr. Seismol Res. Lett. 91, 207–221. https://doi.org/10.1785/0220190124.